The Rating of Compound Sharp-Crested Weirs under Modular and Non-Modular Flow Conditions

by
RR Canto

Thesis presented in partial fulfilment of the
requirements for the degree of
Magister in Engineering (Civil)
at the University of Stellenbosch

Dr Jan Rossouw
Supervisor

February 2000

DECLARATION

I the undersigned do hereby declare that this thesis describes my own original work, except where stated otherwise, and that I have not submitted this work, in entirety or in part, to any other university for a degree.

Rolf Rainer Canto

SYNOPSIS

The compound sharp-crested weir, which consists of two or more notches at different elevations, is the most common type of flow gauging structure found in South Africa. The Department of Water Affairs and Forestry (DWAF) is responsible for the operation of these weirs. They are currently experiencing the following problems regarding flow measurement with compound sharp-crested weirs:

1. During free-flow conditions, also known as modular flows, there is uncertainty about the accuracy of the discharge formulas. Although reliable formulas exist for single notch weirs, it is not clear how they should be modified for compound weirs. Whilst methods have already been developed to deal with compound weirs their accuracy needs to be investigated further.
2. When the weirs become submerged during floods, the upstream water head is affected by downstream water levels and the original formulas are not applicable. It has so far been impossible to calculate discharge accurately under these so-called non-modular flow conditions.

This report summarises the findings of an extensive study which addressed the issues mentioned above. A comprehensive test programme was completed during which variations of compound sharp-crested weirs were tested under both modular and non-modular flow conditions. In the development of new methods care was taken to adhere to internationally accepted standards. This should make South African practice acceptable to others.

One important characteristic of compound weirs is the presence of end contractions. It was found that they have a significant effect on discharge measurement. Generally, the more a weir is contracted, the lower its coefficient of discharge becomes. It was also established that end contractions can ensure excellent aeration for compound weirs.

For modular flow conditions it was possible to develop a discharge formula based on the IMFT equation, which is included in the ISO standards. This new method was found to produce the smallest errors when compared to other existing formulas (average error 0.6%).

During non-modular flow conditions it was noted that end contractions also play an important role, at least during the early stages of submergence. In full-width weirs the upstream water level tends to drop first (due to de-aeration) before it rises again with increasing submergence. Weirs with end contractions do not suffer from this problem.

It was further established that the effect of submergence could be described in terms of an energy loss occurring at the drowned weir. This energy loss is a function of the velocities at the so-called vena contracta of the weir and at the downstream river cross section. As the difference between these velocities increases, the energy loss increases as well.

Two methods were tested to estimate the discharge under submerged conditions. The Villemonte formula works well if the energy losses at the weir are relatively high, while the Wessels method is reliable if the energy losses become smaller. A procedure was developed which indicates when each method is applicable. The test data indicated that the maximum error is up to ±10% at high submergence ratios ($S > 0.80$) if this procedure is followed.

SAMEVATTING

Multikeep-skerpkruinmeetstrukture bestaande uit twee of meer kepe op verskillende vlakke word meestal gebruik om vloeie in Suid-Afrikaanse riviere te meet. Die Departement van Waterwese en Bosbou (DWAF) is verantwoordelik vir die instandhouding van sulke meetstrukture. Hulle ervaar tans die volgende probleme met vloeimeting by multikeep-skerpkruine:

1. Gedurende modulêre (onversuipte) toestande bestaan daar nog onsekerheid oor die akkuraatheid van die formules wat gebruik word om vloeitempo's te bereken. Alhoewel betroubare formules ontwikkel is vir enkelkepe, is dit nie duidelik hoe hulle aangepas kan word sodat hulle ook vir multikepe gebruik kan word nie. Die akkuraatheid van sommige bestaande metodes vir multikepe moet ook ondersoek word.
2. Onder versuipte toestande word die stroom-op watervlak beïnvloed deur die stroom-af watervlak en die formules vir vry-vloei toestande is nie geldig nie. Dit was tot nou toe nie moontlik om vloeitempo's akkuraat te bereken onder hierdie nie-modulêre toestande nie.

Hierdie verslag bied 'n opsomming van die bevindinge van 'n navorsingsprojek wat bogenoemde probleme aangespreek het. 'n Toetsprogram is uitgevoer wat moontlike konfigurasies van multikepe ingesluit het. Die modelle van die meetstrukture is onder beide vry-vloei en versuipte toestande bestudeer. Gedurende die ontwikkeling van nuwe formules vir die berekening van vloeie is daarna gestreef om so veel as moontlik gebruik te maak van internasionale standaarde. Dit behoort Suid-Afrikaanse praktyke vir andere aanvaarbaar te maak.

'n Belangrike eienskap van multikepe is die voorkoms van end-kontraksies. Hulle het 'n groot invloed op vloeimeting en oor die algemeen het 'n keep met groot end-kontraksies 'n laer vloei koëffisient as 'n vol-wydte keep. End-kontraksies is ook baie effektief om skerpkruine te belug.

Vir vry-vloei toestande is gevind dat 'n metode gebaseer op die IMFT vergelyking (ingesluit in ISO standaarde) baie goeie resultate lewer. In vergelyking met ander bestaande metodes gee dié metode die kleinste foute met 'n gemiddelde fout van 0.6%.

Onder versuipte toestande speel end-kontraksies ook 'n belangrike rol, ten minste by beperkte versuiping. As vol-wydte kepe beskou word, kan gesien word dat die stroom-op watervlak eers daal voordat dit weer styg (weens ontlugting). Kepe met end-kontraksies ly nie aan hierdie probleem nie.

Dit is verder bevestig dat versuipte toestande beskryf kan word in terme van 'n energie verlies wat by die versuipte meetstruktuur voorkom. Hierdie energie verlies is 'n funksie van die snelhede by die vena contracta van die keep en by die stroom-af rivier snit. As die verskil tussen die twee snelhede groot is, is die energie velies ook groot.

Twee bestaande metodes vir versuipte toestande is getoets. Villemonte se vergelyking werk goed as die energie verliese groot is, terwyl Wessels se metode beter werk as die verliese klein raak. 'n Prosedure is ontwikkel wat dit moontlik maak om die regte metode te kies vir 'n spesifieke toestand. Vanaf die toetsdata is bepaal dat die maksimum fout ±10% is by hoë grade van versuiping ($S > 0.80$) wanneer bogenoemde prosedure gevolg word.

ACKNOWDLEDGEMENTS

I would like to thank Prof Albert Rooseboom and the Water Research Commission for providing assistance and the necessary funding for this project. Without their help, it would have been impossible to launch such a detailed study on compound sharp-crested weirs.

I would also like to thank the following persons for giving me valuable support throughout the past two years:

- Dr Jan Rossouw for showing a keen interest in my research and spending a lot of time with me to help solve the most complex issues.
- Mr Johan van Heerden and Dr Pieter Wessels from the Department of Water Affairs and Forestry for their useful comments and assistance.
- All undergraduate and postgraduate students involved with this project, and all the personnel in the workshops and the hydraulics laboratory for helping me implement a successful test programme.

Finally, I would like to show my appreciation towards my family and my girlfriend, Sonja, for their encouragement and support.

SYMBOLS AND ACRONYMS USED IN THIS DOCUMENT

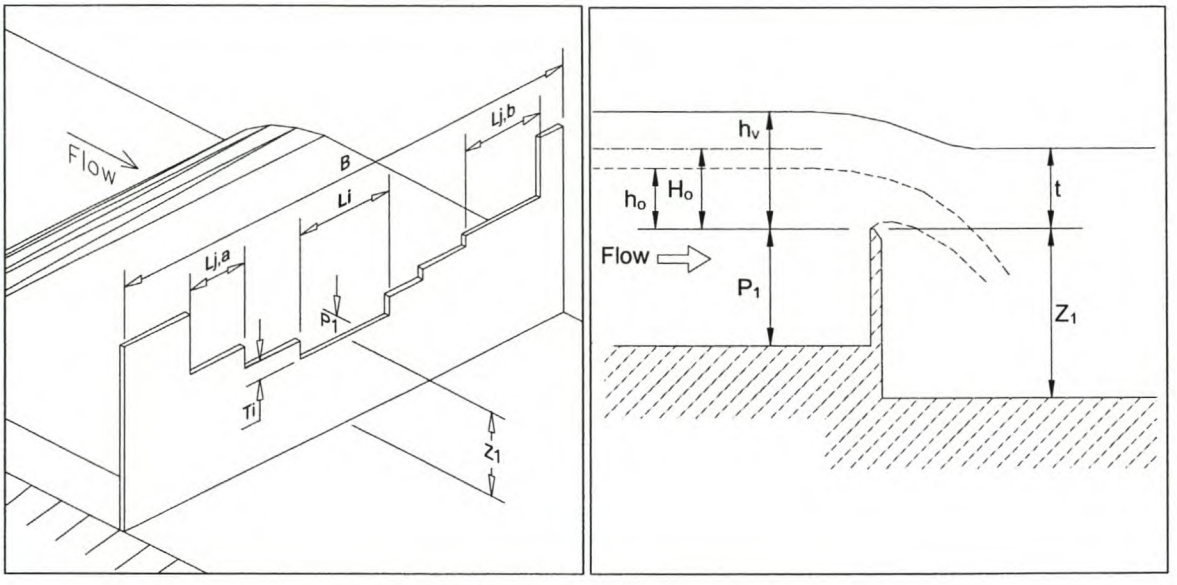

L_i	length of notch i in compound weir
$L_{j,a}$ $L_{j,b}$	length of notches j,a and j,b which are at the same elevation
P_1	pool depth upstream of lowest notch
Z_1	structure height downstream of lowest notch
T_i	step height between notch i and notch i+1
B	total width of approach channel
h_o	upstream water head under modular flow conditions, measured relative to lowest crest in compound weir
H_o	total energy head relative to lowest crest under modular flow conditions
h_v	upstream water head under non-modular flow conditions, measured relative to lowest crest
t	downstream water head under non-modular flow conditions, measured relative to lowest crest
t/h_v	submergence ratio for single notch weirs, also denoted as S

Other symbols not indicated on the sketches:

C_d	coefficient of discharge
g	gravitational acceleration (taken as 9.81 m/s^2)
v	average velocity in approach channel
H_v	total energy head relative to lowest crest under non-modular flow conditions
H_e	effective total energy head for compound weir
P_e	effective pool depth upstream of compound weir
n	correction factor for effective notch length
L_e	effective notch length
Q_o	discharge under modular flow conditions
Q_f	uncorrected discharge calculated with h_v and assuming modular flow conditions
Q_s	estimated discharge under non-modular flow conditions
α	dimensionless constant

A_c	area of vena contracta at drowned weir
v_c	velocity at vena contracta at drowned weir
h_L	energy loss that occurs at a submerged weir
A_o	flow area above crest of weir under free-flow conditions, function of h_o
A_{co}	flow area of vena contracta under free-flow conditions
A_v	flow area above crest of weir under submerged conditions, function of h_v
A_t	flow area above crest of weir under submerged conditions, function of t
A_t/A_v	submergence ratio for compound weirs, also denoted as S'
$A_{t=0}$	area of downstream section when the downstream water head just reaches the lowest crest of a compound weir, i.e. $t = 0$

Acronyms:

DWAF	Department of Water Affairs and Forestry
IMFT	Institut de Mécanique des Fluides de Toulouse
WRC	Water Research Commission
ISO	International Organization for Standardization

LIST OF FIGURES AND TABLES

TABLE OF CONTENTS

Everything flows and nothing stays.

Heraclitus (c.535–c.475 BC) Greek philosopher. *Cratylus* (Plato), 402a

1 INTRODUCTION

Southern Africa will be facing a serious shortage of fresh water in the near future. New water resource projects have to be implemented to augment the current water supplies. It is therefore important to accurately estimate the amount of water still available in the region. This information is essential in the proper identification and planning of new water resource projects.

In order to obtain an estimate of the available water reserves, it is necessary to measure the volumes of water conveyed by the rivers of Southern Africa. Due to the prevailing climate, the rivers carry very little water during most of the hydrological year, while extreme flood events may occur during the wet season. To obtain an accurate estimate of the total volume of water that a particular river can deliver it is necessary to measure the discharge accurately during *all* the seasons. Compound weirs have been specifically developed for this purpose. In contrast to single notch weirs compound weirs have two or more notches at different elevations. These weirs are able to measure both high and low discharges accurately.

In South Africa compound sharp-crested weirs are most frequently used to measure discharges in rivers. Between 70 and 80 percent of all weirs found here are of this type, while the rest consist mainly of Crump weirs, broad-crested weirs as well as flumes. Figure 1.1 below shows a compound sharp-crested weir with notches at three different elevations. Smaller discharges pass over the lowest notch, whilst the higher crests accommodate the excess flow during floods. The water level upstream of the structure is continuously recorded and is used to determine the discharge. This information can be used to calculate the total volume of water that a particular river discharges during a year.

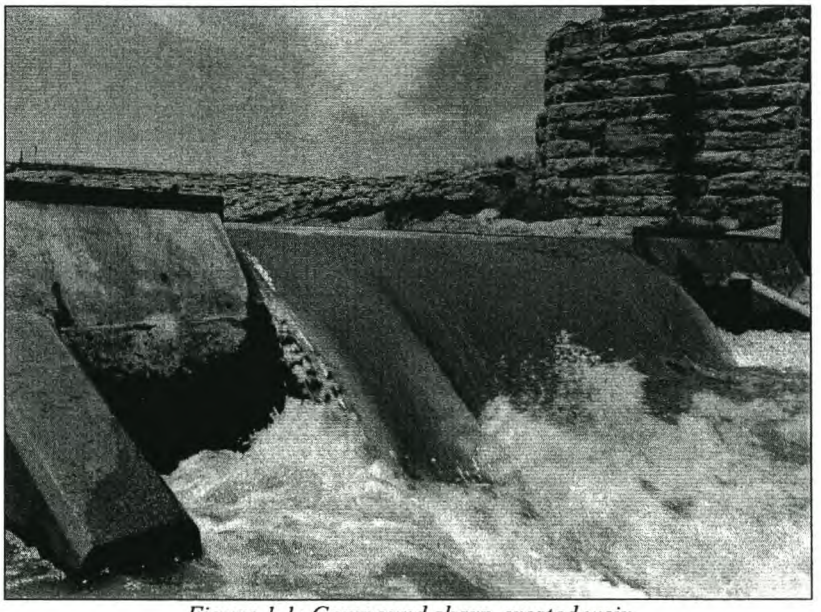

Figure 1.1: Compound sharp-crested weir

The weir in Figure 1.2 has columns between the notches which serve to aerate the area underneath the nappe of the overflowing water.

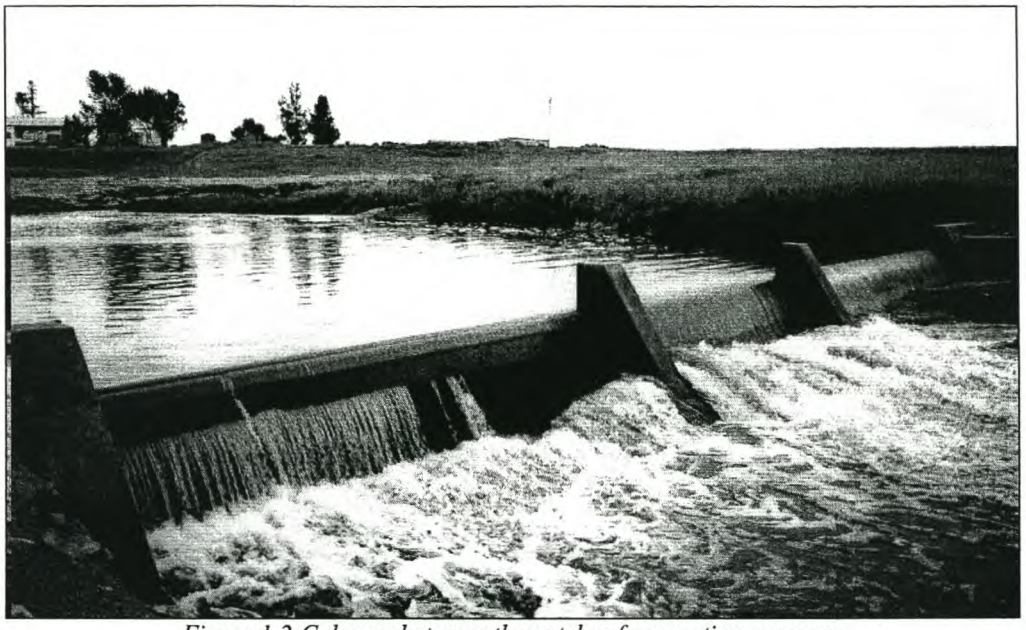

Figure 1.2:Columns between the notches for aeration purposes

This document deals exclusively with the type of flow gauging structure shown in Figures 1.1 and 1.2. The Department of Water Affairs and Forestry (DWAF), which maintains most of the gauging stations in South Africa, currently experiences two major problems with the operation of compound sharp-crested weirs:

- There is still some uncertainty about the accuracy of the formulas that are being used to calculate the discharge under modular flow conditions (i.e. normal operating conditions with smaller discharges).
- During floods, sharp-crested weirs become submerged very quickly. The downstream water head rises above the crest of the weir and the upstream head starts to rise as well. When these so-called non-modular flow conditions prevail, the discharge is a function of both the upstream and downstream water levels, as illustrated on the right in Figure 1.3. The submergence of compound weirs has not been studied comprehensively and discharge calculations are not deemed to be accurate enough.

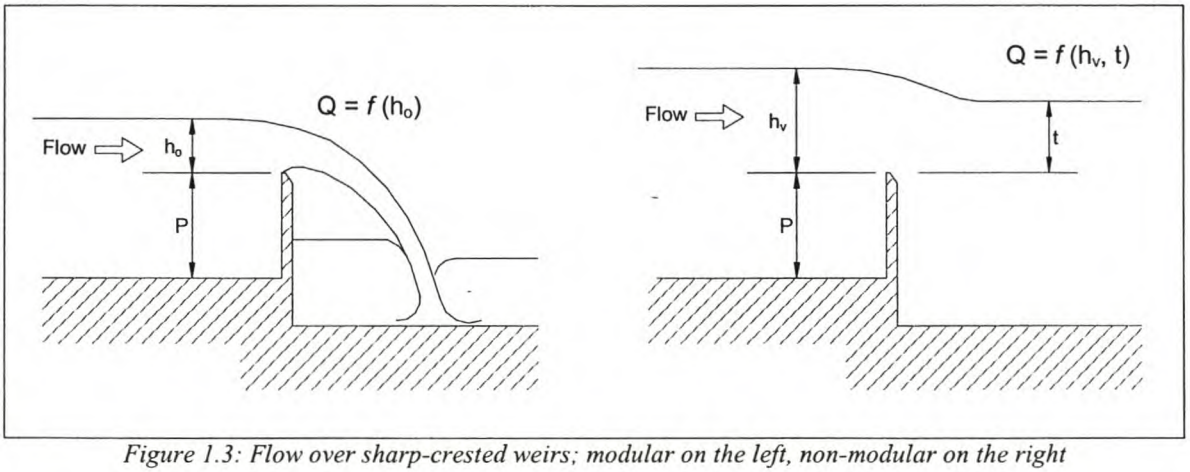

Figure 1.3: Flow over sharp-crested weirs; modular on the left, non-modular on the right

This research project is aimed at finding the most accurate methods to calculate the discharge over compound sharp-crested weirs under both modular and non-modular conditions. Once this has been achieved it will be possible to study more complicated combined flow gauging structures where for example sharp-crested weirs are used in combination with Crump weirs or flumes.

Since South Africa is sharing river resources with other countries in the region (e.g. Lesotho), it will be desirable to adhere to internationally published standards as far as possible. This should ensure that others will accept South African practice.

2 RESEARCH OBJECTIVES

The following objectives have been identified for the study on compound sharp-crested weirs:

1. Modular flow conditions:

- Evaluate existing methods for the calculation of the free-flow discharge over compound sharp-crested weirs. The accuracy of each method is to be tested against existing model data. Some new data will also be generated from additional model tests.
- With the insight gained from the model tests, recommend a method that most accurately calculates the flow rate over a compound sharp-crested weir.
- The recommended discharge formulas should be applicable to a variety of different weir configurations and should be able to accommodate very low as well as extremely high discharges.

2. Non-modular flow conditions:

- Evaluate the best-known methods for the calculation of discharge under submerged conditions. Most of these methods (Villemonte 1947, Wessels 1986) have been developed for single notch weirs only. The data from existing and new model tests will be used to determine the accuracy of each approach.
- Study the submergence process in order to identify the most important parameters influencing non-modular flow conditions.
- Investigate the impact of submergence on compound sharp-crested weirs with the help of model tests.
- Determine whether the methods which have been developed for single notch weirs are also applicable to compound weirs and investigate the accuracy of flow estimation.

The intention is to keep to internationally accepted formulas and methods so that foreign parties should find South African practice acceptable.

3 MODEL TESTS

In order to achieve the above-mentioned objectives it has proven necessary to conduct various model tests on sharp-crested weirs. A large amount of data already exists from previous studies. The following data sets have been used for this project:

3.1 EXISTING DATA FROM PREVIOUS STUDIES

3.1.1 WRC Report No. 442/1/95

The Water Research Commission (WRC) funded a project that dealt with compound sharp-crested weirs under modular flow conditions (Rossouw et al., 1995). All the weirs that were tested were of the configuration shown in Figure 3.1.1.1. They were symmetrical with a lower notch and two higher ones. The two upper notches were at the same elevation and did not have any end contractions on their outsides.

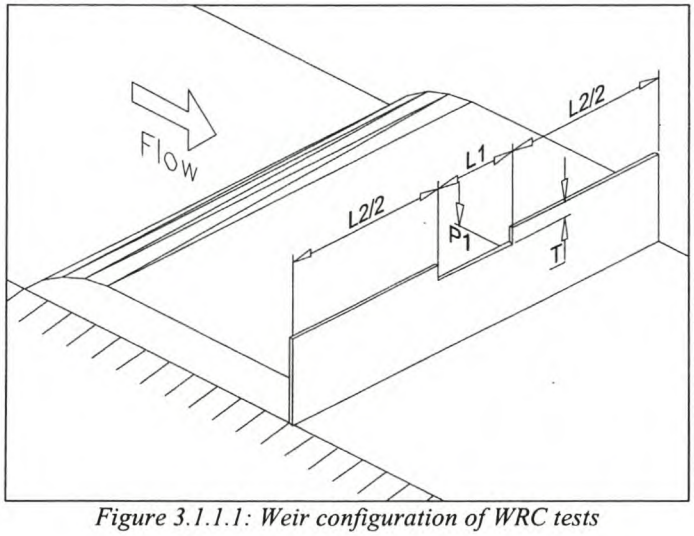

Figure 3.1.1.1: Weir configuration of WRC tests

In the WRC experiments, the notch lengths (L_1 & L_2), pool depth (P) and step height (T) were varied considerably. The data of this study was re-analysed with the new formulas which have been recommended for modular flow conditions.

3.1.2 Data on Submergence from Previous Studies

An extensive study on submergence was performed by Pieter Wessels (Wessels, 1986). He studied the process of submergence with tests on a single notch, full-width sharp-crested weir in a 500 mm wide flume in the laboratories of the Department of Water Affairs and Forestry (DWAF). A wide range of weir configurations was tested, with varying pool depth (P) and structure height (Z). The water levels were measured in stilling wells at distances $4Z$ (upstream) and $10Z$ (downstream) of the crest of the weir.

This data, together with the data from additional model tests described below, was used to analyse the submergence of sharp-crested weirs.

3.2 ADDITIONAL MODEL TESTS

Since no data on submerged compound sharp-crested weirs has been available, most of the additional data are results from tests on compound weirs. Experiments have also been performed on single notch weirs to supplement the work done by Wessels. All the additional data has been generated in the hydraulics laboratory of the Department of Civil Engineering at the University of Stellenbosch. A brief description of the different models follows, after which the test procedure is explained.

3.2.1 Test Series A

All the weirs of *Series A* were tested in a 2-metre wide flume. Figure 3.2.1.1 shows the different weir configurations that were investigated.

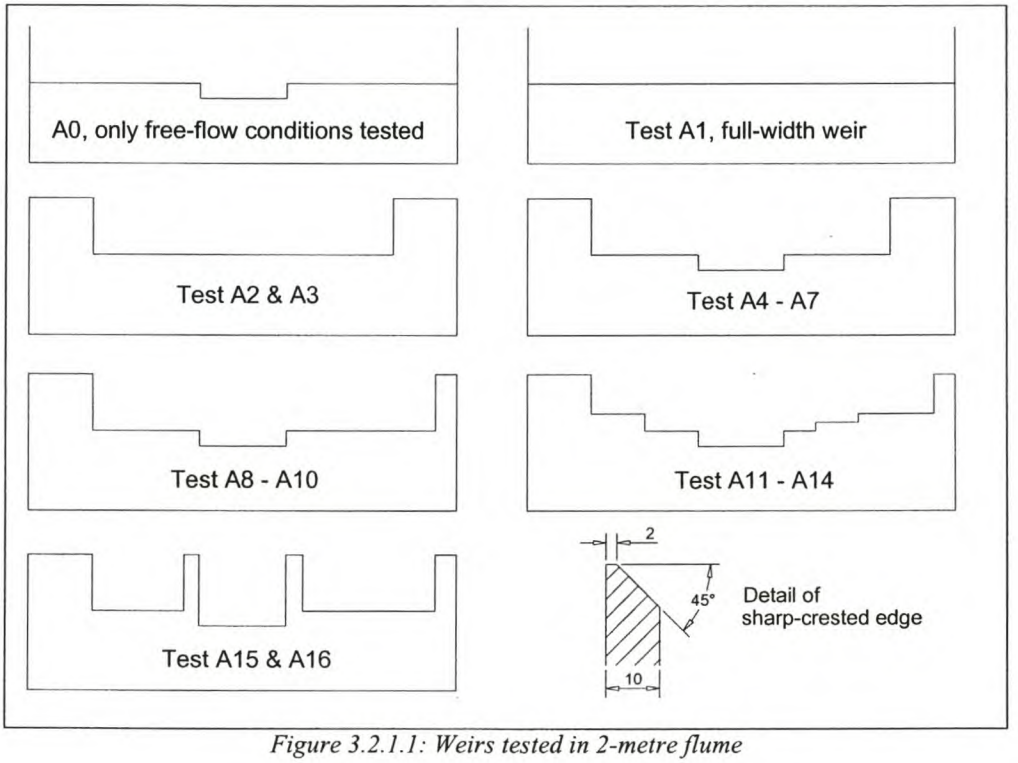

Figure 3.2.1.1: Weirs tested in 2-metre flume

As can be seen from Figure 3.2.1.1, this study was mainly concerned with contracted weirs since most of the prototypes in South Africa are contracted as well. Weir A0 was similar to the ones studied during the WRC project (Section 3.1.1). In order to aerate the nappe effectively during tests A0 and A1, splitters were installed on top of the weirs. These splitters were bent at an angle so that the nappe was split. This in turn allowed air to be fed into the area underneath the nappe. The splitters did not affect the upstream water level in any way. The contracted weirs did not need any extra measures for aeration purposes as air could enter underneath the nappe at the end contractions.

The weirs of tests A15 and A16 had columns between the different notches. Many weirs in South Africa have these columns for extra aeration purposes (see also Figure 1.2). It was therefore decided that their effect on discharge measurement should be analysed as well. Both

the horizontal and vertical edges of all the models were manufactured as indicated in the detail sketch in Figure 3.2.1.1.

The exact dimensions of each individual test weir (together with a sketch) are included on the data sheets in Appendix II.

The complete model set-up in the 2-metre flume is shown in Figure 3.2.1.2. Upstream water levels (points A, B and C) were measured with a point gauge. Due to extremely turbulent conditions downstream of the weir, the water levels at D, E, and F were measured in 100 mm stand pipes that were connected with 10 mm tubes to the respective points. The opening of each tube was aligned at a 90° angle to the direction of flow. The point gauge was used to measure water levels with an accuracy of up to a tenth of a millimetre.

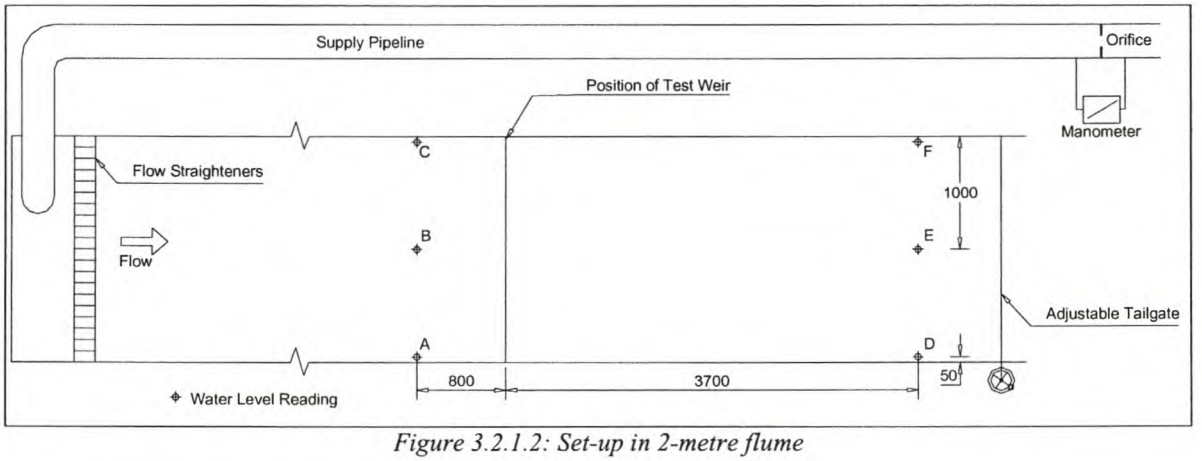

Figure 3.2.1.2: Set-up in 2-metre flume

3.2.2 Test Series B & C

These two series of experiments consisted only of submergence tests on single notch sharp-crested weirs (i.e. no compound weirs). Most experiments were performed on contracted weirs, but some tests on full-width weirs were also included.

Series B and *Series C* included experiments that were done in a 600-mm and a 1000-mm wide flume respectively. The pool depth and structure height was the same for all tests of these series (dimensions can be found on the data sheets in Appendix II).

For *Series B* the upstream and downstream water levels were measured 1420 mm and 3570 mm from the weir respectively. For *Series C* these distances were 2120 mm and 5100 mm respectively.

All the water levels were measured with stand pipes that were connected with tubes to the centres of the flumes. The opening of every tube was aligned at a 90° angle to the direction of flow. With this method the water levels could be recorded with an accuracy of up to half a millimetre. A manometer was used to measure the discharge delivered to the 600-mm flume. The 1000-mm flume had a magnetic flow meter connected to its supply line, but since it had not been fitted according to specifications it could not produce reliable values.

3.2.3 Test Procedure

During each submergence test a constant discharge was maintained which was ensured by a constant head tank in the laboratory. A manometer was connected across an orifice in the supply pipeline to measure the discharge in the system (see Figure 3.2.1.2). Before any experiments were launched, the discharge coefficients for different orifice plates had been determined by calibrating them against discharges measured with standard single notch weirs in the test flume. For this purpose, the Kindsvater & Carter formulas (ISO Standards, 1980) had been used to calculate the discharge at the weirs.

At the beginning of a submergence test the free-flow height upstream of the weir (h_o) was measured. The adjustable tailgate at the end of the flume was then raised which caused the downstream water level to rise, thereby submerging the weir. After changing the tailgate setting a period of ±7 minutes was required to allow the water levels to stabilise before they could be recorded. The tailgate was raised in stages (±10 settings) until all notches of the compound weir were at least 90 percent submerged. At the end of a test the tailgate was lowered and the free-flow height after the test was compared with the one measured at the beginning. Should these levels differ by more than a 1 mm the test was not used for any further analysis, since it implied that conditions had changed during the experiment.

Table 3.2.3.1 summarises all the data used in this research. It includes the associated code (e.g. A4-F), a brief description and the number of experiments for each set. The compound weirs shown in Figure 3.2.1.1 have been analysed under both modular and non-modular flow conditions. Free-flow data (modular conditions) is denoted with an additional 'F', i.e. data set no. A4-F contains the free-flow data for submergence test no. A4.

Code	Description	No. of tests
	MODULAR FLOW CONDITIONS (APPENDIX I):	
WRC-A	Data from previous research on compound sharp-crested weirs	60
WRC-B	More existing data, specifically on shallow and irregular pool depths	28
A0-F	New data, similar to WRC tests	19
A4-F	Free-flow data for submergence test no. A4	45
A8-F	Free-flow data for submergence test no. A8	6
A11-F	Free-flow data for submergence test no. A11	22
A15-F	Free-flow data for submergence test no. A15	17
	NON – MODULAR FLOW CONDITIONS (APPENDIX II):	
Series PW	Tests done by Wessels (existing data)	38
Series A	2-metre flume data	16
Series B	600 mm flume data	7
Series C	1000 mm flume data	5

Table 3.2.3.1: Summary of data used for this project

All the data on modular flow conditions can be found in Appendix I. For each data set in the Appendix, a sketch is given which indicates the type of weir tested. In addition, all the

dimensions and flow data is included. Two discharges are listed; the recorded value as well as the value calculated with the new method for compound weirs under modular flow conditions, which is described in Chapter 4.

Appendix II contains all the data on submergence tests. The individual data sheets contain sketches that describe the particular weir concerned. The observed data includes the free-flow upstream water head (h_o), the discharge measured with the manometer and the upstream and downstream water levels as recorded during a particular submergence test.

Observations that were made during the experiments are recorded in the next section.

3.3 OBSERVATIONS

One of the most significant findings that was made was the important role of end contractions under both modular and non-modular flow conditions. It is known that end contractions can ensure proper aeration of sharp-crested weirs. If a sharp-crested weir is not sufficiently aerated, the air underneath the nappe gets drawn out which causes the nappe to 'cling' to the weir. The lowering of the pressure underneath the nappe in turn leads to a drop in the upstream water head. Since the upstream water head is used to calculate the discharge, significant errors can be expected if it is affected due to poor aeration.

All the test weirs that had end contractions did not show any aeration problems. Fortunately, most prototypes in South Africa also have end contractions and it is not expected that they will experience any aeration problems under normal operating conditions. A very long notch can be aerated sufficiently by constructing a column half way. This will split the nappe in two and will provide additional aeration. The photograph below shows a test weir with two columns. One can clearly see that air can freely enter underneath the nappe at the two columns – and also at the outer end contractions.

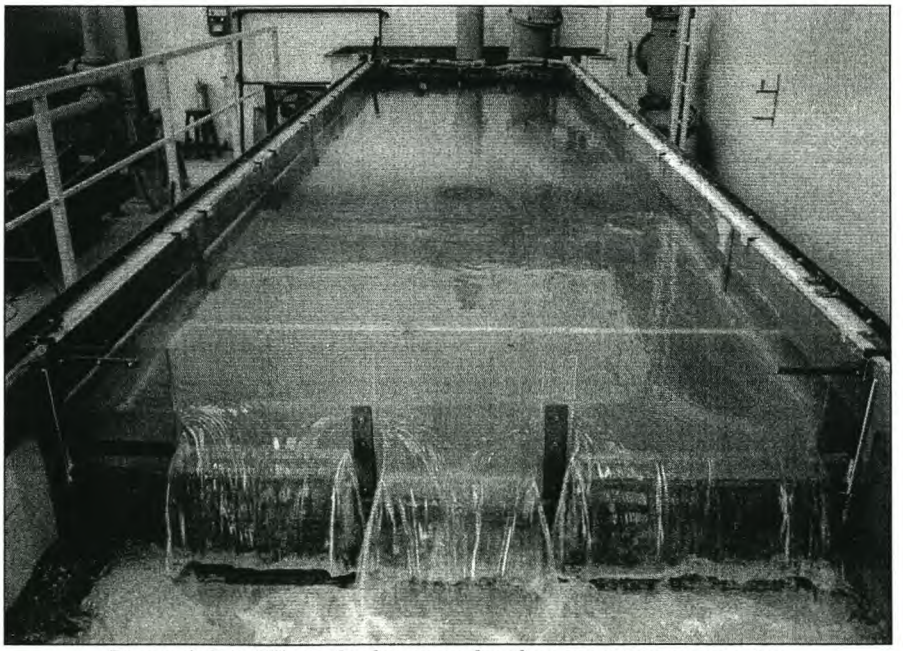

Figure 3.3.1: Effect of columns and end contractions on aeration

For submerged full-width weirs, both Wessels (1986) and Villemonte (1947) mention that the upstream water head drops slightly with low submergence ratios ($t/h_v < 0.20$) before it rises again. The full-width weirs that were tested during this study exhibited the same phenomenon. This is due to the fact that the nappe becomes de-aerated and subnormal pressures occur directly underneath the nappe which causes the water head to drop, i.e. the same discharge is represented by a lower head.

The contracted weirs did not show the same behaviour at low submergence ratios. In these cases the nappes were still receiving adequate aeration from the end contractions and the water heads remained constant. In fact, the water levels did not rise until a submergence ratio of about 0.10 was reached. This implies that no correction is needed for low submergence ratios ($t/h_v < 0.10$).

Furthermore, the contracted weirs were generating far more turbulence downstream than the full-width weirs. This is due to the fact that the streamlines are curved in front of the end contractions in order to flow past the weir, thereby producing 3–dimensional flow patterns (horizontal eddies) downstream of the weir. This is shown schematically in Figure 3.3.2. The greater the end contractions, the larger the downstream eddies become. This suggests that higher energy losses are generated at submerged contracted weirs compared to single notch, full-width weirs, where no horizontal eddies occur.

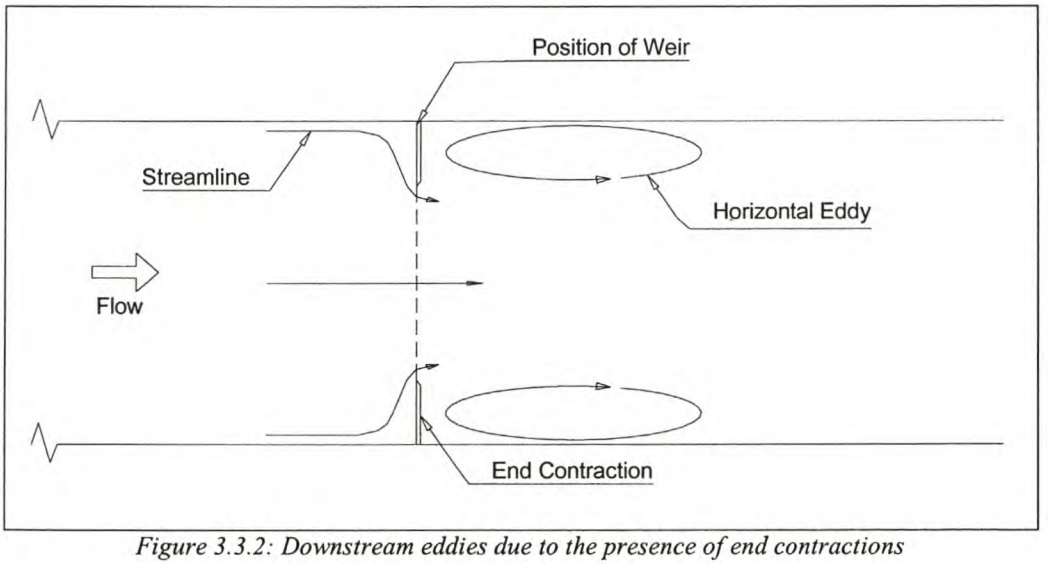

Figure 3.3.2: Downstream eddies due to the presence of end contractions

A number of researchers (Villemonte 1947, Wessels 1986) have indicated in their papers that the flow regime over a sharp-crested weir changes with increasing submergence. The different regimes were also identified during this study on contracted and compound weirs. Two profiles were identified:

- Regime *a*: A plunging nappe that occurs at low submergence ratios. This submerged nappe produces eddies above and below itself. The downstream water level is quite stable during this stage.
- Regime *b*: A surface nappe that occurs at high submergence ratios. Standing waves are produced, which create very turbulent conditions in the tailwater basin. A large eddy can be distinguished below the surface nappe.

Figure 3.3.3 illustrates both regimes. The transition from one regime to the other did not influence the upstream and downstream water levels significantly. In Appendix II (data on non-modular flow conditions) the type of regime is indicated on the data sheets.

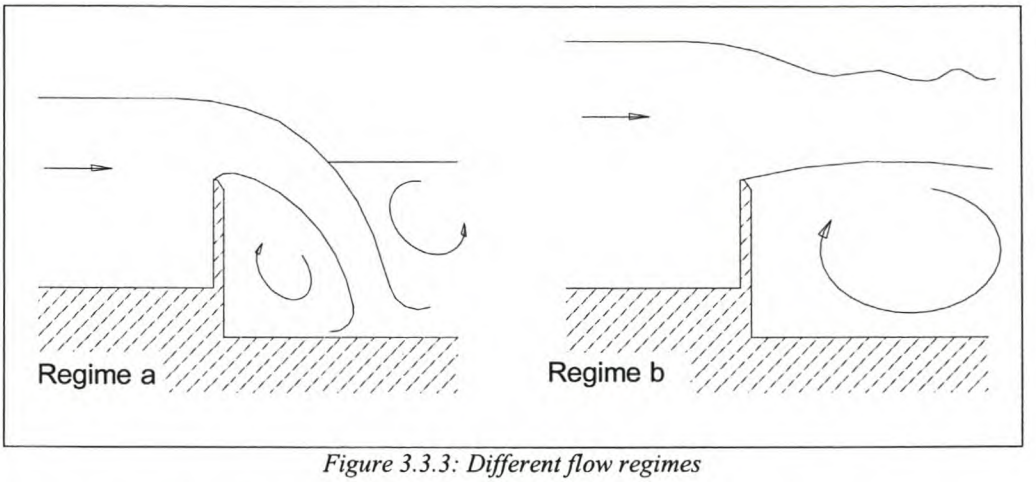

Figure 3.3.3: Different flow regimes

When full-width weirs were tested, regime *a* prevailed up to relatively high submergence ratios (up to $t/h_v = 0.60$). This was not the case for end-contracted weirs, where the transition from one regime to the next occurred at an average ratio of about 0.40.

It was sometimes difficult to identify a certain regime when a compound weir was tested. Since one notch might already be significantly submerged, the others might still be free-flowing, which meant that different regimes were observed at different notches. This led to highly unstable regimes and very turbulent downstream conditions. Figure 3.3.4 shows such a case: Regime *b* is already fully developed at the lower notch while the other two crests are not submerged yet.

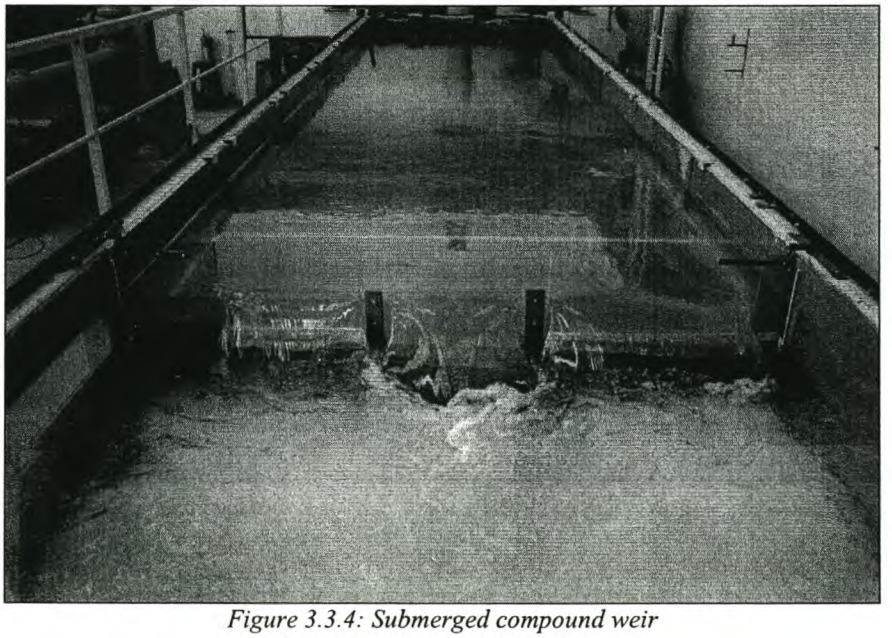

Figure 3.3.4: Submerged compound weir

4 MODULAR FLOW CONDITIONS

4.1 THEORY FOR SINGLE NOTCH WEIRS

Every discharge formula developed for compound weirs is based on the theory of a single notch weir. The formula for single notch weirs is well-known and can be derived from energy principles (Featherstone and Nalluri, 1982):

$$Q = C_d \frac{2}{3}\sqrt{2g}L\left(H_o^{3/2} - \left(\frac{v^2}{2g}\right)^{3/2}\right) \quad , \qquad \text{where} \qquad H_o = h_o + \frac{v^2}{2g}$$

The most detailed studies on compound sharp-crested weirs that have been undertaken in South Africa in the past were those undertaken by DWAF and the WRC. This research is described in more detail in the sections below.

The different methods have been evaluated with the data for modular flow conditions (Appendix I) and the errors have been calculated as follows:

$$Average\ Error = \frac{Q_o - Q_m}{Q_m} \times 100\%$$

Where: Q_o: discharge at weir (as calculated with a certain method)
Q_m: discharge given by manometer

The absolute error is defined as:

$$Average\ Error = \left|\frac{Q_o - Q_m}{Q_m} \times 100\%\right|$$

While the average error gives an indication of the value around which the data is spread, the absolute error gives a better indication of the actual magnitude of the errors. It has been assumed that the discharge given by the manometers is absolutely correct. This is not the case, but since the maximum errors made with the manometers is up to ±2 percent, the assumption is reasonable.

4.2 WRC FORMULA

The research that was sponsored by the WRC (Rossouw et al., 1995) resulted in a formula that is applicable to symmetrical compound weirs with three notches as shown in Figure 4.2.1. It was not known whether or not the WRC formula is also able to deal with weirs with more than two crest elevations, additional notches and more end contractions – which is the case at most gauging stations in South Africa. To be able to calculate the discharge with weirs consisting of more than three notches the formula had to be adapted slightly. These adaptations are explained below.

For the weirs with only three notches the original formula is used (see also Figure 4.2.1):

$$Q = C_d \frac{2}{3}\sqrt{2g}\left(L_1 H_1^{3/2} + L_2 (H_1 - T)^{3/2}\right)$$

Where:

$$C_d = 0.607 + 0.0419\frac{H_e}{P_e}$$

With:

$$H_e = \frac{H_1 L_1 + (H_1 - T)L_2}{L_1 + L_2} \qquad \text{and} \qquad P_e = \frac{P_1 L_1 + P_2 L_2}{L_1 + L_2}$$

$$= H_1 \quad for \quad h_1 < T \qquad\qquad = \frac{P_1 L_1 + (P_1 + h_1)L_2}{L_1 + L_2} \quad for \quad h_1 < T$$

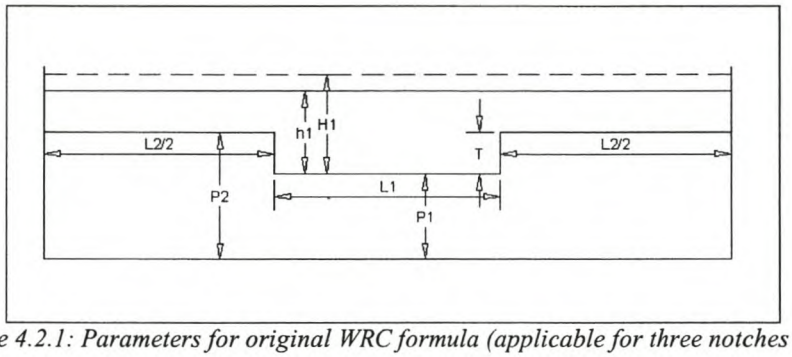

Figure 4.2.1: Parameters for original WRC formula (applicable for three notches only)

In order to calculate the flow over a weir with more than three notches the definitions of H_e and P_e were adapted as follows (only those notches overtopped by water are considered):

$$H_e = \frac{\sum H_i L_i}{\sum L_i} \qquad \text{and} \qquad P_e = \frac{\sum P_i L_i}{\sum L_i}$$

Where:
L_i : width of notch i (i = 1,2,3,....)
H_i : energy level upstream of notch i
P_i : pool depth upstream of notch i

The discharge formula for a weir with any number of notches has the general form:

$$Q = C_d \frac{2}{3}\sqrt{2g}\left(\sum L_i H_i^{3/2}\right) \qquad \text{with } C_d = 0.607 + 0.0419\frac{H_e}{P_e}$$

As the formula makes use of the energy level, H, the solution is obtained through an iterative process.

The WRC formula does not specifically deal with the effect of end contractions. From the additional model tests on contracted weirs it has been proven that end contractions *do* affect the flow over weirs significantly. Generally, an end contraction causes the water level upstream of

a weir to rise, while (for the same discharge) the water head will be lower for a full-width weir. In other words, for two weirs with identical dimensions (same pool depth, notch width) and the same upstream water head, a contracted weir will have a lower discharge.

Since the model weirs on which the WRC formula is based did not have outer end contractions, it can be expected that the method will overestimate the discharge. Figure 4.2.2 shows the results of an analysis of weir data that has been used to derive the WRC formula and some new data from similar tests (i.e. without outer end contractions). It is obvious that for these cases the formula predicts the discharge accurately. Note that the data set of WRC-B represents tests with shallow and irregular pool depths which therefore contain larger errors.

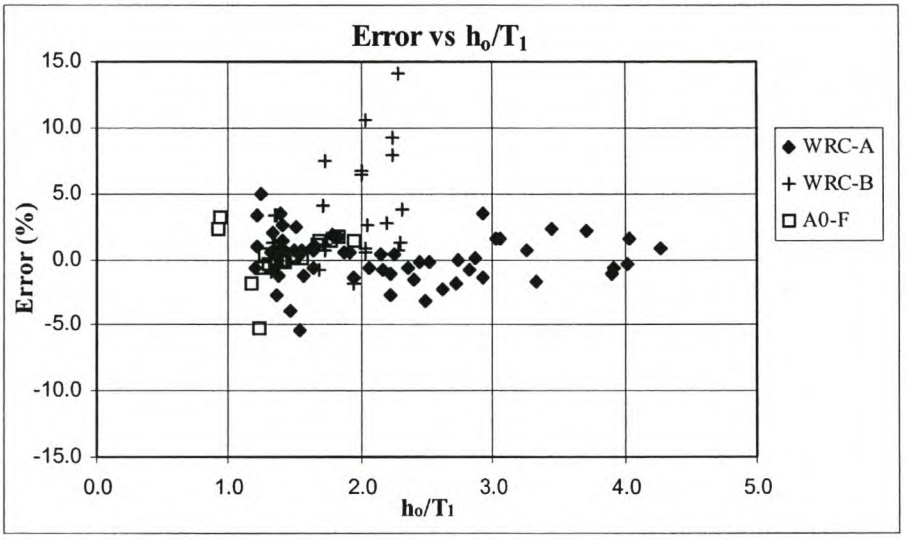

Figure 4.2.2: The WRC formula for weirs without outer end contractions

Figure 4.2.3 shows the errors that are made when weirs with outer end contractions are used to measure the discharge. As can be seen, the WRC formula overestimates the discharge, with the errors increasing with increasing flow rates.

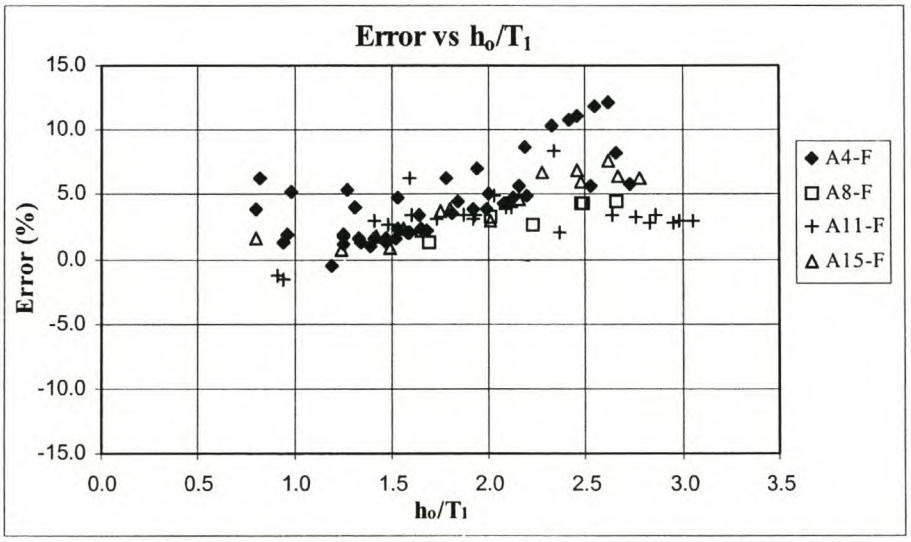

Figure 4.2.3: Errors made when using weirs with outer end contractions

It is clear that the WRC formula cannot accommodate the effect of end contractions. One further negative aspect is that with this method the discharge is calculated by considering the complete weir as one unit, i.e. using only one coefficient of discharge for the whole weir. It is desirable that each notch in a compound weir can be dealt with independently. This will make it possible to analyse more complex gauging stations that consist of sharp-crested weirs in combination with Crump weirs or flumes. The DWAF method employs such an approach and is discussed next.

4.3 THE DWAF FORMULA

The Department of Water Affairs and Forestry (DWAF) has over the years developed its own formulas to deal with all cases of sharp-crested weirs (Delport, Le Roux 1990). Every notch in a compound weir is treated separately as follows (see also Figure 4.3.1):

$$Q = 1.777 L_e C_d (H + 0.001)^{3/2}$$

For a full-width notch $L_e = L$. If the notch is contracted on both sides, L_e is calculated as follows:

$$L_e = L - nh$$

$$n = 0.2 \quad for \quad \frac{H}{L} < 0.35$$

$$n = 0.174\left(\frac{L}{H}\right)^{0.517} - 0.1 \quad for \quad 0.35 \le \frac{H}{L} \le 2.00$$

$$n = 0.0216 \quad for \quad \frac{H}{L} > 2.00$$

If only one side of the notch is contracted, half of the above correction is applied:

$$L_e = L - \frac{1}{2} nh$$

C_d is the correction factor for the pool depth upstream of each notch:

$$C_d = 1 + 0.11\left(\frac{H}{H+P}\right)^{1.24} \quad for \quad \frac{H}{P} \le 3.4$$

$$C_d = 1.145\left(\frac{P}{P+H}\right)^{0.04} \quad for \quad 3.4 < \frac{H}{P} \le 200$$

$$C_d = 0.926 \quad for \quad \frac{H}{P} > 200$$

The above formulas have been developed over many years by numerous researchers and their origins are not well documented.

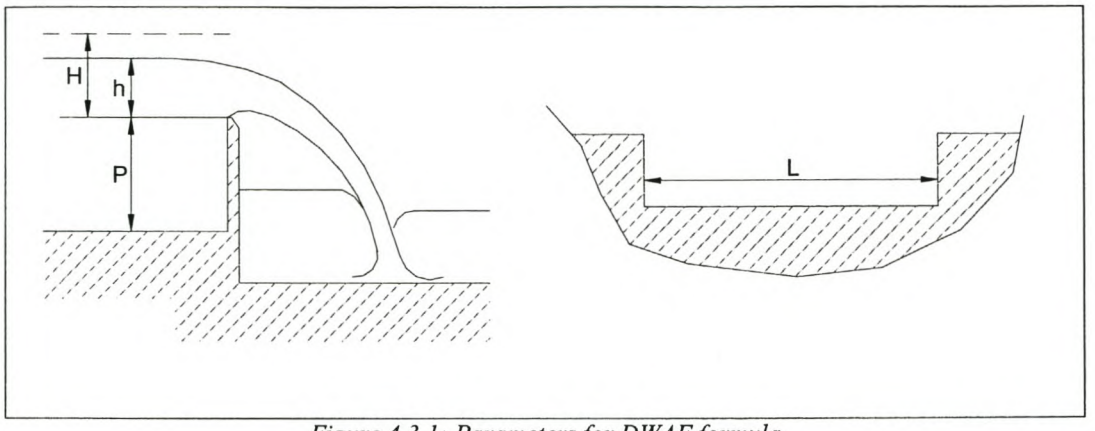

Figure 4.3.1: Parameters for DWAF formula

Figures 4.3.2 and 4.3.3 give an indication of how the errors are distributed when different weirs are analysed.

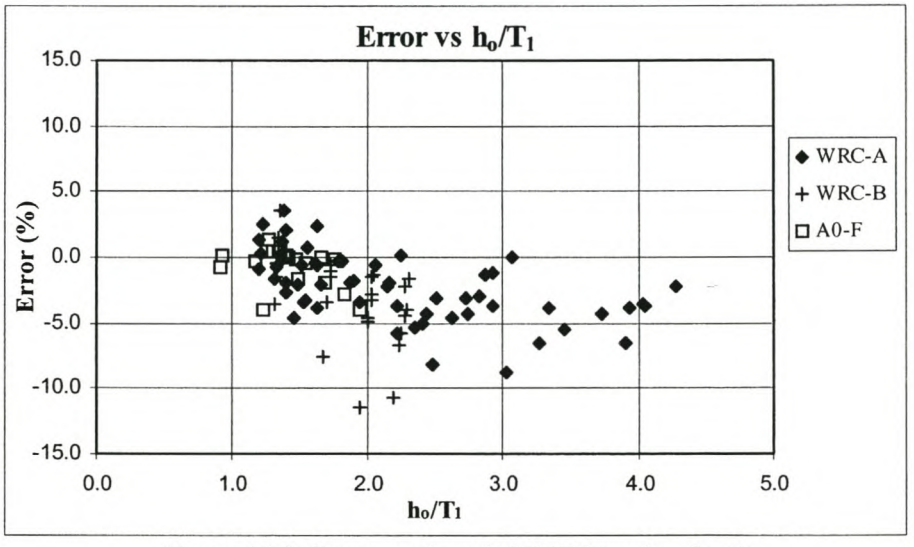

Figure 4.3.2: Errors made with DWAF formula – Part1

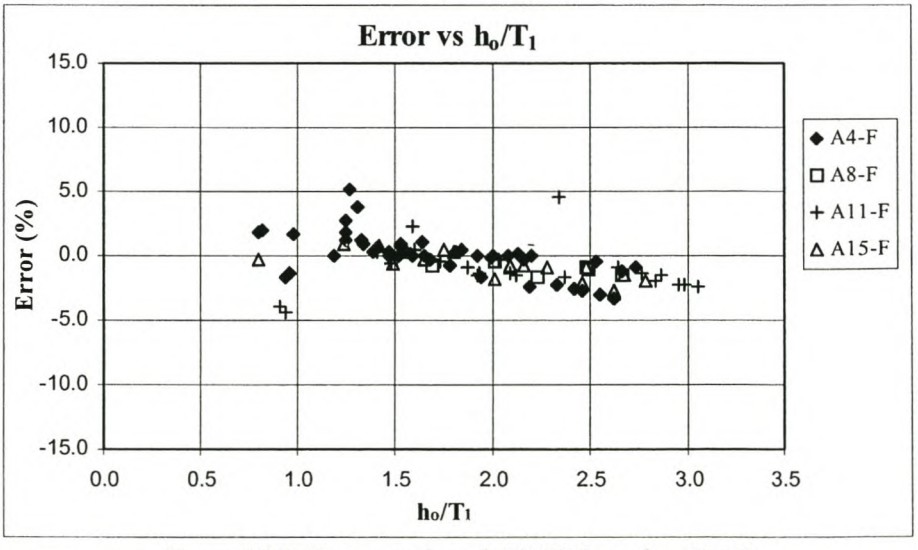

Figure 4.3.3: Errors made with DWAF formula – Part 2

Since the DWAF formula makes adjustments for end contractions the errors are much smaller than those made by the WRC formula. As mentioned earlier, the fact that the DWAF approach considers every notch in a compound weir separately makes it very attractive to use. The only problem is that the formulas listed above are not clearly related to any internationally accepted standards. In the next section a method is derived that uses the IMFT equation as a basis. The IMFT equation is well-known and appears in the ISO Standards (1980).

4.4 IMFT EQUATION FOR COMPOUND WEIRS

The original IMFT equation (Institut de Mécanique des Fluides de Toulouse) is applicable to full-width single notch weirs (ISO Standards, 1980):

$$Q = C_d \frac{2}{3}\sqrt{2g}LH^{3/2}$$

$$C_d = 0.627 + 0.018\frac{H}{P}$$

This formula makes use of the total energy head upstream of the weir (H) and not the upstream water level (h). The formulas for many other flow gauging structures (e.g. flumes, Crump weirs) are also based on the total energy head. Since these structures are sometimes combined with sharp-crested weirs, it is desirable to use the IMFT equation so that the total energy head can be used throughout. It is also believed that by using a formula incorporating the total energy head, one remains closer to the basic form of the originally derived equation for single notch weirs (see Section 4.1).

The problem with the IMFT equation is the fact that it cannot be used for weirs with end contractions. It is furthermore important to check the accuracy of the IMFT equation for higher values of H/P (i.e. high discharges / shallow pool depths). In the next two sections the effects of end contractions and shallow pool depths are discussed in more detail.

4.4.1 End Contractions

From the errors made by the WRC formula (see Section 4.2), it is clear that end contractions have a significant influence on discharge measurement. Their effect therefore has to be taken into account in the new method recommended for compound weirs.

In their classical paper Kindsvater & Carter (1957) have presented a set of equations to determine the flow over full-width and partially end-contracted single notch weirs. It is generally accepted that these formulas are very accurate (they have also been used during this project to calibrate the coefficients of discharge for different orifice plates). Unfortunately these equations are functions of the upstream water level, h, and not the total head, H.

The DWAF formula deals with end contractions by making use of an effective notch length:

$L_e = L - nh$.

Francis (1883) developed this method of adjusting the effective notch length. Roberson et al. (1988) mention that experiments have shown that the effective reduction in the notch length is approximately equal to $0.20h$ when $h/L < 0.33$. DWAF uses $n = 0.20$ when $H/L < 0.35$, which compares favourably. For $H/L > 0.35$, n becomes a function of H/L. It is expected that under

normal operating conditions the *H/L* ratio will remain below 0.35 in the prototypes, i.e. n=0.2 for most of the time.

For the new formulas recommended for compound weirs it has been decided that the IMFT equation will be used as a basis. In addition, DWAF's method for the correction of the effective notch length is incorporated into the new method.

To justify this, the following theoretical comparison is made with the Kindsvater & Carter method. A weir with P = 0.2 m and B = 2.0 m is used. Various contraction ratios (*L/B*) have been tested where the discharge is calculated with the Kindsvater & Carter formulas and with the adapted IMFT equation as proposed above. Figure 4.4.1.1 shows by how much the calculated discharge differs from the one determined by the Kindsvater & Carter equations. One can conclude that the methods correspond well and that the correction made by assuming an effective notch length is acceptable.

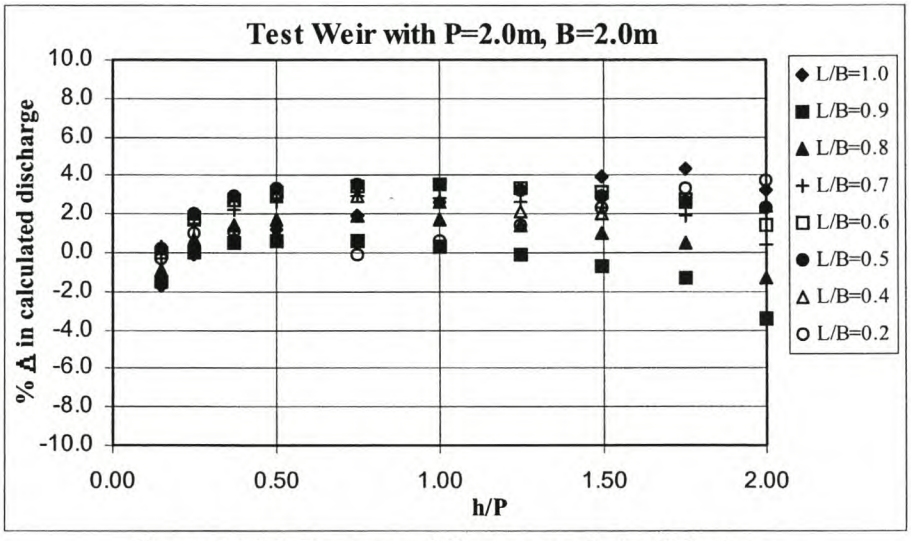

Figure 4.4.1.1: Percentage difference in calculated discharge

4.4.2 Shallow Pool Depths

According to the ISO Standards the IMFT formula is only valid up to *h/P* = 2.5. It is well-known (Swamee, 1988) that for very high values of *H/P* the coefficient of discharge (C_d) should decrease. For the new discharge formula it has been decided that DWAF's coefficient of discharge will be adopted for very high ratios of *H/P*:

Consider the constant terms in the discharge formulas:

$$C_d \frac{2}{3}\sqrt{2g}$$ (IMFT equation)

$$1.777 \times C_d = 1.777 \times 1.145\left(\frac{P}{P+H}\right)^{0.04}$$ (DWAF equation, with C_d for high *H/P* ratios)

Solve for C_d:

$$C_d \frac{2}{3}\sqrt{2g} = 1.777 \times 1.145 \left(\frac{P}{P+H}\right)^{0.04}$$

$$\therefore C_d = 0.689 \left(\frac{P}{P+H}\right)^{0.04}$$

In order to have a continuous function of C_d the following equations can be applied for the indicated ranges of *H/P*:

$$C_d = 0.627 + 0.018\frac{H}{P} \quad \text{for} \quad \frac{H}{P} \leq 1.867 \quad \text{(original IMFT equation)}$$

$$C_d = 0.689 \left(\frac{P}{P+H}\right)^{0.04} \quad \text{for} \quad 1.867 < \frac{H}{P} \leq 15 \quad \text{(adopted from DWAF)}$$

Figure 4.4.2.1 shows how the coefficient of discharge changes with increasing *H/P* ratios.

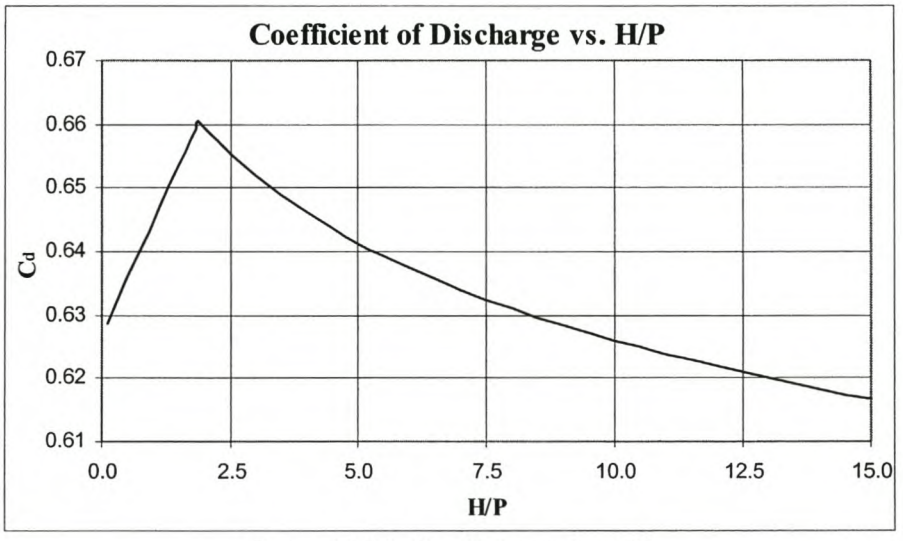

Figure 4.4.2.1: C_d with increasing H/P

From model tests it is known that the transition from one function to the other is not as abrupt as shown on Figure 4.4.2.1, but the errors made by assuming such a transition are negligible as will be shown in the next section.

The test data included experiments with ratios of *H/P* of up to 15. Although it might be possible that the equations are still valid for higher ratios of *H/P*, it is expected that flow conditions at the prototypes will become unstable at this stage and that flow measurement will therefore also become inaccurate.

4.4.3 Summary

The IMFT equation together with the modifications for end contractions and shallow pool depths has been found to give excellent results when it is evaluated with the test data. The complete method is summarised below (refer to Figure 4.4.3.1) and an example calculation is given in Appendix III:

$$Q = C_d \frac{2}{3}\sqrt{2g} L_e H^{3/2}$$

$$C_d = 0.627 + 0.018\frac{H}{P} \qquad \text{for} \quad \frac{H}{P} \le 1.867$$

$$C_d = 0.689\left(\frac{P}{P+H}\right)^{0.04} \qquad \text{for} \quad 1.867 < \frac{H}{P} \le 15$$

For a full-width notch $L_e = L$. For contractions on both sides of the notch L_e is calculated as follows:

$$L_e = L - nh$$

$$n = 0.2 \quad for \quad \frac{H}{L} < 0.35$$

$$n = 0.174\left(\frac{L}{H}\right)^{0.517} - 0.1 \quad for \quad 0.35 \le \frac{H}{L} \le 2.00$$

$$n = 0.0216 \quad for \quad \frac{H}{L} > 2.00$$

If only one side of the notch is contracted half of the above correction is applied:

$$L_e = L - \frac{1}{2}nh$$

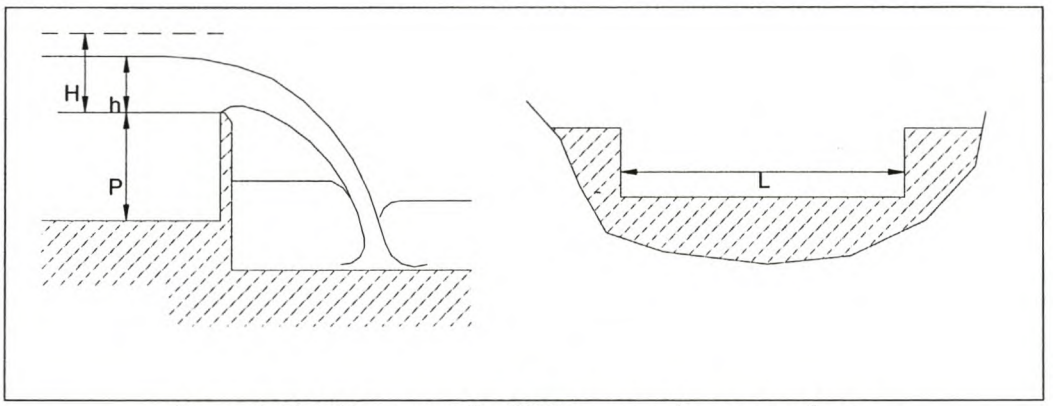

Figure 4.4.3.1: Parameters for IMFT equation for compound weirs

Figures 4.4.3.2 and 4.4.3.3 show the errors that are made when employing this new method. It can be seen that for most cases the errors are well within the ±5 percent margin. The maximum

errors (i.e. bigger than 5 percent) are all from tests where extremely shallow pool depths were involved.

It is also encouraging to see that the errors remain spread around the zero-percent line, i.e. there is no trend that shows that the errors are increasing during higher discharges. This is especially true for the tests indicated in Figure 4.4.3.3. These experiments, which include tests on weirs with up to six notches, end contractions and columns between different notches, closely resemble typical prototype weirs.

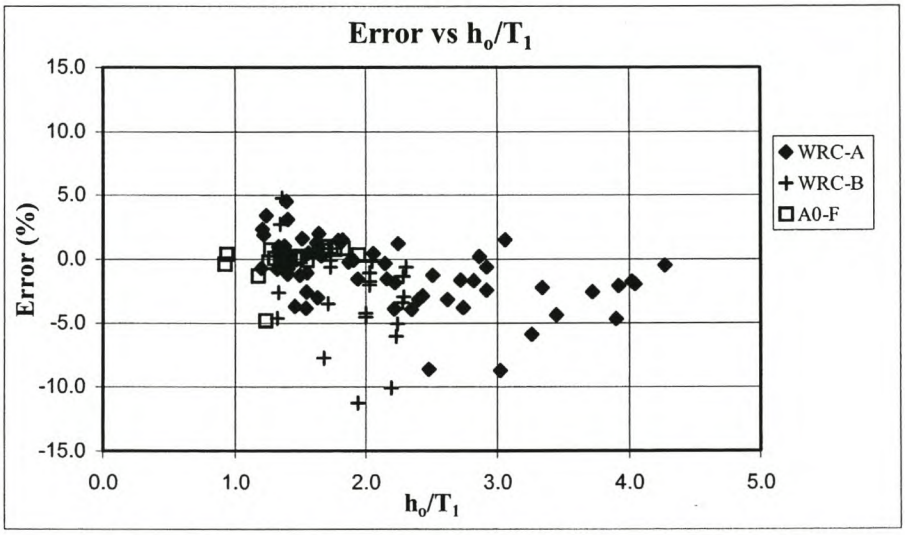

Figure 4.4.3.2: Errors made with adapted IMFT equation –Part1

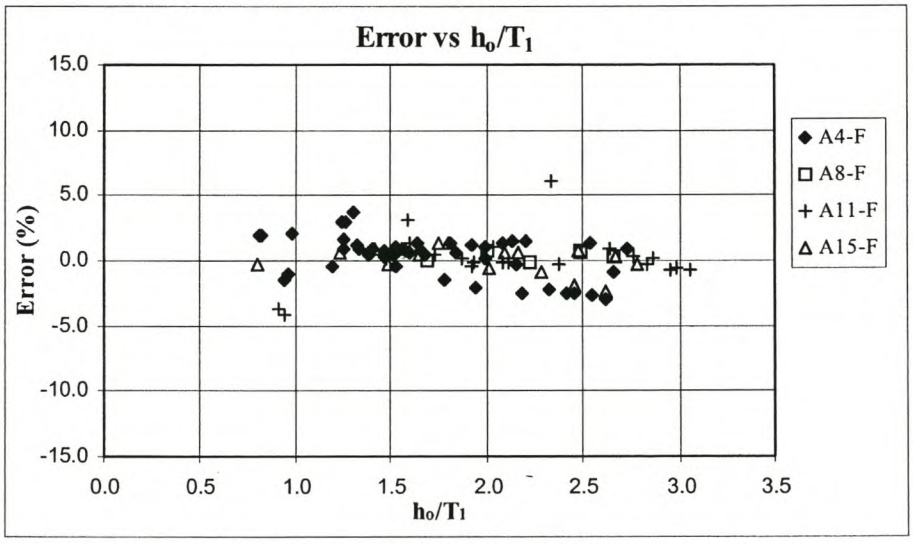

Figure 4.4.3.3: Errors made with adapted IMFT equation – Part2

Table 4.4.3.1 compares the accuracy of the different methods discussed in the previous sections. According to this summary the IMFT equation for compound weirs is the most accurate of all.

	WRC	**DWAF**	**IMFT**
Average Error (%):	2.36	-1.39	-0.59
Average Absolute Error (%):	2.92	2.01	1.70
Standard Deviation (%):	3.14	2.45	2.43
Minimum Error (%):	-5.34	-11.49	-11.27
Maximum Error (%):	14.06	5.22	6.06

Table 4.4.3.1: Summary of all methods; total number of tests analysed: 197

Since it produces the smallest errors, it has been decided that the IMFT formula will be used for the further analyses of non-modular flow conditions.

For the following investigations on non-modular flow conditions, the discharge as calculated by the adapted IMFT formula is assumed to be correct. This means that all errors are calculated relative to the free-flow discharge determined by the method as described in this section.

5 NON-MODULAR FLOW CONDITIONS

When the downstream water level starts to rise above the crest of a sharp-crested weir, the structure is said to become submerged and non-modular flow conditions occur. As the downstream water head (t) rises, the upstream head (h_v) rises as well, so that the discharge is a function of both t and h_v (Figure 5.1). Many methods (Villemonte 1947, Wessels 1986) have been developed to estimate the discharge under non-modular flow conditions. All of them make use of the so-called submergence ratio, which is defined as t/h_v ($0 \leq t/h_v < 1.00$).

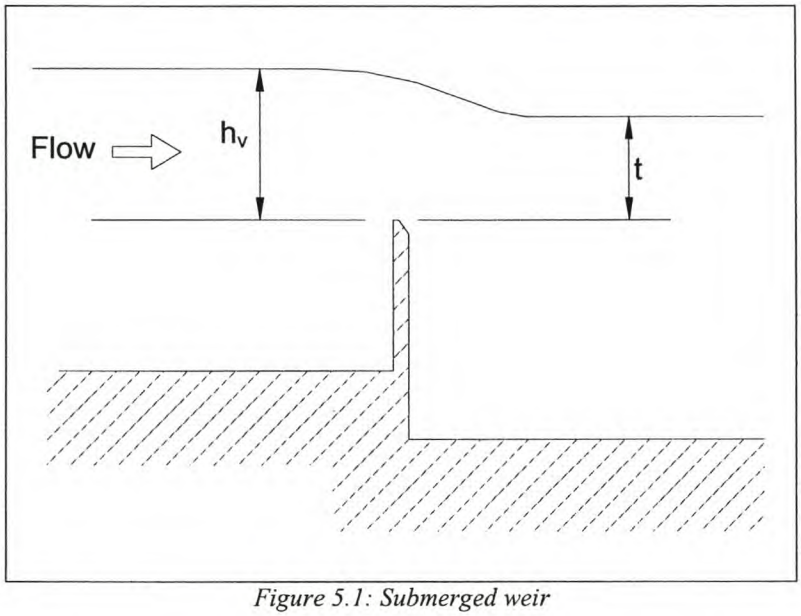

Figure 5.1: Submerged weir

Wessels (1986) gives a summary of the best known methods. They have all been developed for single notch weirs, and it is not known whether they are applicable to compound weirs, too.

There are two approaches to estimate the discharge during submerged conditions:

- By using h_v to obtain an initial estimate of the discharge and then multiplying this discharge with a correction factor (e.g. Villemonte's method).
- By first correcting h_v and then calculating the discharge with the adjusted water head (e.g. Wessels' method).

Almost all methods make use of the ratio t/h_v. During the course of this research project it has been found that the submergence process is indeed dominated by t/h_v, but that other factors also play an important role. It is due to this reason that various methods are sometimes not compatible, i.e. they produce completely different results for seemingly identical conditions.

In the following sections two methods are discussed that are well-known in South Africa. The first is the Villemonte formula which appears frequently in international publications and was developed by Villemonte in 1947. The second method was developed more recently by Wessels and is based on the momentum principle.

5.1 VILLEMONTE FORMULA

Villemonte's equation is based on the superposition principle, where the net flow over the weir is the difference between the free-flow discharge due to head h_v and the free-flow discharge due to head t (Villemonte, 1947). The formula reads as follows:

$$Q_s = Q_f \left[1 - \left(\frac{t}{h_v} \right)^m \right]^{0.385}$$

Where: Q_s : estimated flow under submerged conditions
Q_f : uncorrected discharge calculated with upstream water head, h_v, using free-flow formulas
h_v, t: upstream and downstream water head above crest of weir
m : coefficient with a value of 1.5 for rectangular sharp-crested weirs

Villemonte tested all types of sharp-crested weirs in a 3ft. (0.914 metre) wide flume. Amongst others, his experiments included full-width and partially contracted weirs.

The value of 0.385 in the above equation was derived from tests with relatively low discharges (maximum water head 0.504ft. = 0.154 metre) and low h/P ratios ($h/P \leq 1.00$). The additional test data of this study has proven that the Villemonte equation indeed provides a very good estimation if relatively low discharges are considered. With higher flow rates, typically $h/P >$ 1.00, the formula starts to underestimate the discharge drastically, i.e. the applied correction becomes too big. Villemonte himself included a graph in his classical paper that indicates the necessary correction that has to be applied *after* the discharge has been corrected with his formula. The graph is reproduced in Figure 5.1.1. One can clearly see that the higher the discharge, the greater the additional correction which is required. This trend is expected to continue if the discharge becomes even greater.

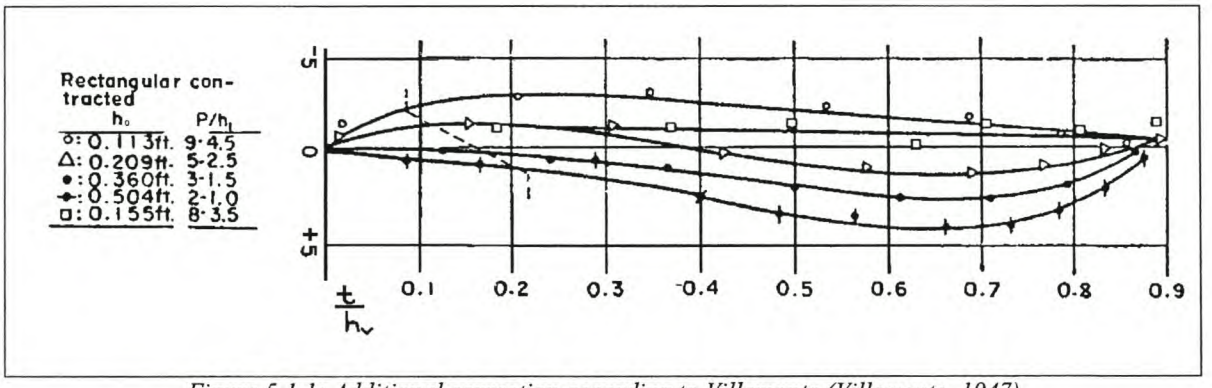

Figure 5.1.1: Additional correction according to Villemonte (Villemonte, 1947)

The data for all the *single notch* weirs of *Series A*, *B* and *C* has been analysed with the original Villemonte equation and the errors are shown in Figure 5.1.2. An example calculation can be found in Appendix III.

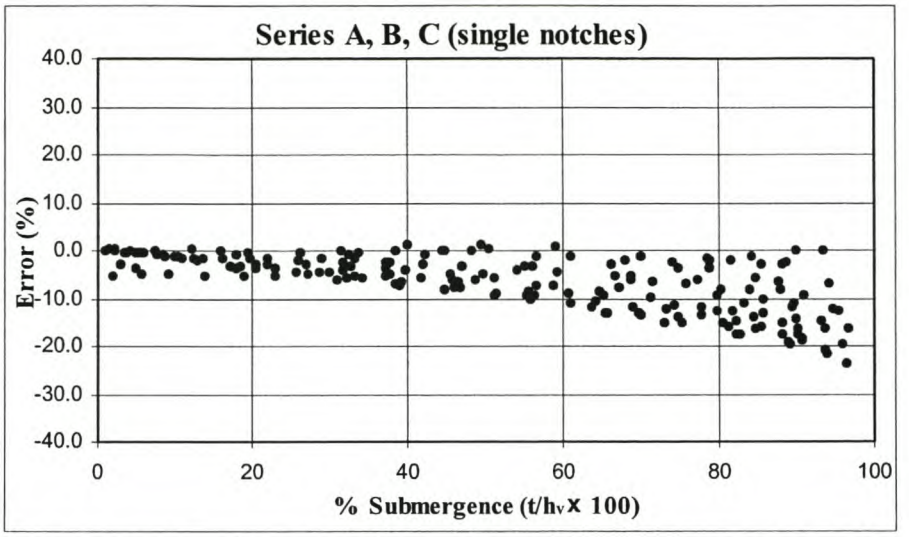

Figure 5.1.2: Errors made with the Villemonte equation (only single notch weirs analysed)

The errors have been calculated as follows:

$$Error = \frac{Q_s - Q_o}{Q_o} \times 100\%$$

Where: Q_s: estimated discharge (as calculated with a certain method, e.g. Villemonte's formula)

Q_o: free-flow discharge at the beginning of a test, calculated with the adapted IMFT equation (Chapter 4)

The larger errors seen in Figure 5.1.2 are from tests with higher discharges, while tests with very low discharges produce small errors. Some tests show errors already at low submergence ratios. These are experiments on full-width weirs that suffer from aeration problems during the initial stages of submergence. As already indicated in Section 3.3, the water level above a full-width weir drops first before it rises again with increasing submergence. The contracted weirs do not suffer from this problem and therefore do not produce any significant errors at low submergence ratios.

Finally, Villemonte made an interesting observation in his paper. He has found that sharp-crested 90° triangular notches perform the best with his formula. The errors for these weirs remain close to zero even at submergence ratios well above 90 percent.

5.2 WESSELS THEORY

Wessels used the momentum principle to derive a method to deal with submerged flow. The theory was developed by considering both free-flow and submerged conditions:

- For a certain Q_o (free-flow) the forces on the weir are analysed.
- For the *same* discharge the forces are analysed under submerged conditions.
- A relationship between the above cases is developed that can be used to determine the free-flow water head, h_o, given h_v and t.

Wessels conducted numerous tests on a 500 mm full-width weir to produce the following formulas (Wessels, 1986):

$$h_o = h_v \frac{\sqrt{1-(t/h_v)^2}}{\alpha}$$

Where:

$$\alpha = \frac{-b+\sqrt{b^2-4c}}{2}$$

$$b = -0.34074 - 0.30623\frac{t}{h_v}$$

$$c = 0.62879\left(\frac{t}{h_v}\right)^2 + 0.10159\frac{t}{h_v} - 0.6096$$

According to Wessels, the maximum errors should not exceed ±5% up to a submergence ratio of 90%. The accuracy can be increased even further by using a graph that Wessels has developed from his laboratory tests. The graph allows for additional effects such as pool depth (P) and structure height (Z) and is included in Appendix IV.

When this theory is used to analyse the data of *Series A*, *B* and *C*, the following errors are found (Figure 5.2.1). An example calculation using Wessels' method can be found in Appendix III.

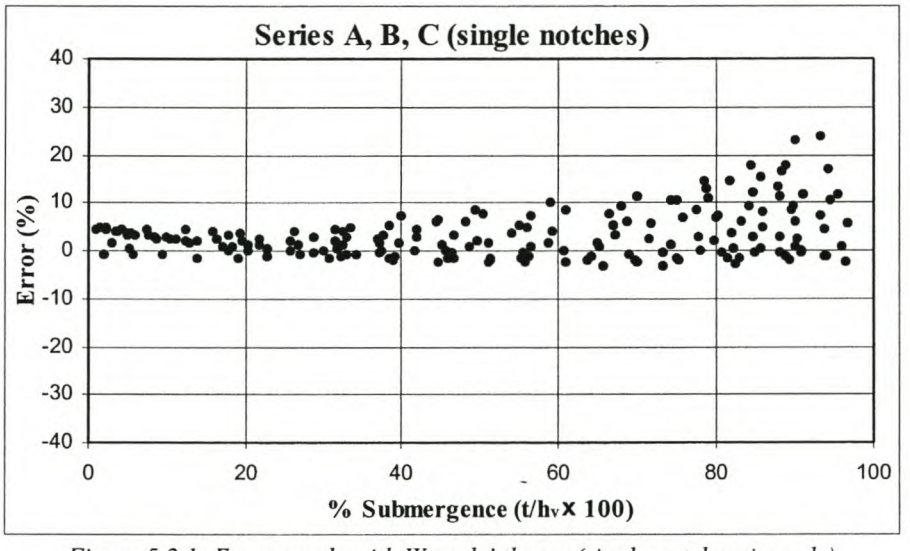

Figure 5.2.1: Errors made with Wessels' theory (single notch weirs only)

From the above graph it is clear that the theory does not work well for all cases. At low submergence ratios the method overestimates the discharge by ±5% when contracted weirs are analysed. This is due to the fact that the method has been developed using only full-width weirs. As described in Section 3.3, full-width weirs suffer from aeration problems at low submergence ratios and therefore perform differently compared to contracted weirs, which generally do not have any aeration problems at low degrees of submergence.

At high submergence ratios the method seems to overestimate the discharge under certain conditions. This happens typically when low flow rates occur. If higher discharges are flowing over the same weir, the method produces much smaller errors.

It can be stated that Villemonte used low discharge rates in his study, while Wessels used relatively higher rates of discharge. This is thought to be the main reason why the two methods are not compatible. If Figure 5.1.2 is compared with Figure 5.2.1 it can be seen that Villemonte's formula indicates a downward trend (corrects too much) while Wessels' method indicates an upward trend (corrects too little).

Generally speaking, the author believes that the momentum principle is not suited to analyse non-modular flow conditions. Consider the weir in figure 5.2.2.

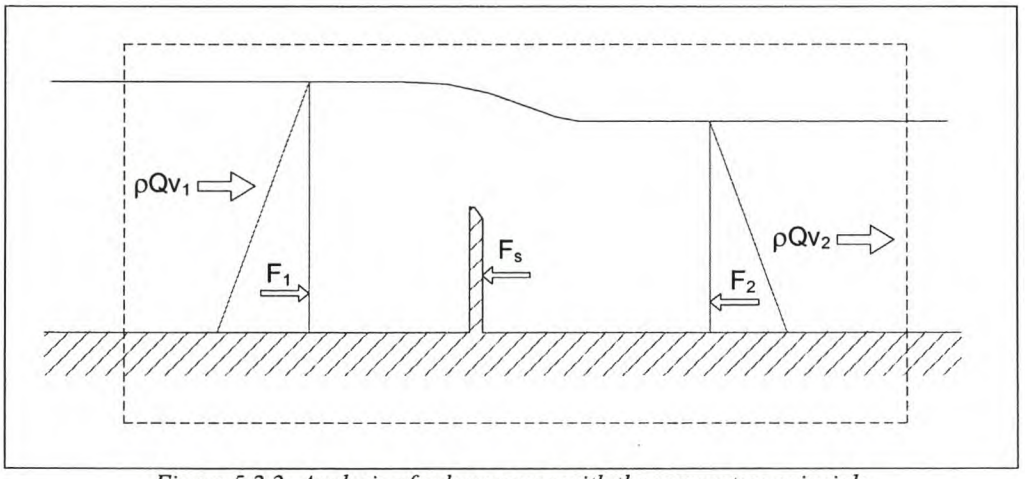

Figure 5.2.2: Analysis of submergence with the momentum principle

If the dashed box indicates the control volume, one can apply the momentum principle as follows:

$$F_1 - F_2 - F_s = \rho Q v_2 - \rho Q v_1$$

Where:

F_1:	upstream hydrostatic force
F_2:	downstream hydrostatic force
F_s:	net force exerted by the weir
ρ:	density of water
Q:	flow rate
v_1:	velocity upstream of the weir
v_2:	velocity downstream of the weir

The following problems arise when this approach is used:

- It is difficult to determine F_s. In addition, F_s becomes very small at high submergence ratios and therefore becomes insignificant.
- At higher submergence ratios ($S \geq 0.60$) the values of the hydrostatic forces (F_1, F_2) become more or less the same because the water levels approach each other. Since they are similar, it means that the difference in forces (F_1 -F_2) is small. Considering the fact that these hydrostatic forces have fairly large numerical values, it means that if a small error is made in

a water level recording it would lead to a significant increase/decrease in one of the forces. This in turn would cause a significant increase/decrease of the term (F_1 -F_2). Since this value is crucial for the estimation of the flow rate, the calculated discharge is likely to be greatly affected by an incorrect water level recording.

Even if it is possible to determine the value of F_s accurately, the determination of the discharge will be very sensitive to the accuracy of the water level recordings.

5.3 IMPORTANT PARAMETERS

It is clear from the previous sections that both the Villemonte and the Wessels methods only work well under certain conditions. Villemonte's formula works well for relatively low discharges which require a fairly large correction factor. Wessels' method in turn is applicable for relatively high discharges and requires a smaller correction compared to Villemonte's equation.

In this section a theoretical investigation is launched to determine the important parameters that affect submergence. The energy principle will be used as a basis and it will be endeavored to explain why the above methods are applicable only under certain conditions.

By assuming that the submergence of sharp-crested weirs is described properly by the energy principle, it can be said that the difference in upstream and downstream water heads can be related to an energy loss occurring at the submerged weir.

If a drowned weir is considered to be similar to a submerged hydraulic jump at a vertical sluice gate in a canal (Figure 5.3.1), where an energy loss occurs due to a sudden enlargement from the vena contracta to the downstream canal cross section, it would mean that the energy loss at a submerged weir is also due to an enlargement from the vena contracta at the weir to the downstream river cross section.

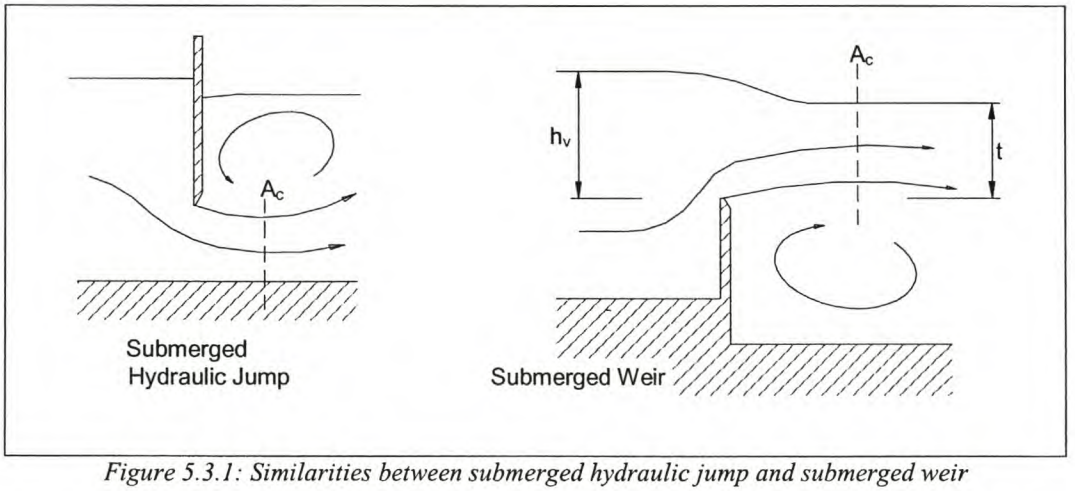

Figure 5.3.1: Similarities between submerged hydraulic jump and submerged weir

It is therefore necessary to find an expression for the vena contracta at submerged weirs so that an estimate of the energy loss can be made.

Analogous to the submerged hydraulic jump, the following formula is developed for the vena contracta at submerged weirs:

The flow area at the weir (A) should be smaller than h_vxL. As an approximation, the flow area is taken as:

$$A = \frac{1}{2}(h_v + t) \times L$$ With L being the width of the weir.

This is analogous to the area of the opening of the sluice gate.

A coefficient of discharge (C_d) should now be included which reflects the effects of a vena contracta, with its reduced flow area, and the true velocity, which is smaller than the theoretical velocity. This coefficient's value is typically 0.60 for sharp-crested sluice gates and the same value is assumed for this investigation. The final expression for the area of the vena contracta at submerged weirs is therefore as follows:

$$A_c = C_d \frac{1}{2}(h_v + t) \times L$$ With $C_d = 0.60$

It should be stated that it is possible to describe the vena contracta in different ways, but the simple formula above is deemed acceptable for the purpose of determining the critical parameters affecting submergence of sharp-crested weirs.

The vena contracta as it is defined above is especially relevant when the surface nappe occurs (regime *b*, see Section 3.3).

It is now possible to formulate an expression for the energy loss due to the sudden enlargement from the vena contracta to the downstream cross section (Featherstone and Nalluri, 1986):

$$h_L = \frac{(v_c - v_2)^2}{2g}$$

Where: h_L: energy loss
v_c: velocity at vena contracta
v_2: velocity at downstream section

The following theoretical calculations are now performed in order to determine the important parameters affecting submergence (see Figure 5.3.2):

- Assume that Q and t are known.
- For a particular weir, estimate h_v and calculate A_c:

  $$A_c = C_d \frac{1}{2}(h_v + t) \times L$$
- Now calculate v_c and then h_L:

  $$h_L = \frac{(v_c - v_2)^2}{2g} \qquad (1)$$

- Determine h_L also by calculating the total energy up- and downstream of the weir:
  $h_L = H_1 - H_2$ (2)
- Iterate h_v until (1) = (2).
- Once h_v is established the theoretical correction factor for the discharge can be calculated as follows:

$$Correction\ factor = \frac{Q_o}{Q_f} \approx \frac{h_o^{3/2}}{h_v^{3/2}}$$

- This theoretical correction factor can be compared to the correction factors proposed by Villemonte and Wessels.

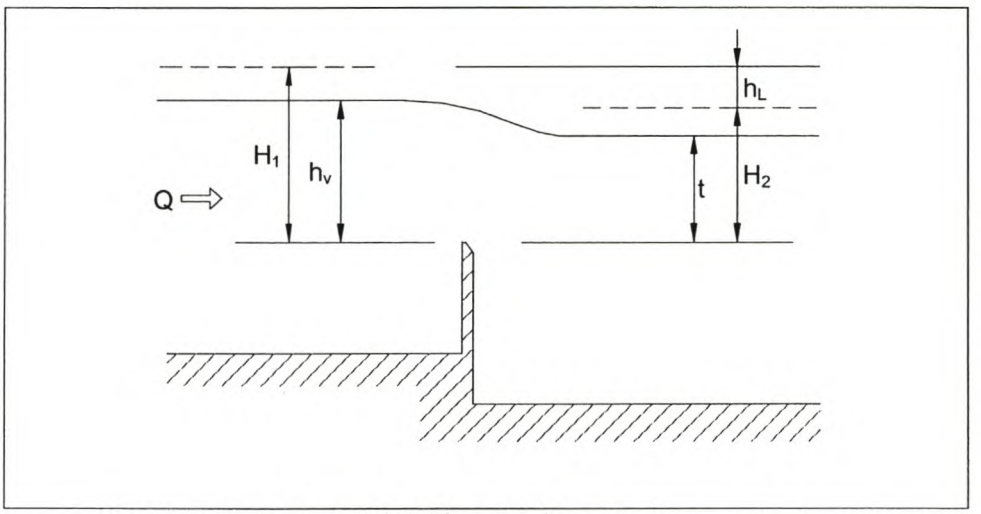

Figure 5.3.2: Theoretical investigation

The parameters that have been investigated are discussed in the next sections.

5.3.1 Pool Depth

A single notch weir with the following properties was used to analyse the effect of pool depth on submergence:

- $B = 1.00$m
- $L = 1.00$m (i.e. full-width)
- $Z = 1.00$m
- $P = 0.10 - 1.00$m
- $Q = 0.015$m^3/s

All of the above quantities, except for the pool depth, remained the same during each calculation. Figure 5.3.1.1 shows the results of the investigation. The graph includes the correction factors that were determined when using Villemonte's and Wessels' method.

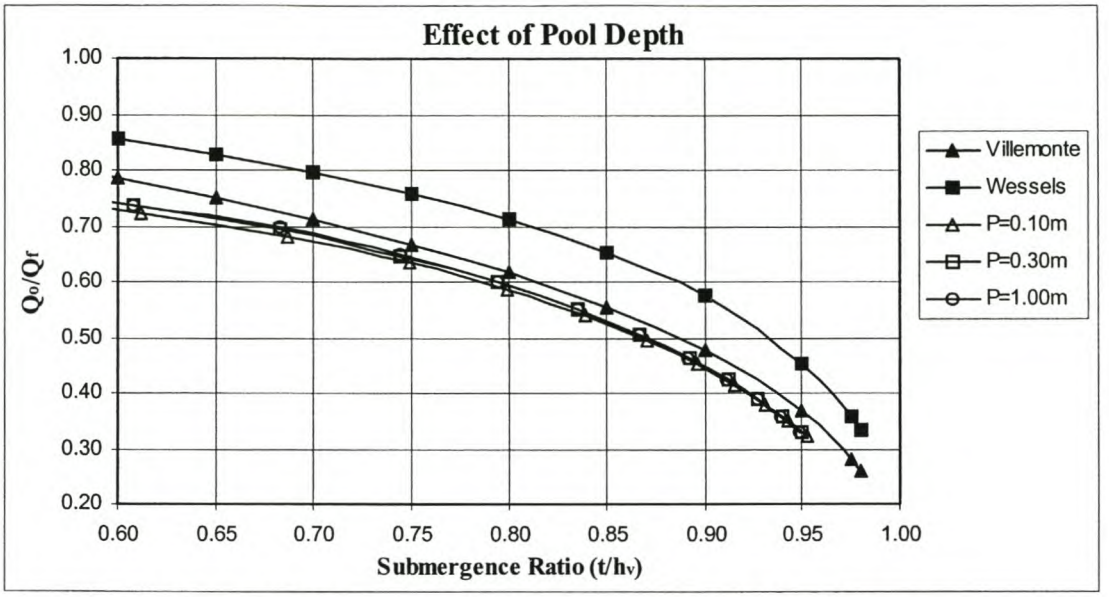

Figure 5.3.1.1: Effect of pool depth on correction factor for submergence

The graph only starts at $t/h_v = 0.60$ for clarity. It is at this submergence ratio where most existing methods start to deviate from each other. In addition, it should be remembered that the vena contracta is defined as if a surface nappe occurs, which happens only at higher submergence ratios.

Although the resulting curves don't fit between the extremes (indicated by the Villemonte and Wessels curves), it is evident that the theoretical curves have almost the same form as these. This is proof that the energy principle can be used to analyse submerged weirs, even when simplifying assumptions are made.

From Figure 5.3.1.1 it is clear that the pool depth does not play a significant role, as the curves do not differ much from each other. This is to be expected, since the energy loss (h_L) is a function of the velocities at the vena contracta and the downstream section (v_c, v_2) and does not depend strongly on upstream conditions.

5.3.2 Structure Height

The weir used to analyse the effect of structure height had the following properties:

- $B = 1.00$m
- $L = 1.00$m (i.e. full-width)
- $Z = 0.25$-1.00m
- $P = 0.25$m
- $Q = 0.060$m^3/s

Once again only one property, in this case the structure height (Z), was varied during the calculations. The results are shown in Figure 5.3.2.1. The theoretical curves are now very close to the actual ones.

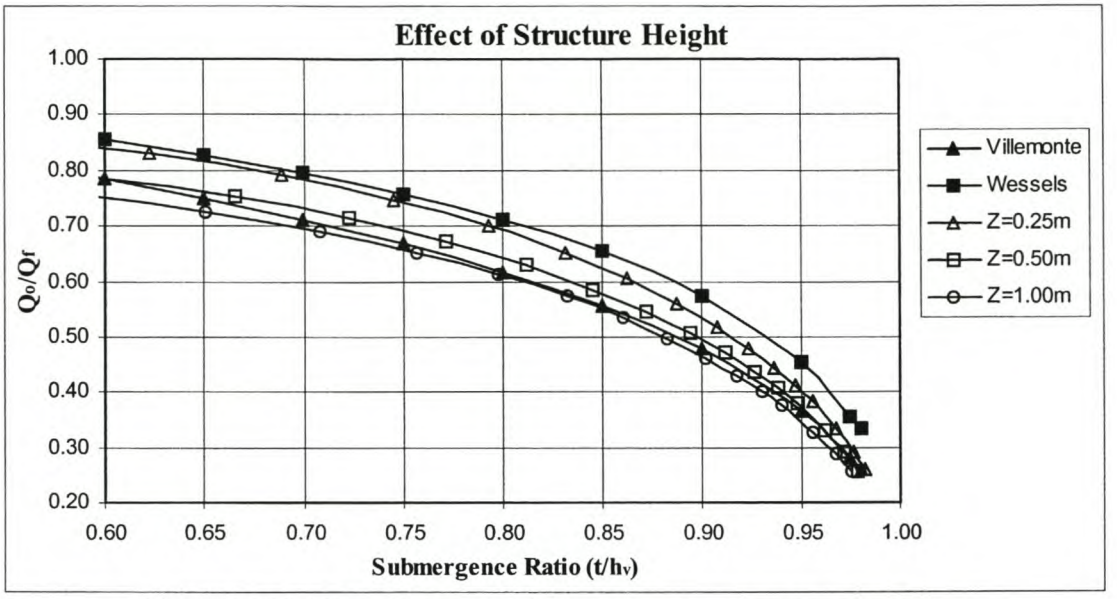

Figure 5.3.2.1: Effect of structure height on correction factor for submergence

From the figure it is clear that when the structure height is increased, the theoretical curves move from the Wessels curve to the Villemonte curve. This means that as the structure height increases, the downstream flow area increases, which leads to a smaller downstream velocity. This in turn causes a greater energy loss since the difference in velocities (v_c–v_2) becomes larger.

Therefore, according to this theoretical study, it can be said that if the relative energy losses increase, the likelihood that Villemonte's formula can be used increases. Conversely, if the relative energy losses decrease, Wessels' approach becomes more reliable.

It is necessary to mention that it is the *relative* energy loss that is important. A higher flow rate over a weir will obviously produce a higher energy loss, but the energy loss divided by the free-flow water head (denoted as h_L/h_o) is much smaller than that for a smaller discharge over the same weir. This was also found to be the case with the actual test data. In the text that follows the relative energy loss is frequently mentioned and is defined as h_L/h_o.

5.3.3 End Contractions

Finally, it was important to look at the effect of end contractions. The properties for this weir were:

- $B = 1.00$m
- $L = 1.00$-0.50m
- $Z = 0.25$m
- $P = 0.25$m
- $Q = 0.060$m^3/s

Only the notch length (L) was changed during the calculations. The final results are shown in Figure 5.3.3.1.

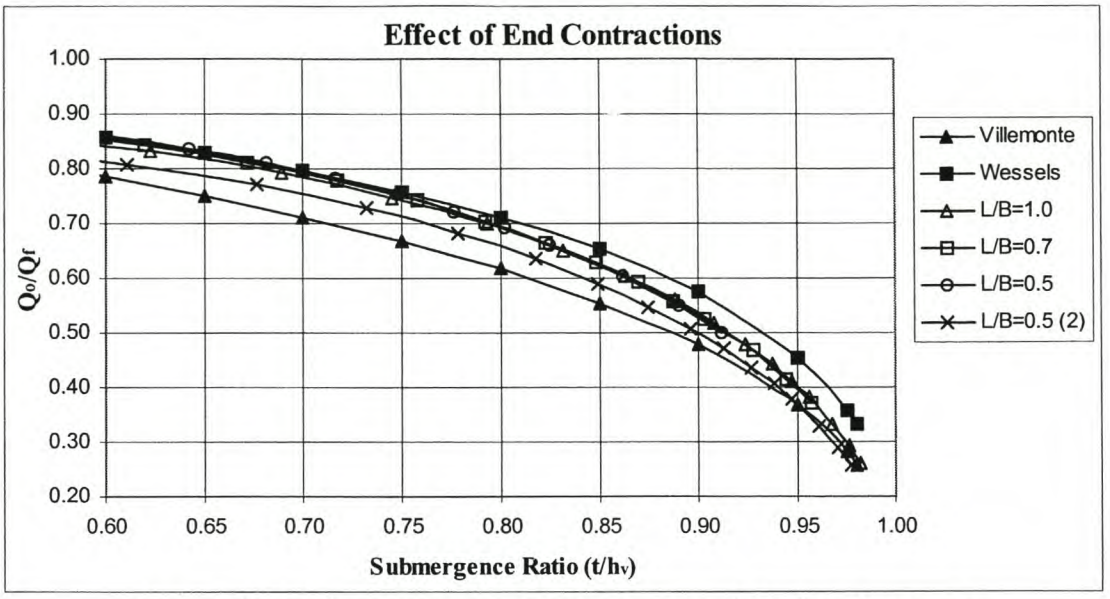

Figure 5.3.3.1: Effect of end contractions on correction factor for submergence

From the graph above it seems that the end contraction ratio (L/B) does not play a significant role. It has to be remembered though that if the same flow rate is used in each of the above cases, the upstream water head increases dramatically when the weir is more contracted. This might have affected the results and therefore one additional case has been included in the above graph, with $L/B = 0.5$ and an upstream water head equal to the one where $L/B = 1.00$ (indicated with crosses). It is evident that in this case the curve moves toward the Villemonte curve.

The author is of the opinion that end contractions do play an important role during submergence, though probably not as much as the structure height. From the observations during the model tests it was found that the end contractions produce very turbulent downstream conditions associated with large eddies. This suggests that the energy losses are much higher in this case than what they would be with full-width weirs.

In the next section two of the model tests will be analysed theoretically in the same fashion as above and then compared to the actual test data. It has to be established whether or not the above theory can actually predict (even roughly) the behaviour of submerged weirs.

5.3.4 Comparison with Actual Test Data

Tests A2 and B3 have been selected to compare the developed theory with actual test data. The exact weir configurations and flow rates of the chosen tests have been used and the theory has been applied in the same way as outlined in Section 5.3. Figure 5.3.4.1 summarises the results of the theoretical approach.

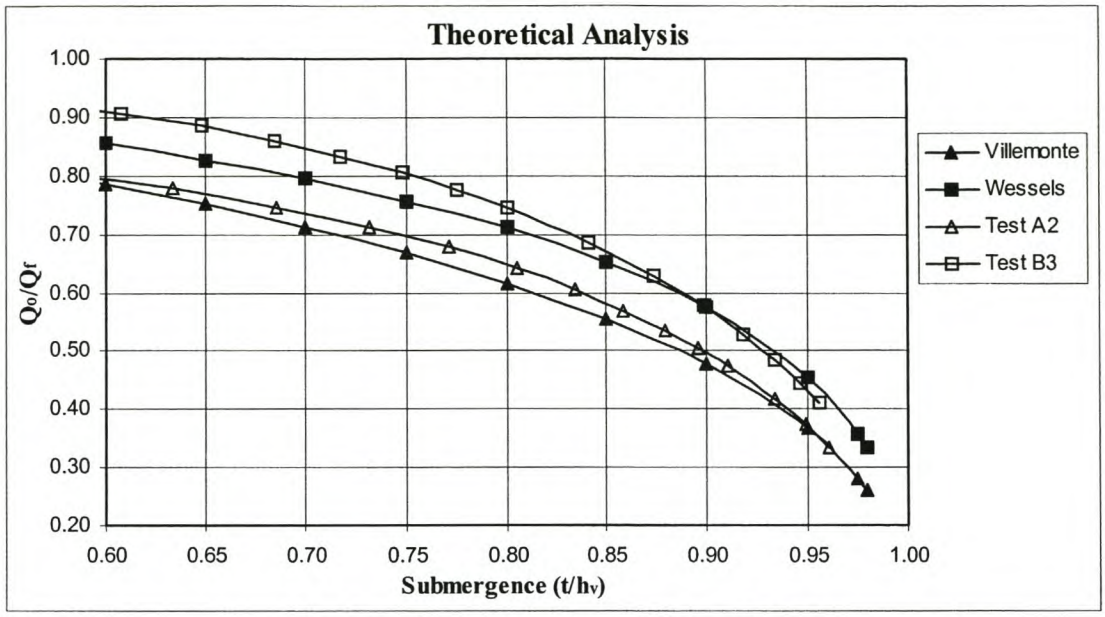

Figure 5.3.4.1: Results of theoretical investigation

According to the theoretical investigation, test A2 will require a large correction similar to the one predicted by Villemonte's formula (smaller Q_o/Q_f - value). This implies that relatively high energy losses are occurring at weir A2. Test B3 on the other hand will require a correction factor that is similar to the one predicted by Wessels.

Figure 5.3.4.2 shows the results when the actual test data is analysed. In this case the actual upstream water head (h_v) was used to calculate an estimate of the discharge. The necessary correction factor could then be calculated by dividing the free-flow by the estimated flow (Q_o/Q_f).

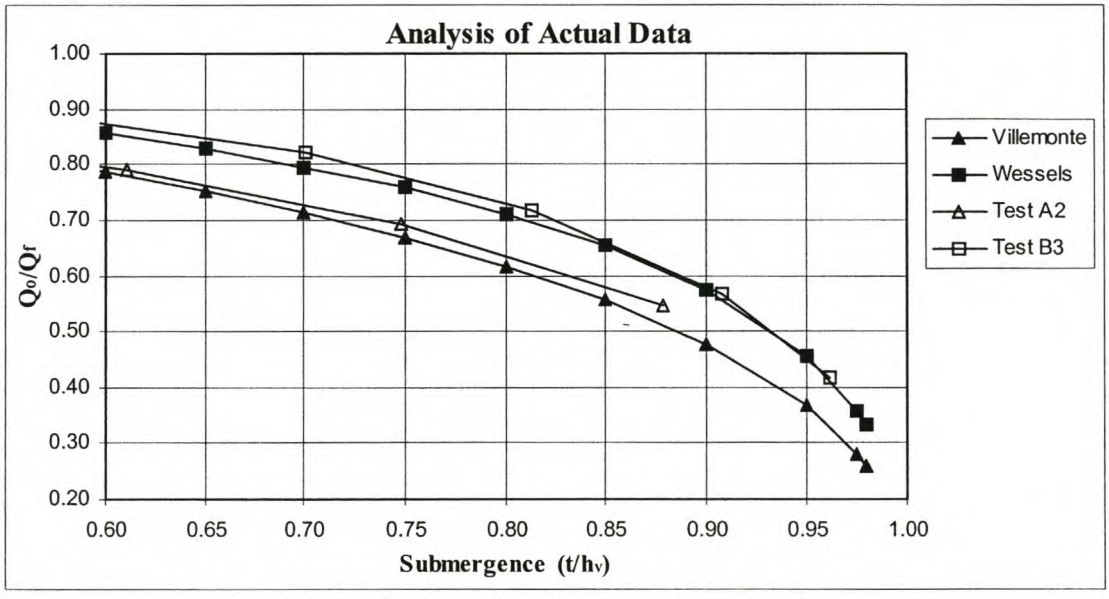

Figure 5.3.4.2: Results when actual data is analysed

The graph in Figure 5.3.4.2 compares favourably with that from the theoretical investigation, i.e. test A2 requires a correction similar to Villemonte's and test B3 requires one similar to Wessels' method.

It can now be stated with confidence that the energy principle forms a sound theoretical basis to study the submergence of sharp-crested weirs. According to this theory the structure height (Z) is the most important factor influencing the performance of drowned weirs. Since the energy loss is a function of the velocities at the vena contracta and at the downstream section, it is actually the flow areas at these sections that determine how much correction is needed. This can best be summarised as follows:

- If the flow area at the vena contracta is much smaller than the flow area at the downstream section, then relatively high energy losses occur at the weir and the Villemonte equation becomes applicable.
- If the flow area at the vena contracta is fairly similar to the downstream flow area, relatively small energy losses occur and Wessels' method is more reliable.

The next section deals with the analysis of compound weirs. A procedure will also be developed which will help decide what method (Villemonte or Wessels) is applicable given a certain problem.

5.4 COMPOUND WEIRS

Before compound weirs are analysed in any detail it is necessary to develop a parameter that will make it possible to compare different kinds of compound weirs (remembering that compound weirs can have any number of notches, columns between the notches etc.). The submergence ratio t/h_v, measured from the lowest crest in the structure, would only consider one notch of a weir. The new parameter should therefore include the fact that some notches in a compound weir might not yet be submerged.

The parameter described in Figure 5.4.1 is thought to be a suitable alternative for the ratio t/h_v:

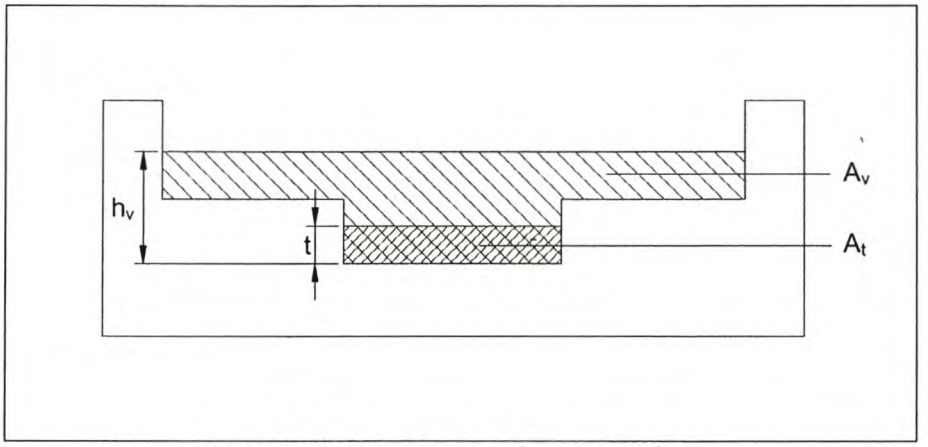

Figure 5.4.1: New parameter for compound weirs

The new parameter is defined as:

$$S' = \frac{A_t}{A_v}$$

Where:

S':		submergence ratio for compound weirs
A_v:		area *above* the crest and a function of h_v
A_t:		area above the crest of the weir and a function of t

This parameter can be thought of as a 2-dimensional extension of the original submergence ratio for single notch weirs. In fact, for single notch weirs $A_t/A_v = t/h_v$. Appendix III includes an example calculation on how A_t/A_v is determined. The parameter described here is only used compare the data from different weirs and is not used in any calculations for the determination of flow rates.

The following two sections illustrate the performance of the Villemonte and the Wessels methods if they are applied to compound weirs.

5.4.1 Villemonte's Formula for Compound Weirs

When the data on non-modular flow conditions was analysed it was found that the Villemonte formula is very easy to apply and works well for most cases. Figure 5.4.1.1 and 5.4.1.2 show the errors that are made when Villemonte's approach is employed.

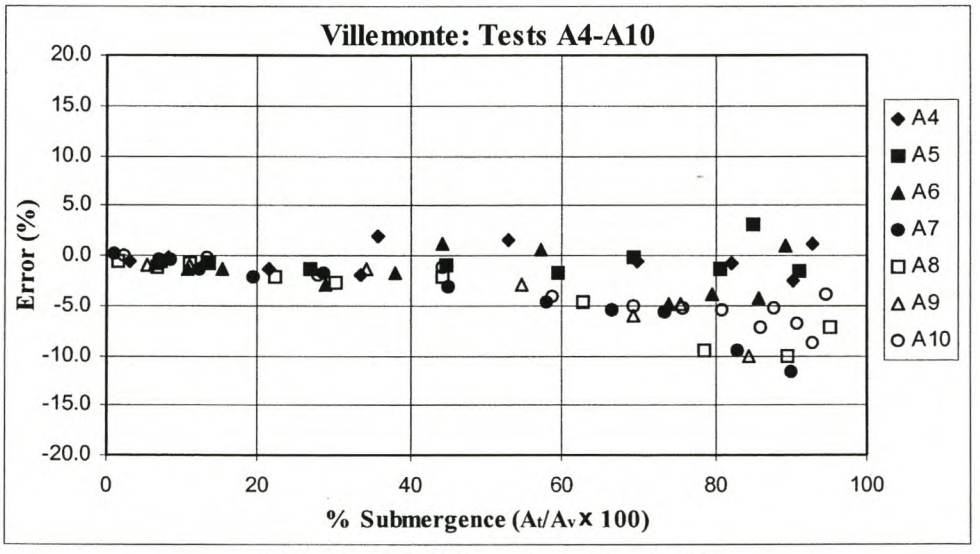

Figure 5.4.1.1: Villemonte results – Part 1

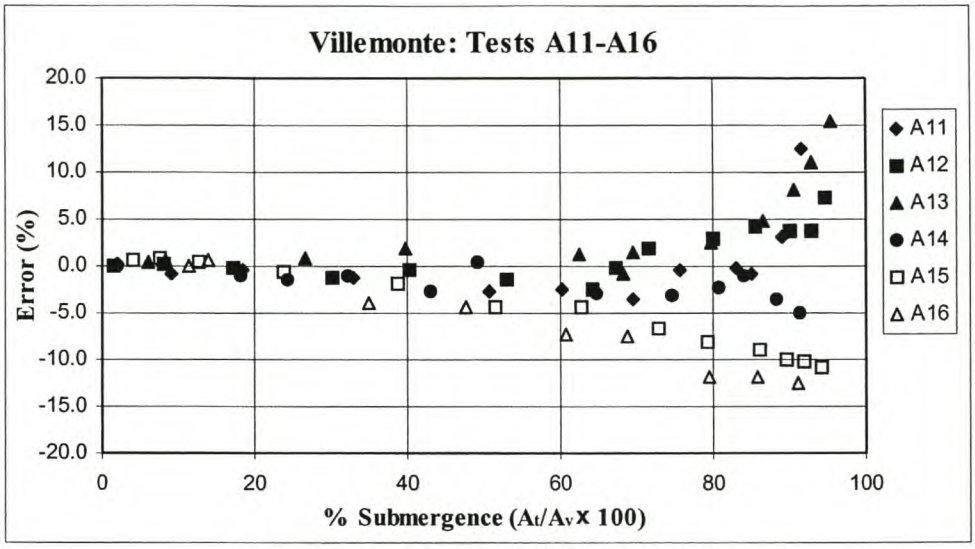

Figure 5.4.1.2: Villemonte results – Part 2

The errors have been plotted against the ratio A_t/A_v as described earlier. From the figures one can conclude that in most cases the errors remain below ±10%. Tests A11 to A13 are the exception to this rule and in these cases Villemonte's formula seems to drastically overestimate the discharge at high ratios of A_t/A_v. These three tests have been conducted with water flowing over only the lower notches of the compound weir concerned. This means that as the structure becomes submerged, the upstream water head rises, which causes the water to start overflowing over the higher crests. As soon as the water reaches the next crest, the errors increase dramatically.

From Section 5.3 it was evident that if the relative energy losses at a submerged weir are high, more correction is needed (smaller Q_o/Q_f – value). The author therefore believes that the increase in errors at high submergence ratios is due to the sudden increase in additional energy losses. It is unlikely that there are weirs in Southern Africa that already start to submerge when water is not even flowing over all the crests. The three tests mentioned above are hence mainly of academic interest.

It was to be expected that Villemonte's formula produces acceptable errors when compound weirs are analysed. Generally, this method is applicable when the relative energy losses are high. Due to end contractions and notches at different elevations the energy losses are likely to be high at compound weirs.

However, if a *very* large discharge is flowing over a compound weir, the author believes that even Villemonte's formula will not work properly anymore. Remembering that the energy loss at a drowned weir is a function of the velocities at the vena contracta and the downstream river section, it can be expected that these become very similar if the respective flow areas have similar size, which is the case during extreme floods (see Figure 5.4.1.3 as an illustration). If the velocities are similar, the relative energy loss becomes small and Villemonte's formula is not expected to perform well – it would probably start to underestimate the discharge as it applies a too great correction (too small Q_o/Q_f – value).

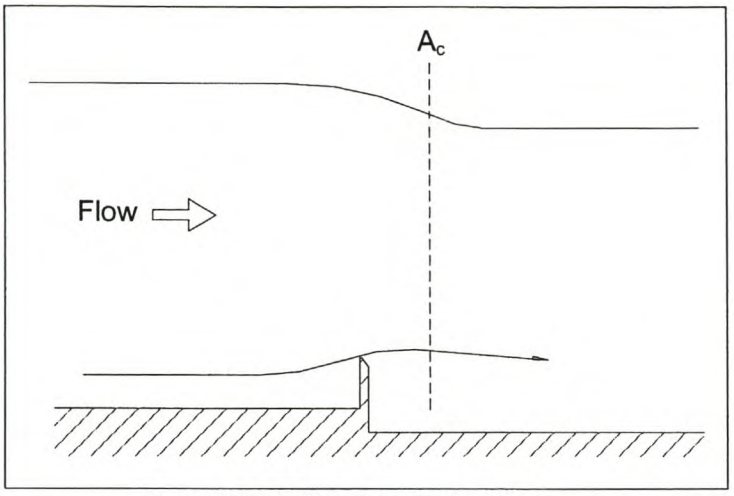

Figure 5.4.1.3: Very high discharge, $v_c \approx v_2$

Unfortunately it was not possible to test very high discharges over compound weirs in the Stellenbosch laboratory, as the test flume only had a limited depth. Although Wessels investigated high flow rates, his experiments only include single notch full-width weirs. The vena contracta for full-width weirs is different to the one of contracted weirs. For this reason the author did not use Wessels' data to draw conclusions on contracted and compound weirs.

5.4.2 Wessels' Method for Compound Weirs

Wessels' method is for the most part overestimating the discharge. This becomes apparent when Figure 5.4.2.1 and 5.4.2.2 are examined. The estimated discharge was calculated with the computer program *DT* which is used by DWAF.

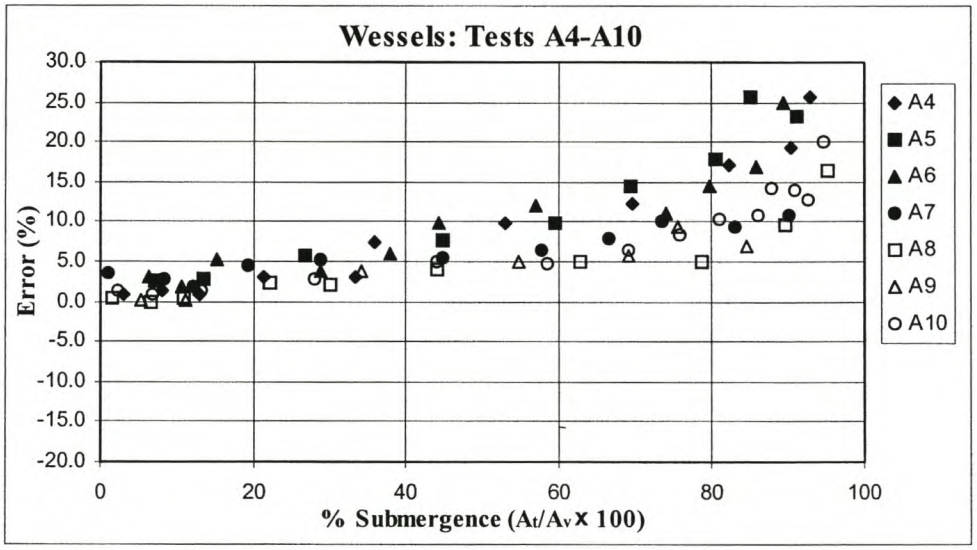

Figure 5.4.2.1: Wessels results – Part1

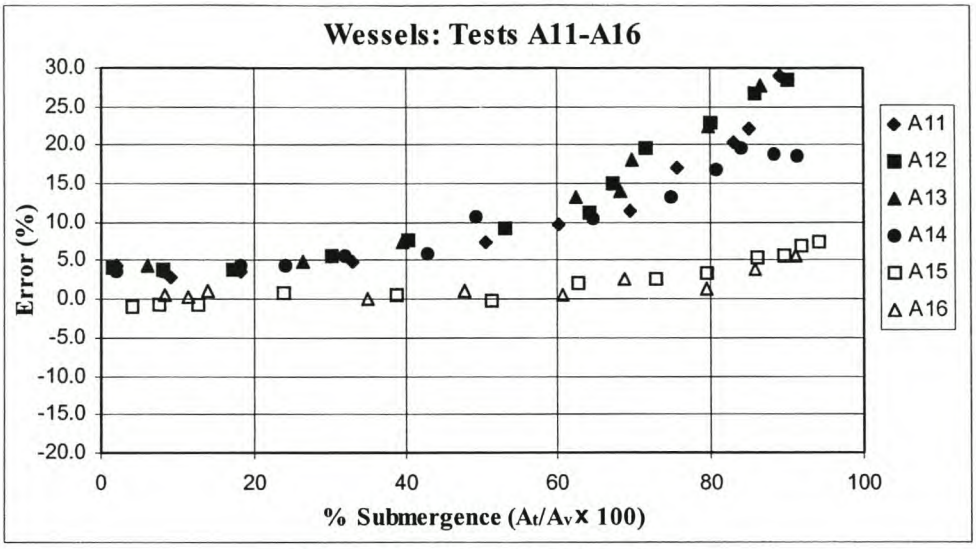

Figure 5.4.2.2: Wessels results – Part 2

Since this method is based on tests with relatively high discharges, which means that the relative energy losses are smaller, the resulting Q_o/Q_f – correction factors are too small. This is the reason why the discharges are overestimated. However, it is expected that when higher discharges are occurring Wessels' method should start to produce acceptable results. As mentioned previously, it was not possible to test very high flow rates in the Stellenbosch laboratory. Thus the range where Wessels' method would have become valid was not reached.

As described in Section 5.2 Wessels makes a correction to the upstream water head (h_v) and then uses this head to calculate the discharge. The author is of the opinion that this is physically not correct if applied to compound weirs and therefore this approach is not preferred. Consider Figure 5.4.2.3, where a compound weir is shown with only the lowest notch submerged. Since the outer crests are still free-flowing, their water heads remain the same, but the water head for the submerged notch has to be corrected. This new head is indicated on the figure and it is clear that there is now a discontinuity in the water level. When the discharge is calculated, additional assumptions will become necessary to calculate the energy level which is nevertheless the same over the whole weir. Villemonte's method on the other hand does not encounter this problem. In this case the discharge is estimated first and only then is a correction factor applied based on the degree of submergence.

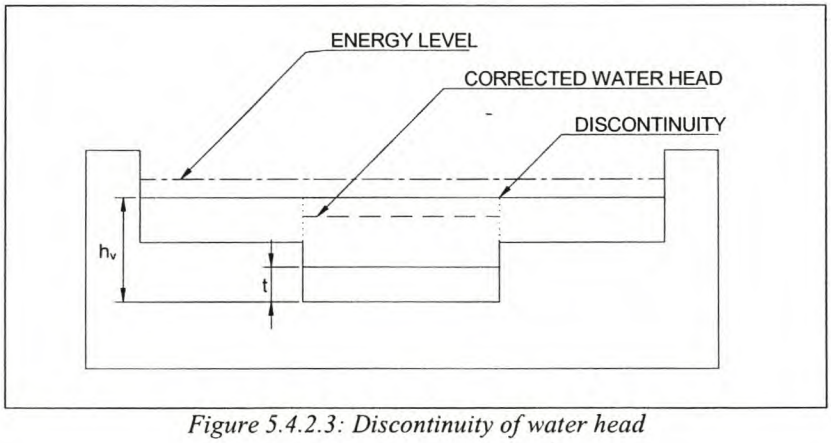

Figure 5.4.2.3: Discontinuity of water head

5.4.3 Summary

The results of the analysis prove that Villemonte's method is preferable to deal with non-modular flow conditions at compound weirs. It has to be stated again though that it was not possible to test extremely high discharges, when Villemonte's formula is not expected to be reliable anymore. Even the currently available data gives the impression that the tests with higher discharges tend to produce slightly larger errors. A parameter has to be identified that indicates when Villemonte's approach is still reliable and when it is advisable to switch over to other methods (or preferably to adjust the Villemonte formula itself).

As was proven earlier, the submergence process is dependent on the difference between the velocities at the vena contracta and at the downstream river section. The velocities in turn are dependent on how large the respective areas are at these sections. Thus if a ratio can be developed which describes the flow area of the vena contracta relative to the one at the downstream section it should be possible to use this ratio to determine whether Villemonte's method is valid or not.

This parameter is now developed as follows (refer to Figure 5.4.3.1).

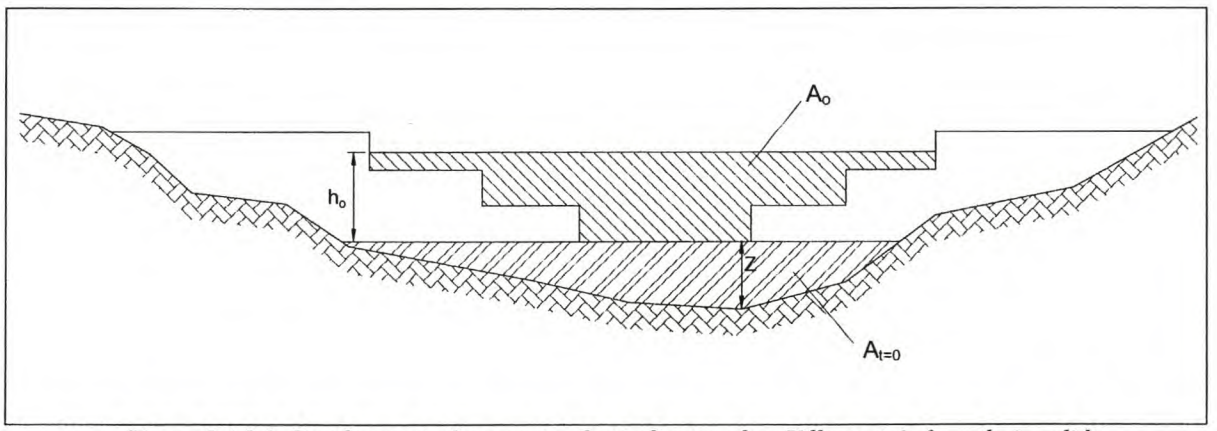

Figure 5.4.3.1: Development of parameter that indicates when Villemonte's formula is valid

If an initial estimate of the discharge can be made with the Villemonte formula it is possible to perform a back calculation to determine the free-flow water head (h_o) for the same flow rate. This water head in turn can be used to calculate the upstream flow area (A_o) that would occur under modular flow conditions. The area of the vena contracta was defined earlier as:

$$A_c = C_d \frac{1}{2}(h_v + t) \times L \qquad \text{With } C_d = 0.60 \text{ (for single notch weirs)}$$

If t=0 then $h_v = h_o$ and the area of the vena contracta under modular flow conditions is:

$$A_{co} = C_d \frac{1}{2} h_o \times L = C_d \frac{1}{2} A_o$$

This expression can now be applied to both single notch and compound weirs to obtain an estimate of the flow area at the vena contracta. The area at the downstream section of the weir when t=0 (i.e. when the structure is *just* becoming submerged) is denoted as $A_{t=0}$.

The author proposes that the ratio $\frac{A_{co}}{A_{t=0}}$ be used as a parameter to establish the limits of application for the Villemonte equation. This ratio gives a good indication of the relative flow areas concerned and therefore also the velocities at the respective sections. The graph in Figure 5.4.3.2 shows the average error made when Villemonte's method is used to calculate the submerged discharge. The average error of each test is plotted against its corresponding $A_{co}/A_{t=0}$ ratio. The graph indicates that as the value of $A_{co}/A_{t=0}$ increases, the average error decreases.

The downward trend of the graph can be explained by realising that a higher $A_{co}/A_{t=0}$ ratio implies that the flow areas at the vena contracta and at the downstream section gradually become closer to each other. The difference in the respective velocities therefore decreases as well and the relative energy loss decreases. If the relative energy loss becomes too small, Villemonte's formula is not reliable anymore, as proven earlier.

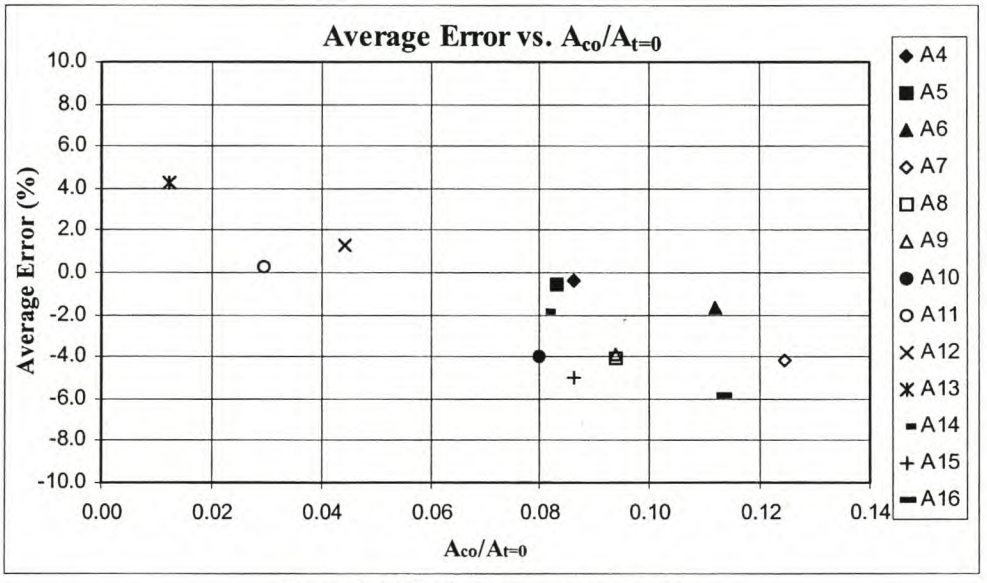

Figure 5.4.3.2: Average error vs. $A_{co}/A_{t=0}$

Given the currently available data on compound sharp-crested weirs, the author proposes that the Villemonte equation be applied if the following is true:

$$0.02 \leq \frac{A_{co}}{A_{t=0}} \leq 0.130$$

It is expected that $A_{co}/A_{t=0}$ will seldom be less than 0.02. Should the ratio be less than 0.02 then the Villemonte formula will still give reasonable results provided that the weir is not submerged too much ($A_t/A_v < 0.80$). At higher values of $A_{co}/A_{t=0}$ the Villemonte equation starts to underestimate the discharge. At this stage it will become preferable to use Wessels' method in place of Villemonte's. The tests where $A_{co}/A_{t=0}$ is high have indicated that the errors produced by the Wessels method are acceptable (maximum error ±10% at submergence ratio of 0.90). It is expected that these errors decrease even further if the discharge becomes greater.

Since no data is available on extremely high flow rates, the limits stated above will have to be verified in future as additional data on compound weirs becomes available.

At this point in time the procedure to estimate the discharge under non-modular flow conditions can thus be summarised as follows (an example calculation can be found in Appendix III):

1. Estimate the discharge with the adapted IMFT equation (Section 4.4.3) and correct this discharge with the Villemonte formula. Each notch in a compound weir is considered separately and their individual flow contributions are added up to obtain the total discharge.
2. Perform a back calculation to determine h_o.
3. Calculate the ratio $A_{co}/A_{t=0}$ and determine if it is within the limits stated above. Should the ratio be higher than the maximum, then repeat the flow estimation with Wessels' method.

Finally, the table below gives a summary of the errors made when the above procedure is followed. It was compiled using all the available data on compound sharp-crested weirs.

Submergence (%)	0-10	10-20	20-30	30-40	40-50	50-60	60-70	70-80	80-90	90-100	0-100
Avg. error (%)	-0.1	-0.7	-1.4	-1.2	-1.5	-2.2	-3.0	-4.1	-3.5	-1.0	-1.9
Std. dev. (%)	0.5	0.8	1.0	1.7	1.7	2.2	2.8	4.5	5.2	8.8	4.3
Abs. error (%)	0.5	0.9	1.6	1.9	1.8	2.6	3.3	5.1	5.0	7.6	3.3

Table 5.4.3.1: Summary of errors made – non-modular flow conditions

6 CONCLUSIONS

The most important findings of this research project can be summarised as follows:

6.1 MODULAR FLOW CONDITIONS

- End contractions can ensure proper aeration for compound sharp-crested weirs. They also have a significant effect on discharge measurement. It was found that this effect could be dealt with by considering an effective notch length.
- The WRC formula is not suited for compound sharp-crested weirs, as it doesn't make specific provision for end contractions. Furthermore, it applies the same coefficient of discharge to the whole weir. This is not desirable because many discharge measurement structures in South Africa consist of different types of gauging structures (flumes, sharp-crested weirs etc.) and it is then better to deal with each section of such a weir separately.
- The formula developed by DWAF works well for all types of compound sharp-crested weirs. It considers both end contractions (by calculating an effective notch length) and shallow pool depths (by using different coefficients of discharge). However, it is not clearly related to any internationally accepted standards.
- It was possible to develop a method for flow calculation which is based on the IMFT equation, which is included in the ISO standards. End contractions are treated by calculating an effective notch length (as in the DWAF formula). A new coefficient of discharge is also included to deal with shallow pool depths. In this way, *H/P* ratios of up to 15 are catered for. Based on all the available test data the average error made when using this new method is 0.59% with a standard deviation of 2.4%. This means that the error varies between –4.2% and +5.5% at the 95% confidence level.

6.2 NON-MODULAR FLOW CONDITIONS

- It was found that the effect of submergence on calculated discharges is not only a function of the ratio t/h_v. It was proven that submergence could be described in terms of the energy loss occurring at a drowned weir. This energy loss is a function of the velocities at the vena contracta and the downstream river section. The greater the difference in these two velocities becomes, the higher the energy loss.
- The Villemonte formula works well if the relative energy losses are fairly large. This typically happens during low discharges or when the downstream section is very large relative to the area of the vena contracta at the drowned weir.
- Wessels' method on the other hand is suitable when the relative energy losses become small.
- Since both methods are only valid under certain conditions, the parameter $A_{co}/A_{t=0}$ was developed which helps to identify the correct procedure to use. This parameter considers the conditions at the vena contracta and at the downstream river section. The currently available data on submerged compound sharp-crested weirs was used to determine the limits when Villemonte's formula is valid and when it is advisable to switch to Wessels' method. According to this test data Villemonte's formula is reliable up to a point when $A_{co}/A_{t=0}$ is equal to 0.130. More data is however needed (especially on very high flows over compound weirs) to establish if this value is indeed correct. From the available data it was determined that the error increases up to ±10% at high submergence ratios ($S > 0.80$) when the above methodology is employed.

- It was also established that when water is only flowing over the lower notches of a compound weir and is already becoming submerged, then a dramatic increase in errors occurs as the weir becomes further submerged. This is due to the sudden increase in energy losses as the upstream water level rises, which causes the water to start flowing over the higher notches.

7 RECOMMENDATIONS

7.1 MODULAR FLOW CONDITIONS

It is recommended that the adapted IMFT equation for compound sharp-crested weirs, as outlined in Section 4.4.3, be used to determine the discharge under modular flow conditions. This method was found to produce the smallest errors (average error 0.6%) and is based on an internationally recognised formula.

The formula can be used with *H/P* ratios of up to 15. For *H/P* ratios greater than 15 it is expected that the errors will increase. The author is of the opinion that at this point the gauging structure would become unreliable and discharge calculations would be affected by inaccurate water level recordings.

With regards to the operation of sharp-crested weirs in general, it is recommended that future weirs be constructed with end contractions. These provide sufficient aeration that is needed for accurate flow measurement. Should a notch be very long, it is possible to divide it into two or more notches with aeration columns, which also provide an effective way to aerate the nappe of the overflowing water.

7.2 NON-MODULAR FLOW CONDITIONS

It is recommended that the procedure described in Section 5.4.3 be used to calculate the discharge under non-modular flow conditions. According to this procedure, the discharge over each notch of a compound weir is initially estimated using the adapted IMFT formula (Section 4.4.3). The individual flow rates are then corrected with the Villemonte formula depending on the degree of submergence. The total discharge is obtained by summing up the contributions of all the notches.

To check whether the Villemonte formula was valid during the calculation the ratio $A_{co}/A_{t=0}$ needs to be calculated. Its value should remain below 0.130 for Villemonte's equation to be reliable. If the ratio has surpassed that value, it is recommended that the method developed by Wessels be used to calculate the discharge. The ratio of $A_{co}/A_{t=0} = 0.130$ was derived from the currently available data on compound weirs. As additional data becomes available this value should be verified.

In order to keep the $A_{co}/A_{t=0}$ ratio low, it is recommended that for future weirs the downstream section should be as large as possible. This will ensure that a high energy loss occurs at the weir during submerged conditions and the likelihood that Villemonte's formula is valid increases.

It is further advised that gauging structures be constructed in such a fashion that they will not already become submerged when water is flowing over the lower notches only. If this is achieved, large errors will be avoided during the estimation of the discharge.

7.3 FURTHER RESEARCH

Should the funds become available to do further research on compound sharp-crested weirs, it is advised that very high flow rates be tested. Since large flumes typically have limited depths, it might become necessary to test a miniature model in a smaller flume with greater depth. It is important to do further tests on high flows to establish the exact point at which Villemonte's formula becomes unreliable.

Should more data become available, it is also recommended that the Villemonte equation be adapted in such a fashion so that it is always applicable during non-modular flow conditions. It was shown earlier that Wessels' method produces discontinuities in the upstream water head, which is physically not correct. In addition, Villemonte's formula is internationally recognised.

8 REFERENCES

1. Bos (1976): *Discharge Measurement Structures*, Publication No. 161, Delft Hydraulics Laboratory, Delft

2. British Standards Institution, 1981: *Methods of Measurement of Liquid Flow in Open Channels - Thin-plate weirs*. BS3680:Part4A, BSI, London

3. Delport and Le Roux (1990): *Handleiding vir Kalibrasieprogramme* [Manual for Calibration Programs], Department of Water Affairs and Forestry, Pretoria

4. Featherstone and Nalluri (1986): *Civil Engineering Hydraulics*, Blackwell Science

5. Francis and Van Nostrand (1883): *Lowell Hydraulic Experiments*, 4th edition, New York

6. French (1985): *Open-Channel Hydraulics*, McGraw-Hill Book Company

7. International Organization for Standardization, 1980: *Water Flow Measurement in Open Channels Using Weirs and Venturi Flumes – Part1: Thin Plate Weirs*. ISO 1438/1, Geneva

8. Kindsvater and Carter (1957): *Discharge Characteristics of Rectangular Thin Plate Weirs*, Journal of the Hydraulic Engineering Division, ASCE

9. King, Wisler and Woodburn (1948): *Hydraulics*, John Wiley & Sons

10. Massey (1989): *Mechanics of Fluids*, 5th edition, Van Nostrand Reinhod (UK)

11. Roberson, Cassidy and Chaudry (1988): *Hydraulic Engineering*, Houghton Mifflin Company

12. Rossouw, Rooseboom and Wessels (1994): *Laboratory Calibration of Compound Sharp-Crested Weirs and Crump Weirs*. Report to the Water Research Commission by Sigma Beta Consulting Engineers, WRC Report No 442/1/95

13. Schoder and Turner (1929): *Precise Weir Measurements*, Transactions, ASCE, Vol. 93

14. Swamee (August 1988): *Generalized Rectangular Weir Equations*, Journal of Hydraulic Engineering, ASCE

15. Villemonte (December 1947): *Submerged-Weir Discharge Studies*, Engineering News Record

16. Wessels (1986): *Korreksies vir die Effek van Versuiping op Skerpkruinmeetstrukture* [Correction Factors for the Effect of Submergence on Sharp-Crested Weirs], University of Pretoria, M.Eng thesis

17. Wolvaardt (1992): *Invloed van Poeldiepte, Traphoogte en Oorloopwydte op die Kalibrasie van Skerpkruinriviervloeimeetstasies* [Effect of Pool Depth, Step Height and Notch Length on the Calibration of Sharp-Crested Weirs], University of Stellenbosch, M.Eng thesis

18. Wu and Rajaratnam (July 1997): *Submerged Flow Regimes of Rectangular Sharp-Crested Weirs*, Journal of Hydraulic Engineering, ASCE

APPENDIX I
DATA FOR MODULAR FLOW CONDITIONS

Modular Flow Conditions - Existing Data

Data contained in WRC Report 442/1/95

Test nr	L_1 (m)	L_2 (m)	P_1 (m)	T (m)	h_o (m)	h_o/T_1	Q_m† (m^3/s)	Q_o‡ (m^3/s)	%Error
S01	1.177	1.759	0.040	0.050	0.068	1.360	0.050	0.0500	-0.03
S02	1.177	1.759	0.040	0.050	0.124	2.480	0.200	0.1828	-8.60
S03	1.177	1.759	0.040	0.050	0.151	3.020	0.298	0.2720	-8.71
S04	1.177	1.759	0.091	0.050	0.069	1.380	0.049	0.0493	0.67
S05	1.177	1.759	0.091	0.050	0.131	2.620	0.200	0.1937	-3.17
S06	1.177	1.759	0.091	0.050	0.186	3.720	0.394	0.3839	-2.56
S10	1.177	1.759	0.193	0.050	0.136	2.720	0.201	0.1976	-1.67
S11	1.177	1.759	0.193	0.050	0.167	3.340	0.299	0.2923	-2.26
S12	1.177	1.759	0.193	0.050	0.196	3.920	0.402	0.3937	-2.07
S13	1.174	1.761	0.193	0.100	0.121	1.210	0.100	0.1023	2.33
S14	1.174	1.761	0.193	0.100	0.164	1.640	0.200	0.2018	0.89
S15	1.174	1.761	0.193	0.100	0.222	2.220	0.399	0.3834	-3.91
S16	1.174	1.761	0.290	0.103	0.167	1.621	0.200	0.2025	1.27
S17	1.174	1.761	0.290	0.103	0.200	1.942	0.302	0.2973	-1.57
S18	1.174	1.761	0.290	0.103	0.229	2.223	0.400	0.3926	-1.86
S19	0.740	2.192	0.050	0.050	0.078	1.560	0.051	0.0513	0.51
S20	0.740	2.192	0.050	0.050	0.137	2.740	0.201	0.1934	-3.79
S21	0.740	2.192	0.050	0.050	0.163	3.260	0.297	0.2794	-5.91
S22H	0.739	2.196	0.101	0.050	0.077	1.540	0.050	0.0481	-3.86
S23H	0.739	2.196	0.101	0.050	0.141	2.820	0.200	0.1966	-1.70
S24H	0.739	2.196	0.101	0.050	0.195	3.900	0.400	0.3813	-4.69
S25	0.738	2.190	0.100	0.100	0.139	1.390	0.100	0.1046	4.55
S26	0.738	2.190	0.100	0.100	0.179	1.790	0.200	0.2029	1.47
S27	0.738	2.190	0.100	0.100	0.235	2.350	0.399	0.3834	-3.92
S28	0.736	2.197	0.099	0.199	0.246	1.236	0.202	0.2089	3.40
S29	0.736	2.197	0.099	0.199	0.279	1.402	0.301	0.2975	-1.17
S30	0.736	2.197	0.099	0.199	0.308	1.548	0.400	0.3897	-2.58
S31	0.736	2.202	0.205	0.051	0.105	2.059	0.098	0.0984	0.43
S32	0.736	2.202	0.205	0.051	0.146	2.863	0.200	0.2004	0.18
S33	0.736	2.202	0.205	0.051	0.205	4.020	0.399	0.3919	-1.77
S34	0.740	2.196	0.205	0.100	0.140	1.400	0.101	0.1041	3.10
S35	0.740	2.196	0.205	0.100	0.181	1.810	0.199	0.2016	1.30
S36	0.740	2.196	0.205	0.100	0.240	2.400	0.399	0.3864	-3.15
S37	0.740	2.196	0.206	0.201	0.245	1.219	0.197	0.2008	1.92
S38	0.740	2.196	0.206	0.201	0.282	1.403	0.301	0.2988	-0.75
S39	0.740	2.196	0.206	0.201	0.312	1.552	0.398	0.3938	-1.05
S40	0.740	2.196	0.306	0.101	0.184	1.822	0.202	0.2051	1.52
S41	0.740	2.196	0.306	0.101	0.217	2.149	0.302	0.3010	-0.35
S42	0.740	2.196	0.306	0.101	0.139	1.376	0.099	0.1000	1.02
S46	0.496	2.433	0.048	0.049	0.106	2.163	0.101	0.0994	-1.57
S47	0.496	2.433	0.048	0.049	0.143	2.918	0.201	0.1997	-0.63
S48	0.496	2.433	0.048	0.049	0.169	3.449	0.301	0.2877	-4.41
S49	0.495	2.438	0.101	0.050	0.082	1.640	0.047	0.0479	2.02
S50	0.495	2.438	0.101	0.050	0.146	2.920	0.202	0.1971	-2.44
S51	0.495	2.438	0.101	0.050	0.202	4.040	0.398	0.3902	-1.95
S52	0.495	2.437	0.101	0.101	0.147	1.455	0.101	0.0973	-3.71
S53	0.495	2.437	0.101	0.101	0.189	1.871	0.201	0.2005	-0.24
S54	0.495	2.437	0.101	0.101	0.246	2.436	0.399	0.3876	-2.87
S55	0.494	2.446	0.099	0.201	0.265	1.318	0.200	0.1984	-0.78
S56	0.494	2.446	0.099	0.201	0.300	1.493	0.300	0.2963	-1.24
S57	0.494	2.446	0.099	0.201	0.328	1.632	0.400	0.3879	-3.03
S58	0.494	2.438	0.200	0.049	0.110	2.245	0.101	0.1023	1.24
S59	0.494	2.438	0.200	0.049	0.150	3.061	0.200	0.2030	1.50
S60	0.494	2.438	0.200	0.049	0.209	4.265	0.399	0.3970	-0.49
S61	0.492	2.438	0.200	0.100	0.120	1.200	0.050	0.0496	-0.73
S62	0.492	2.438	0.200	0.100	0.191	1.910	0.202	0.2018	-0.10
S63	0.492	2.438	0.200	0.100	0.251	2.510	0.399	0.3940	-1.25
S64	0.495	2.434	0.199	0.201	0.267	1.328	0.199	0.2010	0.99
S65	0.495	2.434	0.199	0.201	0.304	1.512	0.300	0.3048	1.59
S66	0.495	2.434	0.199	0.201	0.333	1.657	0.399	0.3999	0.22

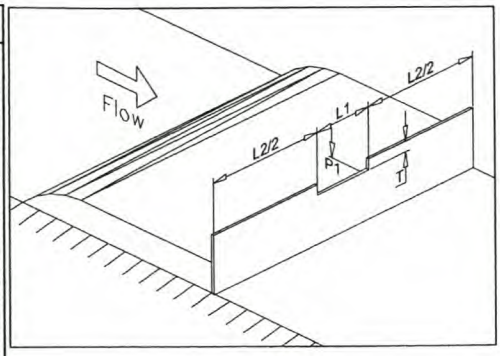

† Discharge determined with manometer

‡ Discharge calculated with adapted IMFT equation (as described in Chapter 4)

Modular Flow Conditions - Existing Data

Data contained in WRC Report 442/1/95

Shallow and irregular pool depths

Test nr	L_1 (m)	L_2 (m)	P_1 (m)	T (m)	h_o (m)	Q_m† (m^3/s)	Q_o‡ (m^3/s)	%Error
SC1	0.738	2.216	0.085	0.104	0.141	0.100	0.1048	4.78
SC2	0.738	2.216	0.085	0.104	0.181	0.201	0.2026	0.80
SC3	0.738	2.216	0.085	0.104	0.213	0.301	0.3004	-0.20
SC4	0.738	2.216	0.085	0.104	0.240	0.398	0.3955	-0.63
SC5	0.738	2.216	0.016	0.103	0.138	0.100	0.0994	-0.58
SC6	0.738	2.216	0.016	0.103	0.178	0.200	0.1987	-0.64
SC7	0.738	2.216	0.016	0.103	0.209	0.301	0.2977	-1.09
SC8	0.738	2.216	0.016	0.103	0.235	0.400	0.3946	-1.36
SC12	0.738	2.216	0.085	0.104	0.139	0.100	0.1007	0.67
SC13	0.738	2.216	0.085	0.104	0.180	0.199	0.1998	0.42
SC14	0.738	2.216	0.085	0.104	0.211	0.299	0.2938	-1.74
SC15	0.738	2.216	0.085	0.104	0.237	0.398	0.3844	-3.43
SC16	0.738	2.216	0.016	0.103	0.137	0.100	0.0974	-2.61
SC17	0.738	2.216	0.016	0.103	0.176	0.200	0.1930	-3.51
SC18	0.738	2.216	0.016	0.103	0.206	0.300	0.2873	-4.22
SC19	0.738	2.216	0.016	0.103	0.231	0.399	0.3789	-5.05
SC23	0.738	2.216	0.085	0.104	0.140	0.100	0.1027	2.71
SC24	0.738	2.216	0.085	0.104	0.180	0.200	0.1998	-0.08
SC25	0.738	2.216	0.085	0.104	0.211	0.300	0.2938	-2.06
SC26	0.738	2.216	0.085	0.104	0.238	0.400	0.3881	-2.99
SC27	0.738	2.216	0.016	0.103	0.137	0.100	0.0974	-2.61
SC28	0.738	2.216	0.016	0.103	0.176	0.200	0.1930	-3.51
SC29	0.738	2.216	0.016	0.103	0.206	0.301	0.2873	-4.54
SC30	0.738	2.216	0.016	0.103	0.230	0.399	0.3750	-6.02
SC34	0.738	2.216	0.016	0.103	0.136	0.100	0.0954	-4.62
SC35	0.738	2.216	0.016	0.103	0.173	0.200	0.1845	-7.75
SC36	0.738	2.216	0.016	0.103	0.200	0.301	0.2671	-11.27
SC37	0.738	2.216	0.016	0.103	0.226	0.400	0.3596	-10.09

† Discharge determined with manometer

‡ Discharge calculated with adapted IMFT equation (as described in Chapter 4)

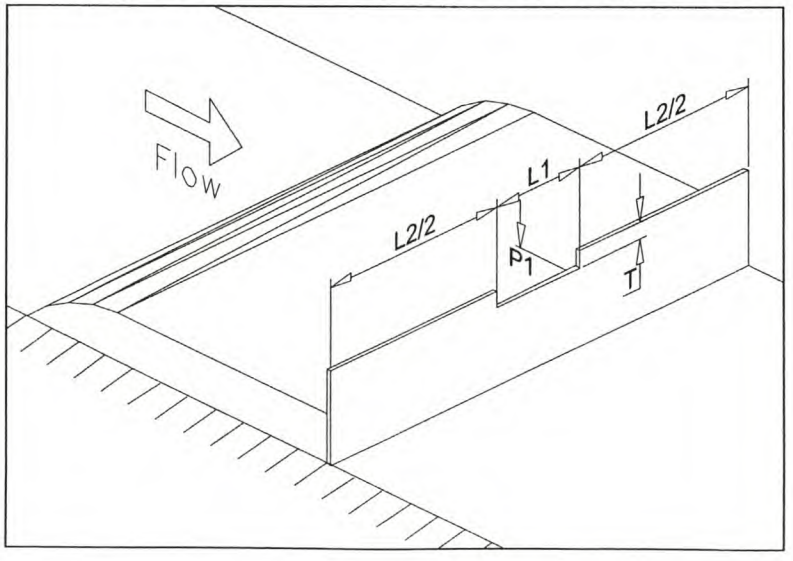

Modular Flow Conditions - Additional Data

Additional data, weirs similar to WRC tests (existing data)

								Manometer					Weir	
Test nr	L_1 (m)	L_2 (m)	B (m)	P_1 (m)	Z_1 (m)	T (m)	h_o (m)	d_1 (m)	d_2 (m)	h_W (m)	C_d	Q_m† (m^3/s)	Q_o‡ (m^3/s)	%Error
A0-F1	0.400	1.600	2.000	0.101	0.310	0.071	0.0662	0.300	0.1629	0.042	0.626	0.0124	0.01244	0.39
A0-F2	0.400	1.600	2.000	0.101	0.310	0.071	0.0873	0.300	0.1629	0.192	0.626	0.0265	0.02523	-4.80
A0-F3	0.400	1.600	2.000	0.101	0.310	0.071	0.0889	0.300	0.1629	0.196	0.626	0.0268	0.02671	-0.26
A0-F4	0.400	1.600	2.000	0.101	0.310	0.071	0.0959	0.300	0.1629	0.310	0.626	0.0337	0.03374	0.20
A0-F5	0.400	1.600	2.000	0.101	0.310	0.071	0.1006	0.300	0.1629	0.415	0.626	0.0390	0.03894	-0.05
A0-F6	0.400	1.600	2.000	0.101	0.310	0.071	0.1043	0.300	0.1629	0.512	0.626	0.0433	0.04329	0.03
A0-F7	0.400	1.600	2.000	0.101	0.310	0.071	0.1097	0.300	0.1629	0.685	0.626	0.0501	0.05001	-0.08
A0-F8	0.400	1.600	2.000	0.101	0.310	0.071	0.1180	0.300	0.1629	1.010	0.626	0.0608	0.06118	0.66
A0-F9	0.400	1.600	2.000	0.101	0.310	0.071	0.1249	0.300	0.1629	1.365	0.626	0.0707	0.07120	0.76
A0-F10	0.400	1.600	2.000	0.101	0.310	0.071	0.0653	0.300	0.1629	0.041	0.626	0.0122	0.01220	-0.40
A0-F11	0.400	1.600	2.000	0.101	0.310	0.071	0.0831	0.300	0.1629	0.131	0.626	0.0219	0.02160	-1.32
A0-F12	0.400	1.600	2.000	0.101	0.310	0.071	0.0899	0.300	0.1629	0.206	0.626	0.0274	0.02766	0.75
A0-F13	0.400	1.600	2.000	0.101	0.310	0.071	0.0923	0.300	0.1629	0.246	0.626	0.0300	0.03001	0.05
A0-F14	0.400	1.600	2.000	0.101	0.310	0.071	0.0952	0.300	0.1629	0.297	0.626	0.0330	0.03300	0.11
A0-F15	0.400	1.600	2.000	0.101	0.310	0.071	0.0996	0.300	0.1629	0.390	0.626	0.0378	0.03780	0.09
A0-F16	0.400	1.600	2.000	0.101	0.310	0.071	0.1057	0.300	0.1629	0.551	0.626	0.0449	0.04499	0.22
A0-F17	0.400	1.600	2.000	0.101	0.310	0.071	0.1192	0.300	0.1629	1.060	0.626	0.0623	0.06288	0.98
A0-F18	0.400	1.600	2.000	0.101	0.310	0.071	0.1295	0.300	0.1629	1.645	0.626	0.0776	0.07823	0.85
A0-F19	0.400	1.600	2.000	0.101	0.310	0.071	0.1378	0.300	0.1629	2.280	0.626	0.0913	0.09161	0.32

† Discharge determined with manometer

‡ Discharge calculated with adapted IMFT equation (as described in Chapter 4)

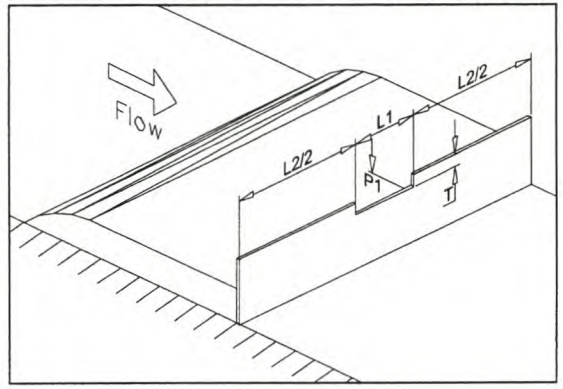

Modular Flow Conditions - Additional Data

Weirs with similar configuration as the weir for submergence test no. A4.

									Manometer					Weir	
Test nr	L_1 (m)	$L_{2,a}$ (m)	$L_{2,b}$ (m)	B (m)	P_1 (m)	Z_1 (m)	T_1 (m)	h_o (m)	d_1 (m)	d_2 (m)	h_W (m)	C_d	Q_m† (m^3/s)	Q_o‡ (m^3/s)	%Error
A4-F1	0.400	0.500	0.500	2.000	0.102	0.313	0.071	0.1787	0.300	0.213	1.220	0.604	0.1219	0.1236	1.34
A4-F2	0.400	0.500	0.500	2.000	0.102	0.313	0.071	0.1501	0.300	0.213	0.575	0.604	0.0837	0.0850	1.54
A4-F3	0.400	0.500	0.500	2.000	0.102	0.313	0.071	0.1927	0.300	0.213	1.680	0.604	0.1431	0.1444	0.91
A4-F4	0.400	0.500	0.498	2.000	0.101	0.313	0.071	0.0664	0.300	0.1629	0.044	0.626	0.0127	0.0125	-1.44
A4-F5	0.400	0.500	0.498	2.000	0.101	0.313	0.071	0.0676	0.300	0.1629	0.046	0.626	0.0130	0.0128	-1.01
A4-F6	0.400	0.500	0.498	2.000	0.101	0.313	0.071	0.0841	0.300	0.1629	0.118	0.626	0.0208	0.0207	-0.43
A4-F7	0.400	0.500	0.498	2.000	0.101	0.313	0.071	0.0884	0.300	0.1629	0.149	0.626	0.0233	0.0236	0.93
A4-F8	0.400	0.500	0.498	2.000	0.101	0.313	0.071	0.0925	0.300	0.1629	0.179	0.626	0.0256	0.0265	3.64
A4-F9	0.400	0.500	0.498	2.000	0.101	0.313	0.071	0.0944	0.300	0.1629	0.210	0.626	0.0277	0.0280	0.87
A4-F10	0.400	0.500	0.498	2.000	0.101	0.313	0.071	0.0980	0.300	0.1629	0.257	0.626	0.0307	0.0308	0.41
A4-F11	0.400	0.500	0.498	2.000	0.101	0.313	0.071	0.1040	0.300	0.1629	0.348	0.626	0.0357	0.0358	0.34
A4-F12	0.400	0.500	0.498	2.000	0.101	0.313	0.071	0.1114	0.300	0.1629	0.486	0.626	0.0422	0.0425	0.70
A4-F13	0.400	0.500	0.498	2.000	0.101	0.313	0.071	0.1170	0.300	0.1629	0.616	0.626	0.0475	0.0478	0.74
A4-F14	0.400	0.500	0.498	2.000	0.101	0.313	0.071	0.0569	0.300	0.1629	0.026	0.626	0.0098	0.0099	1.91
A4-F15	0.400	0.500	0.498	2.000	0.101	0.313	0.071	0.0695	0.300	0.1629	0.047	0.626	0.0131	0.0134	2.05
A4-F16	0.400	0.500	0.498	2.000	0.101	0.313	0.071	0.0885	0.300	0.1629	0.148	0.626	0.0233	0.0236	1.57
A4-F17	0.400	0.500	0.498	2.000	0.101	0.313	0.071	0.0937	0.300	0.1629	0.201	0.626	0.0271	0.0274	1.13
A4-F18	0.400	0.500	0.498	2.000	0.101	0.313	0.071	0.0997	0.300	0.1629	0.278	0.626	0.0319	0.0322	0.88
A4-F19	0.400	0.500	0.498	2.000	0.101	0.313	0.071	0.1038	0.300	0.1629	0.342	0.626	0.0354	0.0356	0.73
A4-F20	0.400	0.500	0.498	2.000	0.101	0.313	0.071	0.1072	0.300	0.1629	0.404	0.626	0.0384	0.0386	0.46
A4-F21	0.400	0.500	0.498	2.000	0.101	0.313	0.071	0.1127	0.300	0.1629	0.515	0.626	0.0434	0.0437	0.63
A4-F22	0.400	0.500	0.498	2.000	0.101	0.313	0.071	0.1188	0.300	0.1629	0.666	0.626	0.0494	0.0496	0.49
A4-F23	0.400	0.500	0.498	2.000	0.101	0.313	0.071	0.1280	0.300	0.1629	0.930	0.626	0.0583	0.0591	1.34
A4-F24	0.400	0.500	0.498	2.000	0.101	0.313	0.071	0.1356	0.300	0.1629	1.215	0.626	0.0667	0.0675	1.18
A4-F25	0.400	0.500	0.498	2.000	0.101	0.313	0.071	0.1407	0.300	0.1629	1.440	0.626	0.0726	0.0733	1.04
A4-F26	0.400	0.500	0.498	2.000	0.101	0.313	0.071	0.1471	0.300	0.1629	1.750	0.626	0.0800	0.0810	1.29
A4-F27	0.400	0.500	0.498	2.000	0.101	0.313	0.071	0.1556	0.300	0.1629	2.235	0.626	0.0904	0.0917	1.46
A4-F28	0.401	0.501	0.498	2.000	0.050	0.259	0.071	0.0582	0.300	0.1629	0.029	0.626	0.0103	0.0105	1.92
A4-F29	0.401	0.501	0.498	2.000	0.050	0.259	0.071	0.0884	0.300	0.1629	0.151	0.626	0.0235	0.0242	2.99
A4-F30	0.401	0.501	0.498	2.000	0.050	0.259	0.071	0.1084	0.300	0.1629	0.440	0.626	0.0401	0.0405	1.07
A4-F31	0.401	0.501	0.498	2.000	0.050	0.259	0.071	0.1162	0.300	0.1629	0.613	0.626	0.0474	0.0480	1.27
A4-F32	0.401	0.501	0.498	2.000	0.050	0.259	0.071	0.1302	0.300	0.1629	1.055	0.626	0.0621	0.0625	0.64
A4-F33	0.401	0.501	0.498	2.000	0.050	0.259	0.071	0.1414	0.300	0.1629	1.545	0.626	0.0752	0.0753	0.18
A4-F34	0.401	0.501	0.498	2.000	0.050	0.259	0.071	0.1529	0.300	0.1629	2.205	0.626	0.0898	0.0896	-0.28
A4-F35	0.401	0.501	0.498	2.000	0.050	0.259	0.071	0.1883	0.300	0.213	1.615	0.604	0.1403	0.1391	-0.83
A4-F36	0.401	0.501	0.498	2.000	0.019	0.228	0.071	0.0898	0.300	0.213	0.048	0.604	0.0242	0.0249	2.90
A4-F37	0.401	0.501	0.498	2.000	0.019	0.228	0.071	0.1081	0.300	0.213	0.132	0.604	0.0401	0.0399	-0.43
A4-F38	0.401	0.501	0.498	2.000	0.019	0.228	0.071	0.1261	0.300	0.213	0.283	0.604	0.0587	0.0579	-1.44
A4-F39	0.401	0.501	0.498	2.000	0.019	0.228	0.071	0.1372	0.300	0.213	0.423	0.604	0.0718	0.0703	-2.11
A4-F40	0.401	0.501	0.498	2.000	0.019	0.228	0.071	0.1549	0.300	0.213	0.737	0.604	0.0948	0.0923	-2.57
A4-F41	0.401	0.501	0.498	2.000	0.019	0.228	0.071	0.1647	0.300	0.213	0.955	0.604	0.1079	0.1055	-2.16
A4-F42	0.401	0.501	0.498	2.000	0.019	0.228	0.071	0.1714	0.300	0.213	1.140	0.604	0.1179	0.1150	-2.45
A4-F43	0.401	0.501	0.498	2.000	0.019	0.228	0.071	0.1741	0.300	0.213	1.220	0.604	0.1219	0.1188	-2.52
A4-F44	0.401	0.501	0.498	2.000	0.019	0.228	0.071	0.1805	0.300	0.213	1.425	0.604	0.1318	0.1283	-2.66
A4-F45	0.401	0.501	0.498	2.000	0.019	0.228	0.071	0.1856	0.300	0.213	1.610	0.604	0.1401	0.1359	-2.93

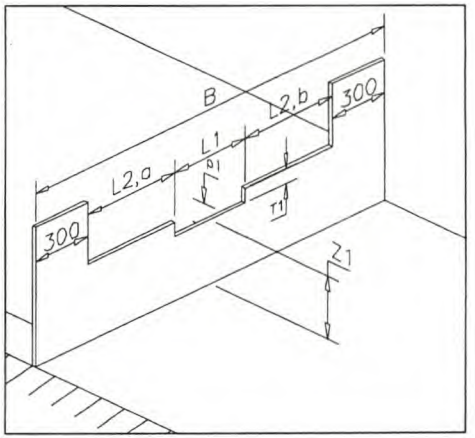

† Discharge determined with manometer

‡ Discharge calculated with adapted IMFT equation (as described in Chapter 4)

Modular Flow Conditions - Additional Data

Weirs with similar configuration as the weir for submergence test no. A8.

									Manometer					Weir	
Test nr	L_1 (m)	$L_{2,a}$ (m)	$L_{2,b}$ (m)	B (m)	P_1 (m)	Z_1 (m)	T_1 (m)	h_o (m)	d_1 (m)	d_2 (m)	h_W (m)	C_d	Q_m† (m^3/s)	Q_o‡ (m^3/s)	%Error
A8-F1	0.401	0.500	0.699	2.000	0.102	0.313	0.071	0.1754	0.300	0.213	1.435	0.604	0.1322	0.1331	0.65
A8-F2	0.401	0.500	0.699	2.000	0.102	0.313	0.071	0.1189	0.300	0.213	0.240	0.604	0.0541	0.0541	-0.01
A8-F3	0.401	0.500	0.699	2.000	0.102	0.313	0.071	0.1415	0.300	0.213	0.545	0.604	0.0815	0.0821	0.78
A8-F4	0.401	0.500	0.699	2.000	0.102	0.313	0.071	0.1878	0.300	0.213	1.935	0.604	0.1535	0.1541	0.33
A8-F5	0.401	0.500	0.699	2.000	0.102	0.313	0.071	0.1752	0.300	0.213	1.425	0.604	0.1318	0.1328	0.76
A8-F6	0.401	0.500	0.699	2.000	0.102	0.313	0.071	0.1572	0.300	0.213	0.900	0.604	0.1047	0.1045	-0.19

† Discharge determined with manometer

‡ Discharge calculated with adapted IMFT equation (as described in Chapter 4)

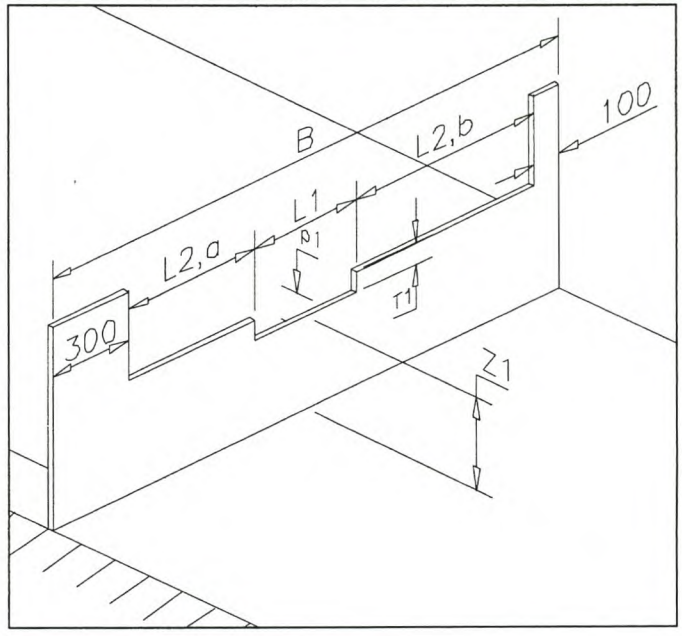

Modular Flow Conditions - Additional Data

Weirs with similar configuration as the weir for submergence test no. A11.

													Manometer					Weir	
Test nr	L_1 (m)	$L_{2,a}$ (m)	$L_{2,b}$ (m)	L_3	$L_{4,a}$	$L_{4,b}$	B (m)	P_1 (m)	Z_1 (m)	T_1 (m)	T_2 (m)	T_3 (m)	h_o (m)	d_1 (m)	d_2 (m)	h_W (m)	C_d	$Q_m^{\dagger}$ (m^3/s)	$Q_o^{\ddagger}$ (m^3/s)	%Error
A11-F1	0.401	0.249	0.148	0.200	0.250	0.350	2.000	0.102	0.313	0.070	0.042	0.039	0.1125	0.300	0.213	0.091	0.604	0.0333	0.0337	1.29
A11-F2	0.401	0.249	0.148	0.200	0.250	0.350	2.000	0.102	0.313	0.070	0.042	0.039	0.1042	0.300	0.213	0.069	0.604	0.0290	0.0290	0.09
A11-F3	0.401	0.249	0.148	0.200	0.250	0.350	2.000	0.102	0.313	0.070	0.042	0.039	0.1215	0.300	0.213	0.127	0.604	0.0393	0.0395	0.40
A11-F4	0.401	0.249	0.148	0.200	0.250	0.350	2.000	0.102	0.313	0.070	0.042	0.039	0.1353	0.300	0.213	0.202	0.604	0.0496	0.0494	-0.43
A11-F5	0.401	0.249	0.148	0.200	0.250	0.350	2.000	0.102	0.313	0.070	0.042	0.039	0.1468	0.300	0.213	0.282	0.604	0.0586	0.0586	-0.08
A11-F6	0.401	0.249	0.148	0.200	0.250	0.350	2.000	0.102	0.313	0.070	0.042	0.039	0.1643	0.300	0.213	0.420	0.604	0.0715	0.0759	6.06
A11-F7	0.401	0.249	0.148	0.200	0.250	0.350	2.000	0.102	0.313	0.070	0.042	0.039	0.1857	0.300	0.213	0.850	0.604	0.1018	0.1026	0.85
A11-F8	0.401	0.249	0.148	0.200	0.250	0.350	2.000	0.102	0.313	0.070	0.042	0.039	0.1992	0.300	0.213	1.220	0.604	0.1219	0.1216	-0.30
A11-F9	0.401	0.249	0.148	0.200	0.250	0.350	2.000	0.102	0.313	0.070	0.042	0.039	0.2097	0.300	0.213	1.565	0.604	0.1381	0.1373	-0.60
A11-F10	0.401	0.249	0.148	0.200	0.250	0.350	2.000	0.102	0.313	0.070	0.042	0.039	0.2147	0.300	0.213	1.755	0.604	0.1462	0.1450	-0.81
A11-F11	0.401	0.250	0.148	0.200	0.250	0.350	2.000	0.103	0.313	0.070	0.042	0.039	0.0664	0.300	0.213	0.014	0.604	0.0131	0.0125	-4.11
A11-F12	0.401	0.250	0.148	0.200	0.250	0.350	2.000	0.103	0.313	0.070	0.042	0.039	0.0992	0.300	0.213	0.056	0.604	0.0261	0.0263	0.83
A11-F13	0.401	0.250	0.148	0.200	0.250	0.350	2.000	0.103	0.313	0.070	0.042	0.039	0.1119	0.300	0.213	0.086	0.604	0.0324	0.0334	3.12
A11-F14	0.401	0.250	0.148	0.200	0.250	0.350	2.000	0.103	0.313	0.070	0.042	0.039	0.1314	0.300	0.213	0.177	0.604	0.0464	0.0465	0.17
A11-F15	0.401	0.250	0.148	0.200	0.250	0.350	2.000	0.103	0.313	0.070	0.042	0.039	0.1359	0.300	0.213	0.205	0.604	0.0500	0.0499	-0.19
A11-F16	0.401	0.250	0.148	0.200	0.250	0.350	2.000	0.103	0.313	0.070	0.042	0.039	0.1489	0.300	0.213	0.300	0.604	0.0605	0.0604	-0.15
A11-F17	0.401	0.250	0.148	0.200	0.250	0.350	2.000	0.103	0.313	0.070	0.042	0.039	0.1671	0.300	0.213	0.517	0.604	0.0794	0.0792	-0.24
A11-F18	0.401	0.250	0.148	0.200	0.250	0.350	2.000	0.103	0.313	0.070	0.042	0.039	0.2013	0.300	0.213	1.275	0.604	0.1246	0.1248	0.12
A11-F19	0.401	0.250	0.148	0.200	0.250	0.350	2.000	0.103	0.313	0.070	0.042	0.039	0.2079	0.300	0.213	1.510	0.604	0.1356	0.1347	-0.71
A11-F20	0.401	0.249	0.148	0.200	0.250	0.350	2.000	0.102	0.313	0.070	0.042	0.039	0.1431	0.300	0.213	0.248	0.604	0.0550	0.0555	1.00
A11-F21	0.401	0.249	0.148	0.200	0.250	0.350	2.000	0.102	0.313	0.070	0.042	0.039	0.0641	0.300	0.213	0.013	0.604	0.0123	0.0119	-3.70
A11-F22	0.401	0.249	0.148	0.200	0.250	0.350	2.000	0.102	0.313	0.070	0.042	0.039	0.1945	0.300	0.213	1.075	0.604	0.1144	0.1148	0.33

† Discharge determined with manometer

‡ Discharge calculated with adapted IMFT equation (as described in Chapter 4)

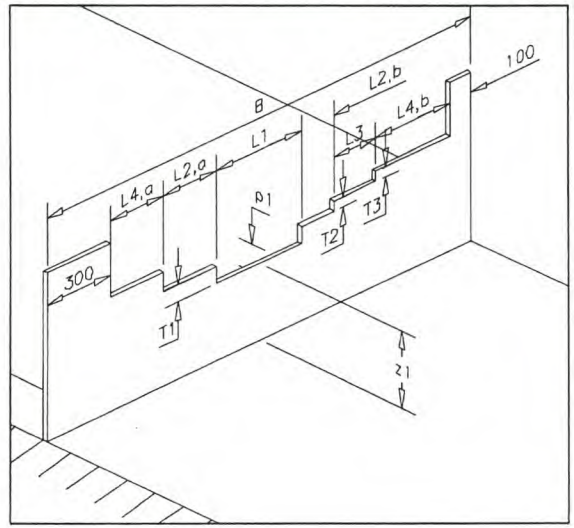

Modular Flow Conditions - Additional Data

Weirs with similar configuration as the weir for submergence test no. A15.

									Manometer					Weir	
Test nr	L_1 (m)	$L_{2,a}$ (m)	$L_{2,b}$ (m)	B (m)	P_1 (m)	Z_1 (m)	T_1 (m)	h_o (m)	d_1 (m)	d_2 (m)	h_W (m)	C_d	Q_m† (m^3/s)	Q_o‡ (m^3/s)	%Error
A15-F1	0.401	0.430	0.618	2.000	0.102	0.313	0.071	0.1750	0.300	0.213	1.170	0.604	0.1194	0.1203	0.76
A15-F2	0.401	0.430	0.618	2.000	0.102	0.313	0.071	0.1050	0.300	0.213	0.115	0.604	0.0374	0.0373	-0.22
A15-F3	0.401	0.430	0.618	2.000	0.102	0.313	0.071	0.1417	0.300	0.213	0.480	0.604	0.0765	0.0761	-0.53
A15-F4	0.401	0.430	0.618	2.000	0.102	0.313	0.071	0.1884	0.300	0.213	1.600	0.604	0.1396	0.1401	0.35
A15-F5	0.401	0.430	0.618	2.000	0.102	0.313	0.071	0.1962	0.300	0.213	1.905	0.604	0.1524	0.1519	-0.27
A15-F6	0.401	0.430	0.619	2.000	0.101	0.313	0.071	0.0567	0.300	0.1629	0.027	0.626	0.0099	0.0099	-0.27
A15-F7	0.401	0.430	0.619	2.000	0.101	0.313	0.071	0.0873	0.300	0.1629	0.144	0.626	0.0230	0.0231	0.58
A15-F8	0.401	0.430	0.619	2.000	0.101	0.313	0.071	0.1003	0.300	0.1629	0.296	0.626	0.0329	0.0332	0.96
A15-F9	0.401	0.430	0.619	2.000	0.101	0.313	0.071	0.1100	0.300	0.1629	0.472	0.626	0.0416	0.0419	0.94
A15-F10	0.401	0.430	0.619	2.000	0.101	0.313	0.071	0.1165	0.300	0.1629	0.632	0.626	0.0481	0.0483	0.39
A15-F11	0.401	0.430	0.619	2.000	0.101	0.313	0.071	0.1237	0.300	0.1629	0.825	0.626	0.0549	0.0557	1.39
A15-F12	0.401	0.430	0.619	2.000	0.101	0.313	0.071	0.1270	0.300	0.1629	0.935	0.626	0.0585	0.0592	1.31
A15-F13	0.401	0.430	0.619	2.000	0.101	0.313	0.071	0.1476	0.300	0.1629	1.880	0.626	0.0829	0.0834	0.53
A15-F14	0.401	0.430	0.619	2.000	0.101	0.313	0.071	0.1526	0.300	0.1629	2.175	0.626	0.0892	0.0897	0.61
A15-F15	0.401	0.430	0.618	2.000	0.050	0.259	0.071	0.1623	0.300	0.213	0.895	0.604	0.1044	0.1035	-0.93
A15-F16	0.401	0.430	0.618	2.000	0.050	0.259	0.071	0.1748	0.300	0.213	1.250	0.604	0.1234	0.1210	-1.94
A15-F17	0.401	0.430	0.618	2.000	0.050	0.259	0.071	0.1865	0.300	0.213	1.650	0.604	0.1418	0.1383	-2.43

† Discharge determined with manometer

‡ Discharge calculated with adapted IMFT equation (as described in Chapter 4)

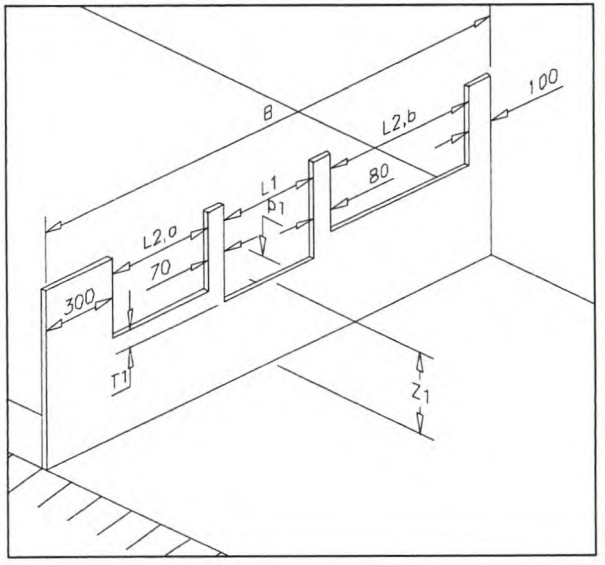

APPENDIX II
DATA FOR NON-MODULAR FLOW CONDITIONS

Submergence Tests Done by Wessels (Existing Data)

Full-width, single notch weirs

PW-1		PW-2		PW-3		PW-4		PW-5	
Z =	0.505 m	Z =	0.505 m	Z =	0.505 m	Z =	0.505 m	Z =	0.505 m
P =	0.505 m	P =	0.505 m	P =	0.505 m	P =	0.505 m	P =	0.505 m
h_o =	0.1593 m	h_o =	0.1801 m	h_o =	0.1018 m	h_o =	0.1414 m	h_o =	0.1922 m
L =	0.5 m	L =	0.5 m	L =	0.5 m	L =	0.5 m	L =	0.5 m
h_v (mm)	t (mm)	h_v (mm)	t (mm)	h_v (mm)	t (mm)	h_v (mm)	t (mm)	h_v (mm)	t (mm)
154.9	0.2	175.0	3.4	99.7	1.1	137.4	0.1	187.0	0.3
159.7	25.3	177.8	20.4	101.5	11.2	139.8	14.5	186.7	1.4
165.0	51.7	180.2	34.7	104.0	25.1	142.7	30.0	189.6	18.7
176.0	94.4	183.4	50.4	106.3	37.1	146.3	47.0	192.3	35.4
185.9	119.7	186.7	65.2	110.5	52.4	150.2	63.1	196.5	54.1
202.9	156.9	189.9	78.9	115.2	66.5	154.2	79.4	199.7	70.4
214.4	177.0	194.7	96.7	121.7	83.1	160.4	96.9	202.5	81.0
219.8	185.4	199.9	115.1	131.1	100.1	168.0	115.6	204.8	90.9
228.1	198.1	206.4	132.6	139.2	116.9	177.1	135.4	209.9	107.5
252.0	229.7	212.8	148.4	153.8	138.3	189.4	157.0	216.6	129.1
266.5	248.4	220.5	165.6	166.5	154.8	204.4	180.4	226.2	153.5
325.4	315.0	228.1	180.5	183.7	175.4	227.1	210.9	238.4	180.0
399.8	330.9	239.4	199.7			250.3	238.7	255.9	212.0
354.0	346.4	252.2	219.8			281.7	274.5	276.5	241.9
369.3	362.3	266.2	239.4					302.5	276.8
		281.8	259.9					331.6	311.9
		297.5	279.2					367.0	352.4
		314.7	299.5					411.0	400.0
								464.8	457.0

Submergence Tests Done by Wessels (Existing Data)

Full-width, single notch weirs

PW-6		PW-7		PW-8		PW-9		PW-10	
Z =	0.505 m	Z =	0.505 m	Z =	0.505 m	Z =	0.505 m	Z =	0.505 m
P =	0.505 m	P =	0.505 m	P =	0.505 m	P =	0.290 m	P =	0.29 m
h_o =	0.2214 m	h_o =	0.223 m	h_o =	0.1221 m	h_o =	0.1203 m	h_o =	0.1569 m
L =	0.5 m	L =	0.5 m	L =	0.5 m	L =	0.5 m	L =	0.5 m
h_v (mm)	t (mm)	h_v (mm)	t (mm)	h_v (mm)	t (mm)	h_v (mm)	t (mm)	h_v (mm)	t (mm)
214.7	1.4	216.2	0.1	119.4	2.8	117.3	1.4	152.7	0.1
217.0	18.4	219.2	21.0	121.6	14.9	120.5	20.2	155.5	16.2
219.9	35.6	222.6	41.2	124.4	28.8	124.4	38.5	158.7	34.8
224.4	59.7	226.6	62.6	127.7	43.9	128.7	58.3	162.3	52.0
229.6	83.1	232.1	87.3	131.5	60.4	134.0	74.7	166.2	69.3
236.3	110.3	239.6	116.1	137.5	78.5	142.6	97.4	171.2	88.4
244.9	138.8	248.0	143.4	146.6	101.0	154.2	121.0	179.4	112.2
256.7	170.5	260.3	177.8	154.6	118.1	170.1	147.0	189.7	137.2
270.8	200.3	274.0	207.3	168.2	141.1	190.9	175.2	202.4	162.7
288.4	234.2	291.8	239.9	186.6	167.4	220.3	210.6	220.7	192.0
309.6	266.8	314.2	274.8	207.4	193.6	256.3	250.4	247.0	227.5
334.9	302.6	339.5	309.3	237.0	227.8			281.2	268.8
368.6	342.8	373.0	349.9	274.8	269.4			326.7	318.7
408.6	390.0	413.0	396.8						
444.7	430.0	452.7	440.1						
489.8	478.2	497.1	487.3						

Submergence Tests Done by Wessels (Existing Data)

Full-width, single notch weirs

PW-11		PW-12		PW-13		PW-14		PW-15	
Z =	0.505 m	Z =	0.505 m	Z =	0.505 m	Z =	0.505 m	Z =	0.505 m
P =	0.29 m	P =	0.29 m	P =	0.160 m	P =	0.16 m	P =	0.16 m
h_o =	0.186 m	h_o =	0.2484 m	h_o =	0.222 m	h_o =	0.1981 m	h_o =	0.1592 m
L =	0.5 m	L =	0.5 m	L =	0.5 m	L =	0.5 m	L =	0.5 m
h_v (mm)	t (mm)	h_v (mm)	t (mm)	h_v (mm)	t (mm)	h_v (mm)	t (mm)	h_v (mm)	t (mm)
182.0	0.7	240.4	0.0	215.7	1.5	192.4	0.0	155.6	0.1
183.9	16.1	243.0	17.9	217.6	18.7	194.6	15.9	157.8	16.6
186.1	31.3	246.6	40.6	220.8	38.4	197.5	34.6	161.1	36.2
189.5	49.0	251.5	68.7	224.6	59.8	200.6	52.1	164.9	55.5
192.8	65.3	258.4	101.2	228.2	79.2	203.5	68.3	169.9	76.7
196.9	83.7	266.0	131.1	234.2	106.8	207.9	90.0	175.5	97.5
202.5	104.6	274.2	160.3	243.7	142.6	214.4	114.9	183.8	122.1
210.0	127.8	283.5	190.9	251.8	167.8	224.2	145.1	196.3	150.6
220.2	153.8	299.9	227.2	265.0	199.9	237.5	178.0	211.4	178.2
236.5	188.1	321.1	267.2	286.3	240.8	257.5	215.8	232.1	209.4
257.4	222.2	356.4	319.9	318.9	288.7	285.1	257.4	263.7	249.6
275.6	248.5	410.4	387.9	367.0	349.7	327.6	311.2	307.8	299.7
312.1	294.0	494.1	481.2	426.4	415.9	389.6	380.5	375.3	371.4
382.1	372.7			495.7	488.9				
475.3	470.4								

Submergence Tests Done by Wessels (Existing Data)

Full-width, single notch weirs

PW-16		PW-17		PW-18		PW-19		PW-20	
Z =	0.505 m	Z =	0.505 m	Z =	0.505 m	Z =	0.29 m	Z =	0.29 m
P =	0.16 m	P =	0.06 m	P =	0.06 m	P =	0.06 m	P =	0.06 m
h_o =	0.132 m	h_o =	0.1203 m	h_o =	0.1867 m	h_o =	0.188 m	h_o =	0.148 m
L =	0.5 m	L =	0.5 m	L =	0.5 m	L =	0.5 m	L =	0.5 m
h_v (mm)	t (mm)	h_v (mm)	t (mm)	h_v (mm)	t (mm)	h_v (mm)	t (mm)	h_v (mm)	t (mm)
129.2	0.6	118.0	0.4	181.2	0.0	182.5	2.7	143.5	0.5
131.6	16.2	120.2	15.7	183.9	19.6	183.7	20.1	145.6	18.1
134.5	32.1	122.7	31.5	186.6	36.0	185.8	39.7	148.0	35.8
137.9	48.6	126.0	48.3	190.5	62.2	188.3	59.3	150.6	51.7
142.4	68.4	129.3	63.4	198.1	95.5	192.2	80.5	154.7	72.9
149.1	89.6	133.6	78.5	205.5	126.5	196.9	100.9	159.6	92.5
156.4	108.6	139.3	95.4	218.0	159.3	203.2	125.0	164.5	109.3
166.3	129.9	146.1	111.4	231.6	190.2	214.7	160.4	169.3	128.2
178.7	151.5	155.8	130.8	249.2	221.3	230.1	190.3	186.6	158.0
195.8	177.2	169.2	152.2	277.6	260.5	246.8	218.8	217.9	203.8
222.6	210.8	194.9	185.8	328.5	319.5	276.2	259.9	278.8	273.4
264.8	258.4	235.2	231.0			339.4	332.6		

Submergence Tests Done by Wessels (Existing Data)

Full-width, single notch weirs

PW21		PW-22		PW-23		PW-24		PW-25	
Z =	0.29 m	Z =	0.29 m	Z =	0.29 m	Z =	0.29 m	Z =	0.29 m
P =	0.06 m	P =	0.06 m	P =	0.16 m	P =	0.16 m	P =	0.16 m
h_o =	0.1267 m	h_o =	0.1055 m	h_o =	0.1628 m	h_o =	0.2082 m	h_o =	0.1177 m
L =	0.5 m	L =	0.5 m	L =	0.5 m	L =	0.5 m	L =	0.5 m
h_v (mm)	t (mm)	h_v (mm)	t (mm)	h_v (mm)	t (mm)	h_v (mm)	t (mm)	h_v (mm)	t (mm)
123.2	1.6	102.5	0.1	157.2	1.2	201.0	0.8	114.3	1.0
125.0	16.7	104.4	10.6	159.4	18.0	202.5	17.6	116.5	16.3
127.6	32.9	106.1	21.1	161.8	33.3	204.7	35.6	119.0	30.4
130.6	50.5	107.4	31.2	164.7	49.9	207.2	51.3	121.6	44.3
134.7	68.6	109.2	40.6	168.7	69.9	210.4	71.0	125.3	60.6
138.9	84.1	111.3	51.4	174.0	92.5	214.4	90.8	130.2	77.1
144.3	98.7	115.1	65.5	180.7	114.3	219.1	110.3	135.9	91.0
153.6	120.8	120.9	82.6	189.5	135.2	224.4	130.1	143.5	108.7
163.4	139.8	127.1	97.2	201.4	159.9	230.8	150.1	155.6	130.7
178.3	162.8	135.3	113.4	212.4	180.2	241.5	176.2	175.5	159.5
201.0	191.4	146.6	131.8	234.4	212.2	255.8	204.8	208.6	199.2
252.0	247.6	169.7	161.4	275.0	261.6	279.0	243.4	254.5	249.3
308.6	306.5	205.2	200.9	328.1	320.6	314.1	291.3		
						369.9	356.9		
						447.6	440.0		

Submergence Tests Done by Wessels (Existing Data)

Full-width, single notch weirs

PW-26		PW-27		PW-28		PW-29		PW-30	
Z =	0.29 m	Z =	0.29 m	Z =	0.29 m	Z =	0.29 m	Z =	0.29 m
P =	0.16 m	P =	0.29 m	P =	0.29 m	P =	0.29 m	P =	0.29 m
h_o =	0.1966 m	h_o =	0.1482 m	h_o =	0.1001 m	h_o =	0.2207 m	h_o =	0.1848 m
L =	0.5 m	L =	0.5 m	L =	0.5 m	L =	0.5 m	L =	0.5 m
h_v (mm)	t (mm)	h_v (mm)	t (mm)	h_v (mm)	t (mm)	h_v (mm)	t (mm)	h_v (mm)	t (mm)
189.2	1.1	143.1	0.9	97.6	0.5	213.0	0.0	177.7	0.8
190.7	14.5	144.7	11.3	99.6	13.9	213.8	11.6	179.5	15.4
193.0	32.8	146.4	23.3	101.1	22.5	214.9	21.6	182.4	34.3
195.9	51.7	148.2	33.4	103.5	34.5	216.7	36.8	186.4	57.3
199.6	71.8	150.9	46.9	106.5	46.9	219.6	54.5	191.0	79.8
203.4	90.4	154.2	62.4	110.4	60.3	223.2	74.9	196.0	99.1
208.0	110.1	157.6	76.8	115.8	74.7	229.3	103.1	202.6	121.2
215.3	134.8	162.0	91.6	123.6	92.4	236.8	130.5	210.8	142.9
223.6	155.5	167.6	106.8	133.7	110.9	246.8	160.5	226.7	177.1
235.6	182.3	175.6	125.9	148.2	132.3	260.3	192.8	254.4	222.6
251.9	211.5	194.8	161.7	171.2	161	282.5	233.7	298.4	279.1
278.2	250.2	220.2	199.0	203.3	196.8	323.2	293.2	362.8	351.9
318.7	302.2	267.1	255.4	264.2	261.2	385.5	368.1	437.1	430.6
369.2	358.2	323.8	316.9			452.7	441.8		
421.2	413.6								

Submergence Tests Done by Wessels (Existing Data)

Full-width, single notch weirs

PW-31		PW-32		PW-33		PW-34		PW-35	
Z =	0.182 m	Z =	0.182 m	Z =	0.182 m	Z =	0.182 m	Z =	0.29 m
P =	0.18 m	P =	0.18 m	P =	0.082 m	P =	0.087 m	P =	0.29 m
h_o =	0.1311 m	h_o =	0.0996 m	h_o =	0.1077 m	h_o =	0.0894 m	h_o =	0.1956 m
L =	0.5 m	L =	0.5 m	L =	0.5 m	L =	0.5 m	L =	0.5 m
h_v (mm)	t (mm)	h_v (mm)	t (mm)	h_v (mm)	t (mm)	h_v (mm)	t (mm)	h_v (mm)	t (mm)
126.6	0.6	96.5	0.6	104.3	1.8	86.4	0.4	188.4	6.5
128.4	16.3	98.1	13.4	105.6	13.4	87.5	9.4	190.6	22.5
130.5	31.7	99.1	19.6	107.2	23.6	88.9	18.9	192.2	40.2
133.1	47.0	100.1	25.8	109.1	35.8	90.7	29.3	196.1	59.5
136.6	63.3	102.2	36.8	111.2	46.7	92.6	39.0	200.7	80.6
140.8	79.7	104.6	47.5	114.4	60.7	94.8	48.5	207.5	109.5
146.1	96.0	107.7	59.4	118.8	75.7	97.7	58.8	218.6	143.3
152.6	111.7	111.7	71.8	125.7	93.6	101.5	69.7	234.9	178.7
161.5	129.8	117.2	84.8	134.0	110.8	106.6	81.6	256.6	217.6
173.8	150.6	124.4	99.3	149.3	135.1	114.1	96.0	285.7	258.7
186.9	169.3	135.3	117.4	170.4	162.1	126.7	115.3	312.6	292.8
202.1	188.6	151.9	139.9	198.4	193.8	146.2	139.8	351.0	337.0
217.6	207.0	180.1	173.2			178.1	175.0		
233.9	225.4	211.3	206.7						
250.1	242.8								
270.0	264.3								
295.6	291.3								

Submergence Tests Done by Wessels (Existing Data)

Full-width, single notch weirs

PW-36		PW-37		PW-38	
Z =	0.29 m	Z =	0.29 m	Z =	0.505 m
P =	0.29 m	P =	0.29 m	P =	0.505 m
h_o =	0.1655 m	h_o =	0.1285 m	h_o =	0.2729 m
L =	0.5 m	L =	0.5 m	L =	0.5 m
h_v (mm)	t (mm)	h_v (mm)	t (mm)	h_v (mm)	t (mm)
159.9	4.2	124.4	0.7	264.7	1.9
161.4	17.1	126.6	16.1	266.5	18.2
164.2	33.2	129.0	29.7	270.6	43.2
166.9	49.7	131.8	43.8	274.4	61.5
170.2	65.7	134.9	57.3	280.3	91.0
174.9	83.9	139.9	75.5	287.3	119.1
180.6	104.6	146.1	93.3	295.0	146.3
187.3	123.0	154.6	112.6	305.0	177.9
201.8	155.1	167.4	137.3	315.4	216.9
219.6	186.3	186.6	166.3	331.1	250.9
238.0	213.5	212.6	199.1	350.9	287.9
263.6	245.9	239.5	230.1	381.1	335.0
296.6	284.3	261.3	253.3	422.0	390.3
330.5	320.7			496.9	477.6

Test No: A1

Configuration:	
L =	2.000 m
P =	0.173 m
Z =	0.383 m

Flow - Weir:	
h_o =	0.1061 m
Q_o† =	0.1359 m^3/s

Flow - Manometer:	
d_1 =	0.300 m
d_2 =	0.213 m
C_d =	0.604
h_W =	1.450 m
Q_m =	0.1329 m^3/s

† IMFT (original)

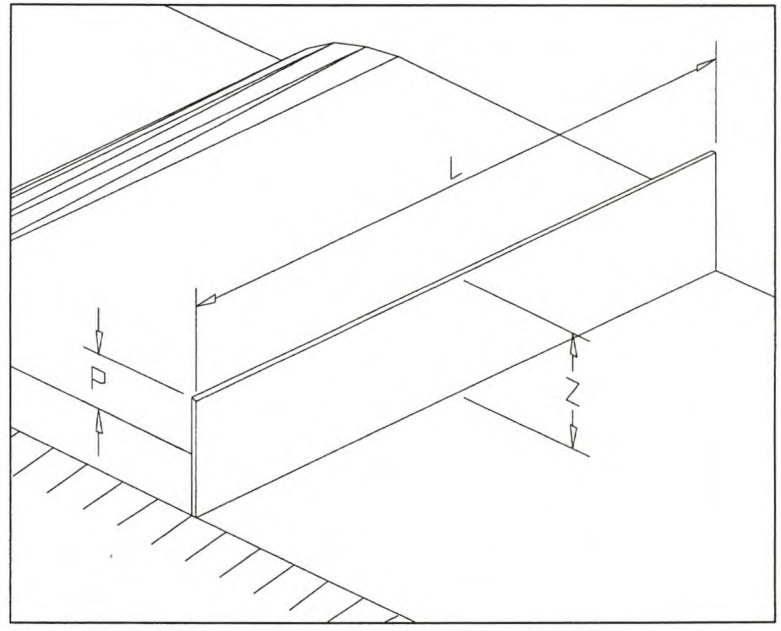

Water levels above crest-centre (mm):						Regime**:	Comment:
A	B (h_v)	C	D	E (t)	F		
106.3	105.9	106.3	-	-	-	-	modular conditions
104.7	104.4	104.6	0.8	3.2	2.0	a	submerged, D & F oscillate slightly, E is fairly stable
106.4	106.8	107.7	14.7	17.4	15.9	a	
112.3	112.0	112.8	40.3	42.3	42.0	a	
119.8	119.5	119.7	66.6	65.9	68.3	b	very rough standing wave
127.0	127.3	127.6	87.9	87.6	87.9	b	
138.6	138.6	139.0	110.8	110.7	111.6	b	smooth standing wave, D & F still oscillating, E is OK
149.7	149.7	150.3	128.4	128.4	129.2	b	
161.7	162.0	162.3	146.2	145.6	146.5	b	very smooth standing wave
174.9	174.6	175.4	162.0	162.7	162.8	b	very smooth standing wave, minor oscillations
188.3	188.4	188.4	178.4	178.3	178.5	b	no std. wave distinguishable

** a = Plunging Nappe; b = Surface Nappe

Test No: A2

Configuration:	
B =	2 m
L =	1.4 m
P =	0.173 m
Z =	0.383 m

Flow - Weir:	
h_o =	0.1216 m
Q_o† =	0.1128 m^3/s

Flow - Manometer:	
d_1 =	0.300 m
d_2 =	0.213 m
C_d =	0.604
h_W =	0.980 m
Q_m =	0.1093 m^3/s

† IMFT (adapted as described in Chapter 4)

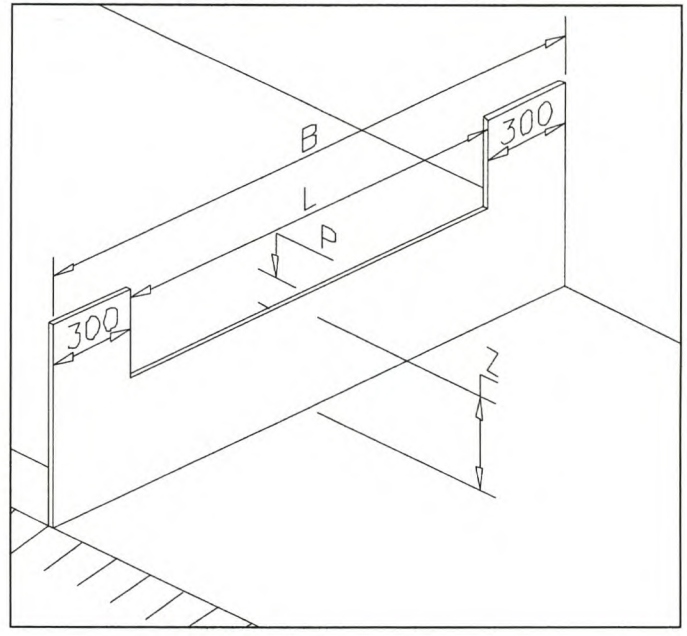

Water levels above crest-centre (mm):						Regime**:	Comment:
A	B (h_v)	C	D	E (t)	F		
122.2	121.6	122.5	-	-	-	-	modular conditions
122.4	121.9	122.8	4.7	2.7	4.4	a	some air still underneath nappe
122.2	121.9	122.3	15.6	5.1	9.3	a	submerged, no air underneath nappe
124.2	123.9	124.5	24.9	27.1	24.3	a-b	very unstable regime, downstream levels oscillate
128.4	127.6	128.6	46.0	41.4	44.7	b	stable regime, rough standing wave
133.7	133.5	134.5	58.7	59.7	59.1	b	
143.7	142.9	143.3	88.2	87.3	90.1	b	smooth standing wave, oscillations are getting smaller
156.6	156.1	157.1	116.1	116.8	117.4	b	smooth standing wave
151.0	150.6	151.1	106.2	99.7	104.1	b	
183.9	183.3	184.0	160.2	161.1	159.8	b	

** a = Plunging Nappe; b = Surface Nappe

Test No: A3

Configuration:	
B =	2 m
L =	1.4 m
P =	0.172 m
Z =	0.383 m

Flow - Weir:	
h_o =	0.1348 m
Q_o† =	0.1321 m^3/s

Flow - Manometer:	
d_1 =	0.300 m
d_2 =	0.213 m
C_d =	0.604
h_W =	1.360 m
Q_m =	0.1287 m^3/s

† IMFT (adapted as described in Chapter 4)

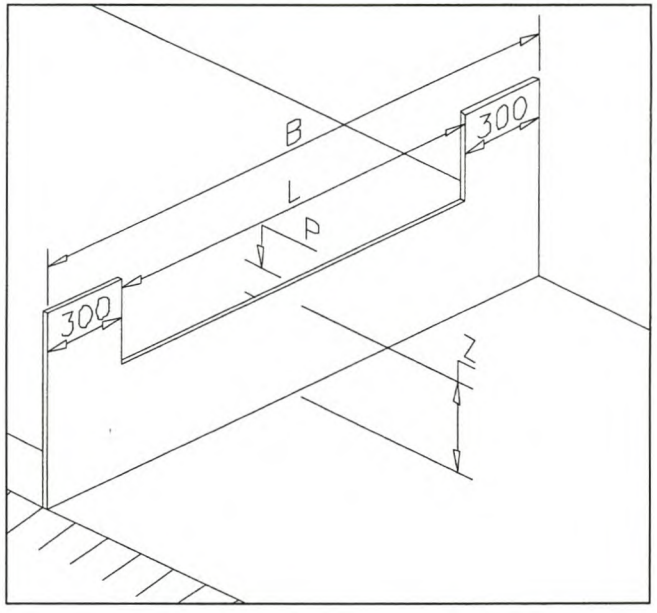

Water levels above crest-centre (mm):						Regime**:	Comment:
A	B (h_v)	C	D	E (t)	F		
136.0	134.7	136.0	-	-	-	-	modular conditions
136.2	135.1	136.2	6.5	2.0	6.4	a	weir well aerated
135.6	134.8	136.0	10.3	5.0	13.0	a	relatively well aerated (± 60% air under nappe)
135.9	135.7	136.4	16.4	10.1	13.7	a	poor aeration (± 5% air underneath nappe)
138.1	136.9	138.7	30.7	24.5	25.0	a-b	
140.4	139.5	140.7	42.6	40.3	44.5	b	
143.4	142.4	143.9	52.4	47.8	52.9	b	
147.4	146.7	147.9	64.4	58.5	65.1	b	
152.9	152.0	153.2	79.6	75.2	81.3	b	
159.1	158.7	159.8	96.8	93.6	97.9	b	
169.2	168.6	169.9	119.7	118.1	119.5	b	
182.5	182.0	182.7	143.2	142.8	144.2	b	
198.1	197.7	198.2	168.3	166.8	168.7	b	
223.1	222.8	223.4	201.3	200.5	202.6	b	

** a = Plunging Nappe; b = Surface Nappe

Test No: A4

Configuration:	
B =	2 m
L_1 =	0.400 m
$L_{2,a}$ =	0.500 m
$L_{2,b}$ =	0.500 m
T_1 =	0.071 m
P_1 =	0.102 m
Z_1 =	0.313 m

Flow - Weir:	
h_o =	0.1787 m
Q_o † =	0.1236 m^3/s
Flow - Manometer:	
d_1 =	0.300 m
d_2 =	0.213 m
C_d =	0.604
h_W =	1.220 m
Q_m =	0.1219 m^3/s

† IMFT (adapted as described in Chapter 4)

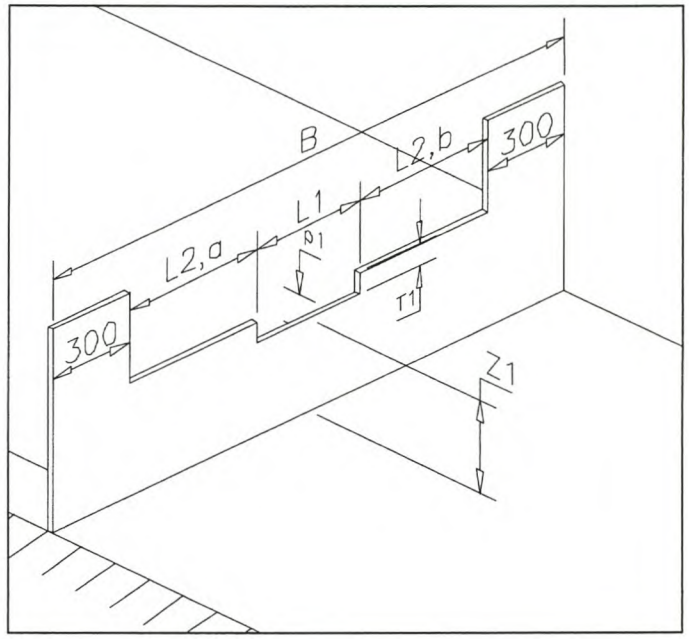

Water levels relative to lowest crest (mm):						Regime**:	Comment:
A	B (h_v)	C	D	E (t)	F		
179.5	178.8	179.9	-	-	-	-	modular conditions
179.7	178.6	179.8	7.5	13.9	8.2	a	L_1 is ±50% aerated
181.2	180.1	181.4	32.8	36.7	35.1	a	L_1 completely submerged
182.2	181.2	182.6	58.4	59.2	60.0	a	L_1 submerged, L_2 fully aerated
183.6	182.9	184.2	81.2	78.8	81.7	a	L_1 submerged, L_2 still well aerated
186.9	186.1	187.5	97.4	95.6	98.6	a-b	L_1 & L_2 completely submerged
191.5	190.6	192.0	112.1	100.6	112.1	b	
200.8	199.6	201.0	136.0	129.2	136.3	b	
214.8	213.8	215.0	168.4	164.5	170.1	b	
236.4	236.2	237.0	206.5	203.1	207.4	b	
264.4	263.8	264.2	243.0	242.9	244.0	b	
288.8	288.0	288.8	273.1	271.2	273.9	b	

** a = Plunging Nappe; b = Surface Nappe

Test No: A5

Configuration:	
B =	2.000 m
L_1 =	0.401 m
$L_{2,a}$ =	0.501 m
$L_{2,b}$ =	0.498
T_1 =	0.071 m
P_1 =	0.050 m
Z_1 =	0.259 m

Flow - Weir:	
h_o =	0.1529 m
Q_o † =	0.0896 m^3/s
Flow - Manometer:	
d_1 =	0.300 m
d_2 =	0.1629 m
C_d =	0.626
h_W =	2.205 m
Q_m =	0.0898 m^3/s

† IMFT (adapted as described in Chapter 4)

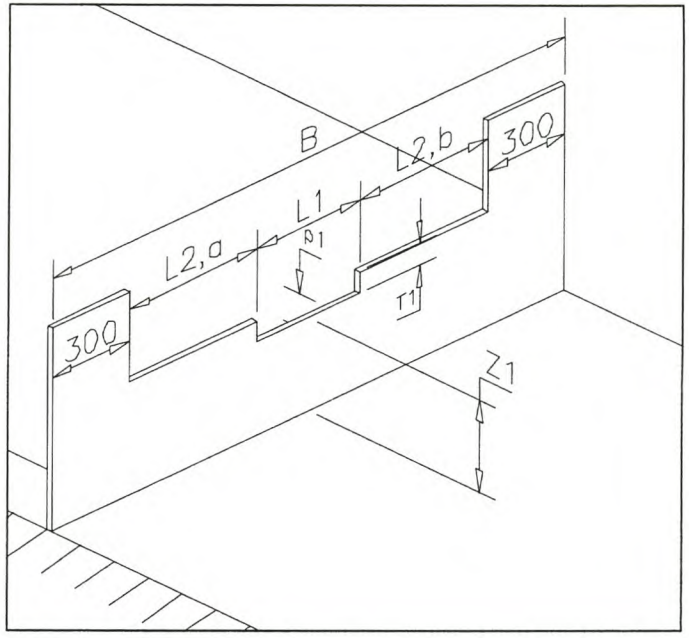

Water levels relative to lowest crest (mm):						Regime**:	Comment:
A	B (h_v)	C	D	E (t)	F		
154.1	152.9	154.4	-	-	-	-	modular conditions
154.4	153.5	155.1	23.4	25.6	24.6	a	L_1 submerged
156.2	155.1	156.5	51.1	49.1	52.7	a	
159.4	158.4	160.1	84.1	79.3	84.6	a	L_1 & L_2 completely submerged. D, E, F levels oscillate (±5mm)
165.7	164.7	165.7	106.8	101.6	106.9	b	downstream levels oscillate a lot
172.8	172.3	173.3	125.0	123.1	128.2	b	still a lot of oscillations
182.8	181.8	182.8	148.3	141.6	149.3	b	
197.0	196.3	197.2	173.5	167.9	174.9	b	
211.6	211.0	211.9	192.7	187.0	194.0	b	
227.9	227.6	228.4	214.9	211.7	215.1	b	

** a = Plunging Nappe; b = Surface Nappe

Test No: A6

Configuration:	
B =	2.000 m
L_1 =	0.401 m
$L_{2,a}$ =	0.501 m
$L_{2,b}$ =	0.498
T_1 =	0.071 m
P_1 =	0.050 m
Z_1 =	0.259 m

Flow - Weir:	
h_o =	0.1883 m
Q_o † =	0.1391 m^3/s
Flow - Manometer:	
d_1 =	0.300 m
d_2 =	0.213 m
C_d =	0.604
h_W =	1.615 m
Q_m =	0.1403 m^3/s

† IMFT (adapted as described in Chapter 4)

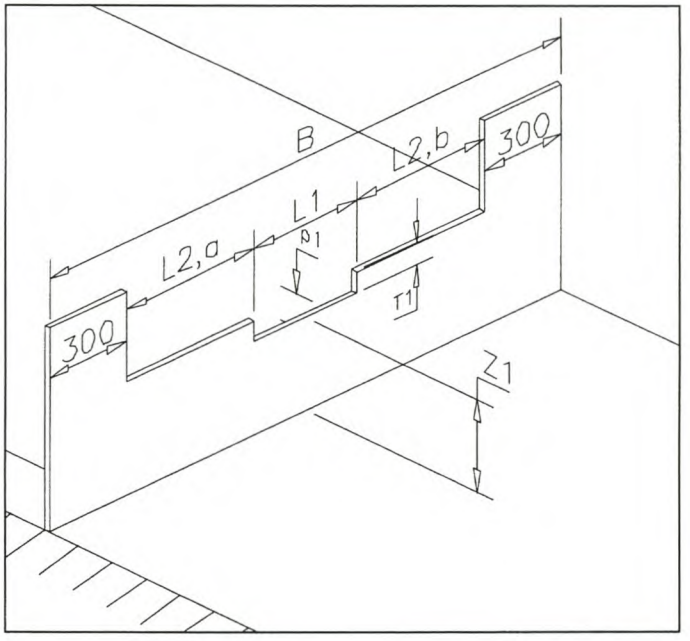

Water levels relative to lowest crest (mm):						Regime**:	Comment:
A	B (h_v)	C	D	E (t)	F		
190.2	188.3	190.7	-	-	-	-	modular conditions
190.5	188.7	191.0	18.9	31.3	15.5	a	L_1 submerged
191.5	189.5	191.8	42.1	52.0	42.6	a	
193.2	191.3	193.4	72.7	72.0	74.0	a	
195.1	193.5	195.6	96.3	91.6	98.7	a	L_1 & L_2 completely submerged
200.0	198.6	200.4	110.0	106.7	116.8	b	Rough standing wave occurs downstream. D, E, F oscillate
205.9	204.7	206.2	128.0	118.6	135.8	b	
215.4	213.6	215.8	158.1	143.6	157.3	b	
228.5	227.7	229.1	187.5	181.5	187.9	b	still some oscillations
240.9	240.1	241.6	207.6	201.4	206.5	b	
258.7	257.3	258.9	235.3	227.8	234.7	b	
280.6	280.0	281.0	259.7	255.2	261.4	b	

** a = Plunging Nappe; b = Surface Nappe

Test No: A7

Configuration:		Flow - Weir:	
B =	2.000 m	h_o =	0.1856 m
L_1 =	0.401 m	Q_o † =	0.1359 m^3/s
$L_{2,a}$ =	0.501 m	**Flow - Manometer:**	
$L_{2,b}$ =	0.498	d_1 =	0.300 m
T_1 =	0.071 m	d_2 =	0.213 m
P_1 =	0.019 m	C_d =	0.604
Z_1 =	0.228 m	h_W =	1.610 m
		Q_m =	0.1401 m^3/s

† IMFT (adapted as described in Chapter 4)

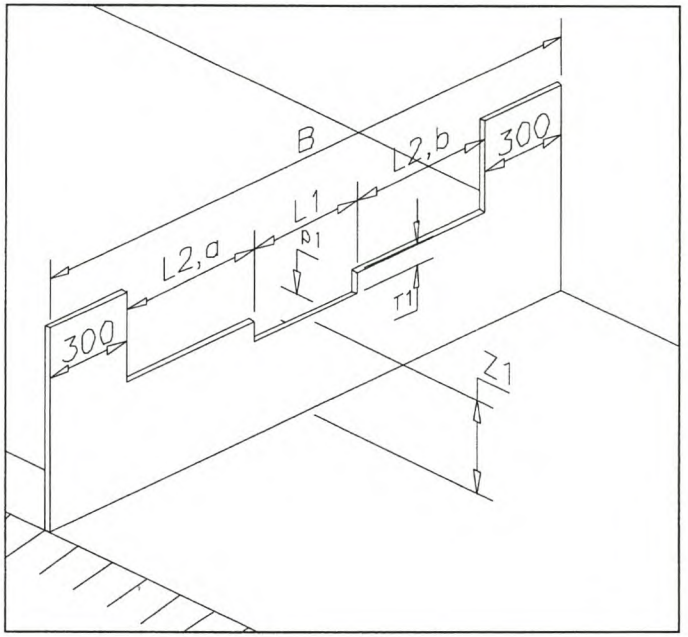

Water levels relative to lowest crest (mm):						Regime**:	Comment:
A	B (h_v)	C	D	E (t)	F		
188.3	185.8	188.5	-	-	-	-	modular conditions
188.1	185.9	188.7	11.9	5.3	14.8	a	L_1 submerged, L_2 free-flowing
189.1	186.9	189.6	36.8	39.5	37.9	a	
189.4	187.3	190.0	55.1	57.9	55.9	a	
190.6	188.7	191.0	81.0	77.2	82.2	a	L_2 still well aerated
193.8	191.9	195.4	98.9	91.0	100.6	a-b	L_1 & L_2 submerged
200.2	198.2	200.5	126.6	116.8	126.2	b	rough wave, large oscillations downstream
207.6	205.8	207.6	147.9	140.4	149.9	b	
215.6	213.9	216.1	163.4	159.5	167.6	b	
225.2	223.1	224.3	185.1	177.4	186.6	b	
238.8	237.7	239.0	209.7	205.6	212.1	b	
263.9	262.7	264.4	244.8	241.5	246.1	b	

** a = Plunging Nappe; b = Surface Nappe

Test No: A8

Configuration:	
B =	2 m
L_1 =	0.401 m
$L_{2,a}$ =	0.500 m
$L_{2,b}$ =	0.699 m
T_1 =	0.071 m
P_1 =	0.102 m
Z_1 =	0.313 m

Flow - Weir:	
h_o =	0.1754 m
Q_o † =	0.1331 m^3/s
Flow - Manometer:	
d_1 =	0.300 m
d_2 =	0.213 m
C_d =	0.604
h_W =	1.435 m
Q_m =	0.1322 m^3/s

† IMFT (adapted as described in Chapter 4)

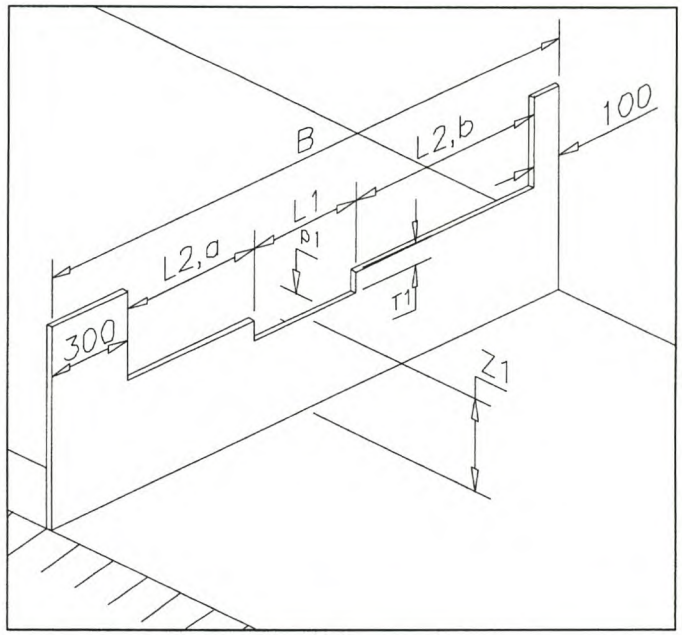

Water levels relative to lowest crest (mm):						Regime**:	Comment:
A	B (h_v)	C	D	E (t)	F		
176.2	175.4	176.1	-	-	-	-	modular conditions
176.5	175.0	176.1	6.1	7.5	8.1	a	L_1 poorly aerated (±5% air underneath nappe)
177.4	175.6	176.9	30.8	32.1	33.0	a	L_1 submerged, L_2 still fully aerated
178.7	177.3	178.2	55.3	54.5	56.4	a	
180.3	179.1	180.3	84.1	80.9	84.7	a	
181.9	180.8	181.2	94.9	91.3	93.2	a	L_1 & L_2 completely submerged
188.3	187.0	188.1	113.1	111.9	112.4	b	
199.0	197.2	198.0	147.1	143.5	143.7	b	
213.9	212.5	213.4	178.8	178.5	177.1	b	
243.8	242.8	243.4	225.2	222.8	223.5	b	
291.5	291.1	291.4	281.2	279.9	280.3	b	

** a = Plunging Nappe; b = Surface Nappe

Test No: A9

Configuration:	
B =	2 m
L_1 =	0.401 m
$L_{2,a}$ =	0.500 m
$L_{2,b}$ =	0.699 m
T_1 =	0.071 m
P_1 =	0.102 m
Z_1 =	0.313 m

Flow - Weir:	
h_o =	0.1752 m
Q_o † =	0.1328 m^3/s
Flow - Manometer:	
d_1 =	0.300 m
d_2 =	0.213 m
C_d =	0.604
h_W =	1.425 m
Q_m =	0.1318 m^3/s

† IMFT (adapted as described in Chapter 4)

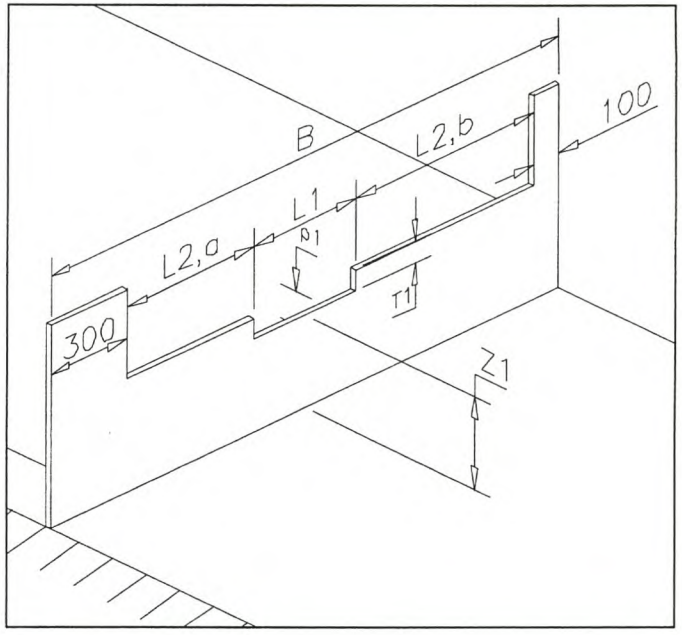

Water levels relative to lowest crest (mm):						Regime**:	Comment:
A	B (h_v)	C	D	E (t)	F		
176.1	175.2	176.1	-	-	-	-	modular conditions
176.5	175.3	176.4	25.0	26.4	26.5	a	L_1 submerged, L_2 free-flowing
178.0	176.9	178.0	57.2	54.9	58.5	a	
184.0	183.2	183.6	104.5	97.4	102.1	a-b	L_1 & L_2 submerged
193.8	192.3	193.6	133.6	129.2	132.7	b	rough standing wave
203.0	202.5	202.8	159.2	156.6	154.7	b	smooth standing wave
213.0	212.2	212.8	176.8	173.2	175.7	b	
226.0	224.6	225.4	198.4	197.8	197.8	b	

** a = Plunging Nappe; b = Surface Nappe

Test No: A10

Configuration:		Flow - Weir:	
B =	2 m	h_o =	0.1572 m
L_1 =	0.401 m	Q_o † =	0.1045 m^3/s
$L_{2,a}$ =	0.500 m	**Flow - Manometer:**	
$L_{2,b}$ =	0.699 m	d_1 =	0.300 m
T_1 =	0.071 m	d_2 =	0.213 m
P_1 =	0.102 m	C_d =	0.604
Z_1 =	0.313 m	h_W =	0.900 m
		Q_m =	0.1047 m^3/s

† IMFT (adapted as described in Chapter 4)

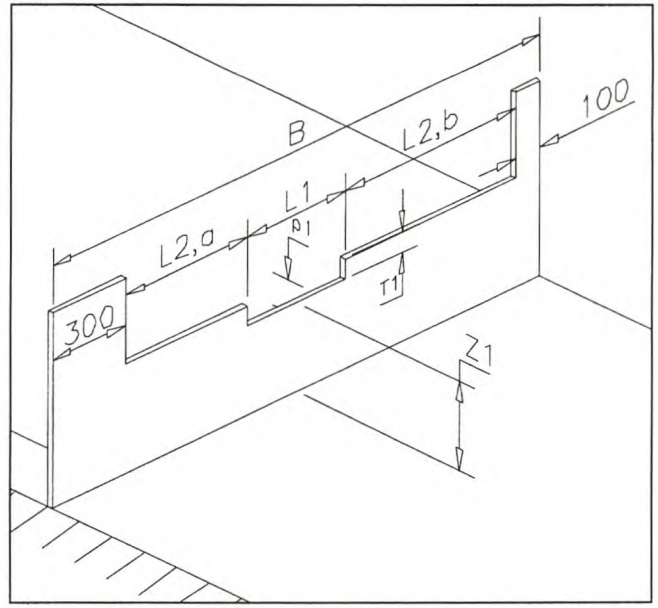

Water levels relative to lowest crest (mm):						Regime**:	Comment:
A	B (h_v)	C	D	E (t)	F		
158.3	157.2	158.0	-	-	-	-	modular conditions
158.2	157.4	158.1	9.6	9.5	9.1	a	L_1 well aerated (±85% air underneath nappe of L_1)
158.8	158.0	158.5	27.9	29.4	29.6	a	L_1 submerged, L_2 free-flowing
160.6	160.0	160.7	59.1	57.0	59.9	a	L_1 submerged, L_2 free-flowing
163.1	162.2	161.8	83.5	83.4	85.4	a-b	
168.7	168.1	168.8	107.4	103.6	105.4	b	L_1 & L_2 submerged, rough standing wave
173.9	173.6	174.0	124.4	123.6	124.5	b	
182.0	181.5	182.4	142.6	142.1	142.2	b	smooth standing wave
189.6	188.8	189.6	157.4	155.9	156.7	b	
197.6	196.8	197.9	172.3	169.4	170.6	b	
207.0	206.4	206.9	185.2	184.9	185.2	b	very smooth standing wave
214.5	214.1	214.7	196.6	194.4	195.5	b	
225.3	224.6	225.7	210.3	208.9	209.6	b	no wave distinguishable
233.3	232.7	233.6	220.2	219.7	219.7	b	
255.0	254.6	255.4	244.6	244.0	244.7	b	

** a = Plunging Nappe; b = Surface Nappe

Test No: A11

Configuration:	
B =	2 m
L_1 =	0.401 m
$L_{2,a}$ =	0.249 m
$L_{2,b}$ =	0.148 m
L_3 =	0.200 m
$L_{4,a}$ =	0.250 m
$L_{4,b}$ =	0.350 m
T_1 =	0.070 m
T_2 =	0.042 m
T_3 =	0.039 m
P_1 =	0.102 m
Z_1 =	0.313 m

Flow - Weir:	
h_o =	0.1125 m
Q_o † =	0.0337 m^3/s
Flow - Manometer:	
d_1 =	0.300 m
d_2 =	0.213 m
C_d =	0.604
h_W =	0.091 m
Q_m =	0.0333 m^3/s

† IMFT (adapted as described in Chapter 4)

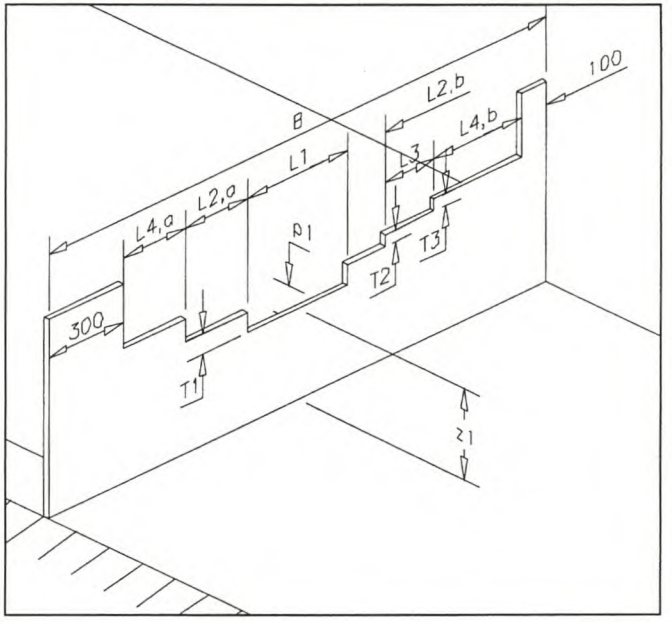

Water levels relative to lowest crest (mm):						Regime**:	Comment:
A	B (h_v)	C	D	E (t)	F		
112.6	112.5	113.1	-	-	-	-	modular flow conditions, flow only over L_1 & L_2
112.9	112.7	113.2	3.9	3.1	3.9	a	L_1 has ±50% air underneath nappe, L_3 not yet overflowing
112.9	112.8	113.5	14.6	14.3	15.3	a	L_1 submerged, L_2 free-flowing, L_3 not yet overflowing
114.6	114.6	115.4	29.1	29.3	29.4	a	
118.3	118.5	118.9	56.6	55.9	56.8	a	L_1 submerged, L_2 free-flowing, L_3 overflowing - but no air underneath nappe
124.0	124.1	124.8	80.0	81.5	81.3	b	L_1 & L_2 submerged, L_3 still unaerated (too little flow)
129.1	128.8	129.8	93.8	93.9	94.6	b	L_1 & L_2 submerged, L_3 finally aerated
134.9	134.8	135.5	107.3	108.3	108.0	b	
142.0	142.0	142.6	120.6	119.7	120.8	b	L_1, L_2, L_3 submerged
150.7	150.7	151.4	134.3	133.7	134.6	b	
159.9	160.0	160.6	147.9	148.2	148.5	b	L_4 overflowing - but no air underneath nappe
170.2	170.3	170.9	161.7	161.3	161.1	b	L_1 - L_4 submerged
181.3	181.3	181.9	174.8	173.4	174.1	b	

** a = Plunging Nappe; b = Surface Nappe

Test No: A12

Configuration:	
B =	2 m
L_1 =	0.401 m
$L_{2,a}$ =	0.249 m
$L_{2,b}$ =	0.148 m
L_3 =	0.200 m
$L_{4,a}$ =	0.250 m
$L_{4,b}$ =	0.350 m
T_1 =	0.070 m
T_2 =	0.042 m
T_3 =	0.039 m
P_1 =	0.102 m
Z_1 =	0.313 m

Flow - Weir:	
h_o =	0.1431 m
Q_o † =	0.0555 m^3/s
Flow - Manometer:	
d_1 =	0.300 m
d_2 =	0.213 m
C_d =	0.604
h_W =	0.248 m
Q_m =	0.0550 m^3/s

† IMFT (adapted as described in Chapter 4)

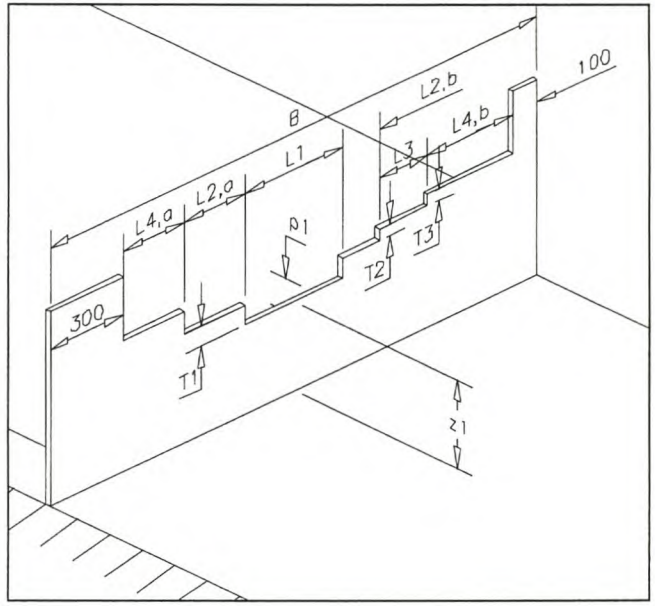

Water levels relative to lowest crest (mm):						Regime**:	Comment:
A	B (h_v)	C	D	E (t)	F		
143.1	143.0	143.9	-	-	-	-	modular flow conditions, flow over L_1 - L_3
143.3	143.1	143.9	3.8	3.7	4.3	a	L_1 has some air (±60%) underneath nappe, L_2 & L_3 ok, L_4 has no flow
144.3	144.1	145.2	18.5	18.9	19.0	a	L_1 submerged, L_2 & L_3 free-flow, L_4 has no flow yet
146.4	145.9	146.5	40.8	40.8	41.5	a	
150.0	149.8	150.5	75.3	72.5	74.4	a	L_1 & L_2 submerged, L_3 free-flowing, L_4 not yet overflowing
154.0	153.8	154.5	88.7	87.9	89.7	a-b	
160.0	159.6	160.2	111.7	110.8	113.1	b	L_1 & L_2 submerged, L_3 free-flowing, L_4 has flow - but no air under nappe
166.9	166.5	167.6	131.0	131.0	133.4	b	L_1-L_3 submerged, L_4 aerated
171.6	171.5	172.3	139.7	140.2	141.7	b	
178.3	178.3	179.0	154.9	152.7	154.2	b	L_1-L_4 submerged
186.9	186.9	187.5	169.3	167.1	169.2	b	
196.6	196.6	197.1	183.1	181.1	183.0	b	
207.1	207.0	207.7	196.5	195.2	196.5	b	
218.0	217.9	218.5	208.9	208.7	209.8	b	
231.6	231.6	232.2	225.1	224.1	225.0	b	

** a = Plunging Nappe; b = Surface Nappe

Test No: A13

Configuration:	
B =	2 m
L_1 =	0.401 m
$L_{2,a}$ =	0.249 m
$L_{2,b}$ =	0.148 m
L_3 =	0.200 m
$L_{4,a}$ =	0.250 m
$L_{4,b}$ =	0.350 m
T_1 =	0.070 m
T_2 =	0.042 m
T_3 =	0.039 m
P_1 =	0.102 m
Z_1 =	0.313 m

Flow - Weir:	
h_o =	0.0641 m
Q_o † =	0.0119 m^3/s
Flow - Manometer:	
d_1 =	0.300 m
d_2 =	0.213 m
C_d =	0.604
h_W =	0.013 m
Q_m =	0.0123 m^3/s

† IMFT (adapted as described in Chapter 4)

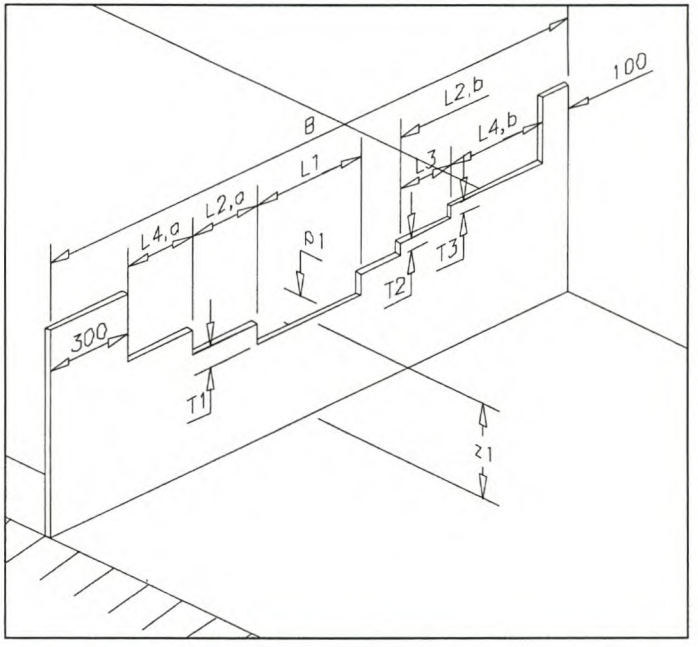

Water levels relative to lowest crest (mm):						Regime**:	Comment:
A	B (h_v)	C	D	E (t)	F		
64.1	64.1	64.7				-	modular conditions, flow over L_1 only
64.6	64.6	65.1	3.8	4.0	4.2	a	L_1 submerged, no flow over L_2 yet
67.1	67.0	68.0	18.0	17.7	17.5	b	
70.0	70.0	70.6	27.0	27.7	28.2	b	
78.1	78.2	78.8	53.7	53.7	54.1	b	flow over L_2 but no air under the nappe of L_2
81.6	81.7	82.4	63.5	63.5	63.5	b	
84.9	84.9	85.4	69.5	69.2	70.0	b	L_2 appears to be submerged
90.6	90.8	91.5	79.2	79.4	79.4	b	L_1 & L_2 definitely submerged
97.8	97.9	98.4	89.3	89.4	89.8	b	
105.7	105.8	106.3	99.2	99.2	99.7	b	
114.1	114.3	114.7	109.3	109.2	109.5	b	
126.2	126.4	127.0	122.7	122.9	123.1	b	L_3 starts overflowing, but almost no difference in water levels

** a = Plunging Nappe; b = Surface Nappe

Test No: A14

Configuration:	
B =	2 m
L_1 =	0.401 m
$L_{2,a}$ =	0.249 m
$L_{2,b}$ =	0.148 m
L_3 =	0.200 m
$L_{4,a}$ =	0.250 m
$L_{4,b}$ =	0.350 m
T_1 =	0.070 m
T_2 =	0.042 m
T_3 =	0.039 m
P_1 =	0.102 m
Z_1 =	0.313 m

Flow - Weir:	
h_o =	0.1945 m
Q_o † =	0.1148 m^3/s

Flow - Manometer:	
d_1 =	0.300 m
d_2 =	0.213 m
C_d =	0.604
h_W =	1.075 m
Q_m =	0.1144 m^3/s

† IMFT (adapted as described in Chapter 4)

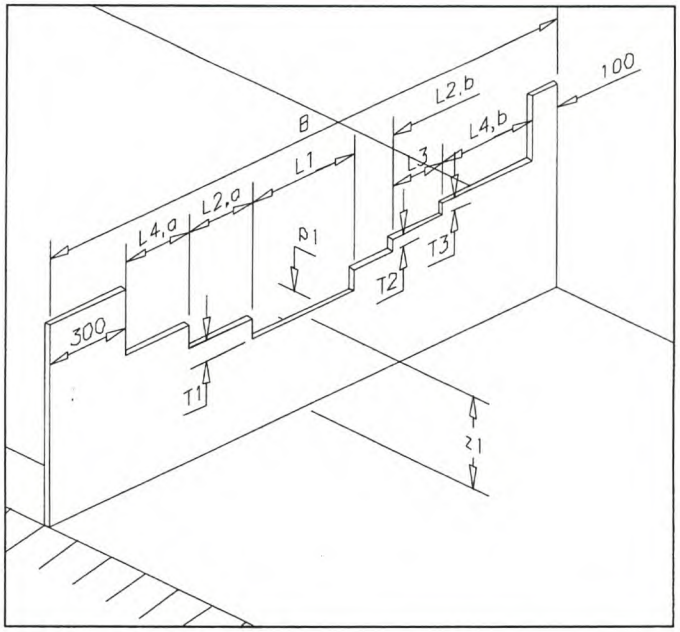

Water levels relative to lowest crest (mm):						Regime**:	Comment:
A	B (h_v)	C	D	E (t)	F		
195.5	194.5	196.1	-	-	-	-	modular conditions, flow over all crests
195.6	194.6	196.3	9.4	9.0	9.3	a	L_1 has ±40% air underneath nappe, L_2 - L_4 free-flowing
197.2	196.1	197.7	36.5	35.1	35.5	a	L_1 submerged, L_2 - L_4 free-flowing
199.0	198.3	199.6	77.2	75.2	77.0	a	L_1 submerged, L_2 becoming submerged (still some air under nappe)
201.2	199.9	201.4	93.3	89.1	92.5	a	L_1 & L_2 submerged, L_3 & L_4 free-flowing
204.8	203.8	205.2	116.3	109.1	115.7	a?	
208.4	208.2	209.3	134.7	132.9	136.9	a-b	L_1-L_3 submerged, L_4 free-flowing
216.6	215.6	216.4	159.6	150.7	154.9	b	L_1-L_4 submerged
224.0	223.3	224.5	181.8	175.6	177.9	b	
235.1	234.6	235.7	200.0	197.7	200.0	b	
245.8	245.6	246.4	218.2	215.2	217.3	b	
254.9	254.5	255.2	232.1	227.9	231.4	b	
265.9	265.1	266.8	248.8	244.3	247.0	b	
278.0	278.0	279.1	262.6	261.8	262.6	b	

** a = Plunging Nappe; b = Surface Nappe

Test No: A15

Configuration:	
B =	2 m
L_1 =	0.401 m
$L_{2,a}$ =	0.430 m
$L_{2,b}$ =	0.618 m
T_1 =	0.071 m
P_1 =	0.102 m
Z_1 =	0.313 m

Flow - Weir:	
h_o =	0.1750 m
Q_o † =	0.1203 m^3/s
Flow - Manometer:	
d_1 =	0.300 m
d_2 =	0.213 m
C_d =	0.604
h_W =	1.170 m
Q_m =	0.1194 m^3/s

† IMFT (adapted as described in Chapter 4)

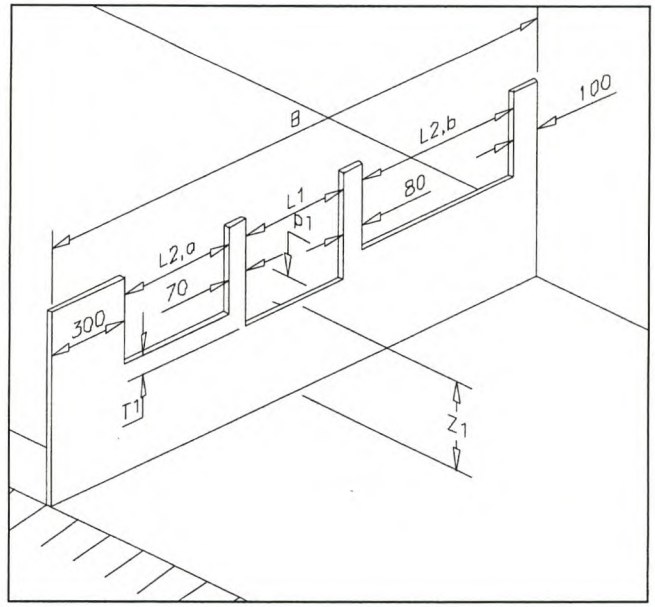

Water levels relative to lowest crest (mm):						Regime**:	Comment:
A	B (h_v)	C	D	E (t)	F		
175.9	174.9	175.8				-	modular conditions
175.9	175.0	175.9	17.8	18.4	18.4	a	±20% air underneath nappe of L_1
176.8	176.0	176.9	38.1	34.9	38.6	a	L_1 submerged, L_2 free-flowing
178.3	177.4	178.5	62.3	57.9	59.7	a	
179.9	179.3	179.9	84.7	81.5	84.6	a-b	L_1 submerged, L_2 ±35% aerated
184.3	183.4	184.2	104.2	102.4	105.2	b	L_1 & L_2 submerged
188.2	187.6	188.8	123.4	121.1	122.0	b	
196.5	196.0	196.8	141.1	142.0	145.4	b	
205.4	205.0	205.7	163.6	163.2	165.6	b	
214.5	213.9	215.0	181.4	180.2	181.9	b	
230.6	229.8	230.6	205.8	204.9	207.0	b	
242.7	241.7	242.9	222.1	221.8	222.8	b	
255.0	254.6	255.1	238.0	238.2	239.1	b	
273.0	272.3	273.3	260.2	259.7	259.6	b	

** a = Plunging Nappe; b = Surface Nappe

Test No: A16

Configuration:	
B =	2 m
L_1 =	0.401 m
$L_{2,a}$ =	0.430 m
$L_{2,b}$ =	0.618 m
T_1 =	0.071 m
P_1 =	0.050 m
Z_1 =	0.259 m

Flow - Weir:	
h_o =	0.1865 m
Q_o † =	0.1383 m^3/s
Flow - Manometer:	
d_1 =	0.300 m
d_2 =	0.213 m
C_d =	0.604
h_W =	1.650 m
Q_m =	0.1418 m^3/s

† IMFT (adapted as described in Chapter 4)

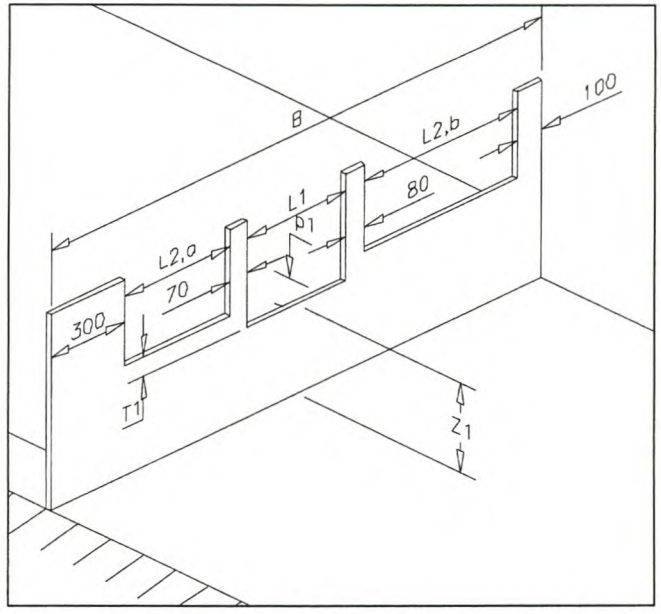

Water levels relative to lowest crest (mm):						Regime**:	Comment:
A	B (h_v)	C	D	E (t)	F		
188.6	186.5	187.5	-	-	-	-	modular flow conditions
189.0	187.4	188.2	36.4	41.4	40.2	a	L_1 submerged
190.3	188.1	189.3	61.8	56.4	58.8	a	
191.5	189.7	190.5	78.0	70.1	76.2	a	L_2 still well aerated
194.2	191.9	193.4	99.8	100.5	104.2	a-b	L_1 & L_2 submerged
199.7	197.9	198.9	120.3	121.2	123.4	b	
206.3	204.5	204.8	144.6	144.3	145.0	b	
214.0	213.1	213.4	162.5	162.6	167.9	b	
226.3	225.1	226.0	190.0	189.6	192.1	b	
242.8	241.7	242.8	216.3	214.5	216.4	b	
265.6	264.8	265.3	247.7	245.8	248.0	b	

** a = Plunging Nappe; b = Surface Nappe

Test No: B1

Configuration:	
L =	0.600 m
P =	0.292 m
Z =	0.292 m

Flow - Weir:	
h_o =	0.1400 m
Q_o † =	0.0608 m^3/s
Flow - Manometer:	
d_1 =	0.300 m
d_2 =	0.213 m
C_d =	0.628
h_w =	0.280 m
Q_m =	0.0607 m^3/s

† IMFT (original)

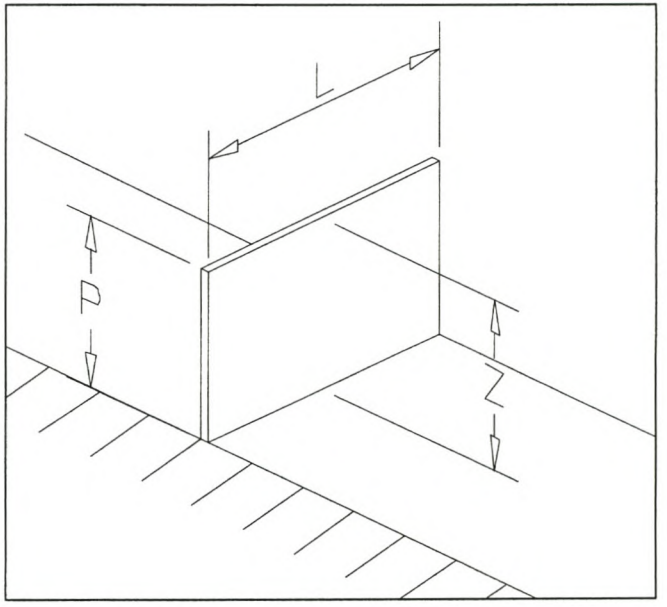

Water levels (mm):		Regime**:
h_v	t	
137.0	7.0	a
139.5	25.0	a
143.5	45.5	a
145.0	54.5	a
146.5	61.0	a
148.0	68.5	a
150.0	73.0	a
154.0	87.0	a
156.0	95.0	a
160.0	104.5	b
169.0	125.5	b
177.5	141.5	b
188.0	159.0	b
199.0	175.5	b
207.0	187.0	b
231.0	216.5	b
270.5	261.5	b

** a = Plunging Nappe; b = Surface Nappe

Test No: B2

Configuration:	
L =	0.600 m
P =	0.292 m
Z =	0.292 m

Flow - Weir:	
h_o =	0.1863 m
Q_o† =	0.0952 m^3/s

Flow - Manometer:	
d_1 =	0.300 m
d_2 =	0.213 m
C_d =	0.628
h_w =	0.679 m
Q_m =	0.0946 m^3/s

† IMFT (original)

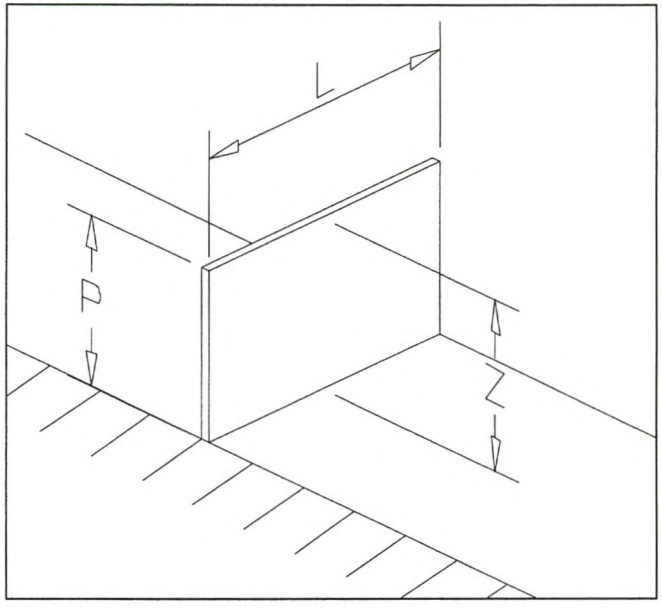

Water levels (mm):		Regime**:
h_v	t	
180.0	3.5	a
181.0	10.5	a
182.0	17.0	a
182.5	25.5	a
184.0	35.0	a
185.5	42.5	a
188.0	58.0	a
191.0	74.5	a
198.5	102.0	a
207.5	132.5	a
222.0	167.0	b
238.0	197.0	b
261.5	232.5	b
299.5	281.5	b
340.5	329.0	b

** a = Plunging Nappe; b = Surface Nappe

Test No: B3

Configuration:	
B =	0.6 m
L =	0.478 m
P =	0.292 m
Z =	0.292 m

Flow - Weir:	
h_o =	0.1850 m
Q_o † =	0.0682 m^3/s
Flow - Manometer:	
d_1 =	0.300 m
d_2 =	0.213 m
C_d =	0.628
h_W =	0.384 m
Q_m =	0.0711 m^3/s

† IMFT (adapted as described in Chapter 4)

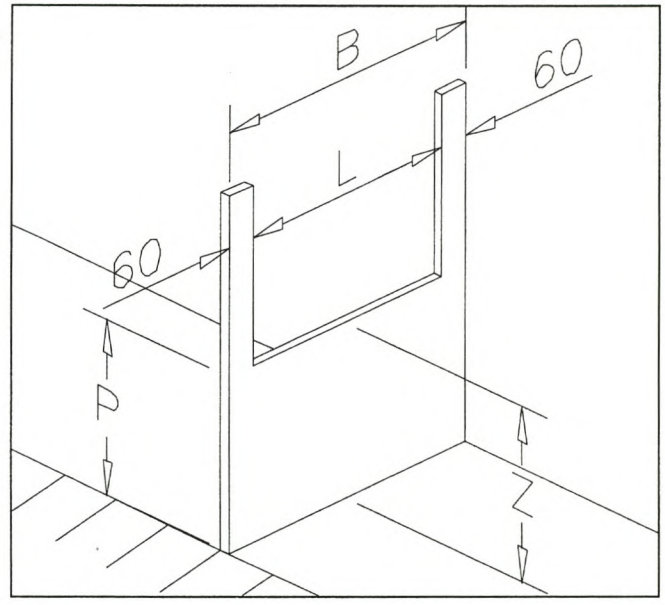

Water levels (mm):		Regime**:
h_v	t	
185.0	4.0	a
185.0	18.5	a
187.5	54.0	a
189.0	64.5	a
194.0	90.5	b
200.5	113.0	b
212.0	148.5	b
233.0	189.5	b
272.5	247.5	b
334.5	321.5	b

** a = Plunging Nappe; b = Surface Nappe

Test No: B4

Configuration:	
B =	0.6 m
L =	0.478 m
P =	0.292 m
Z =	0.292 m

Flow - Weir:	
h_o =	0.1015 m
Q_o † =	0.0280 m^3/s

Flow - Manometer:	
d_1 =	0.300 m
d_2 =	0.213 m
C_d =	0.628
h_W =	0.061 m
Q_m =	0.0283 m^3/s

† IMFT (adapted as described in Chapter 4)

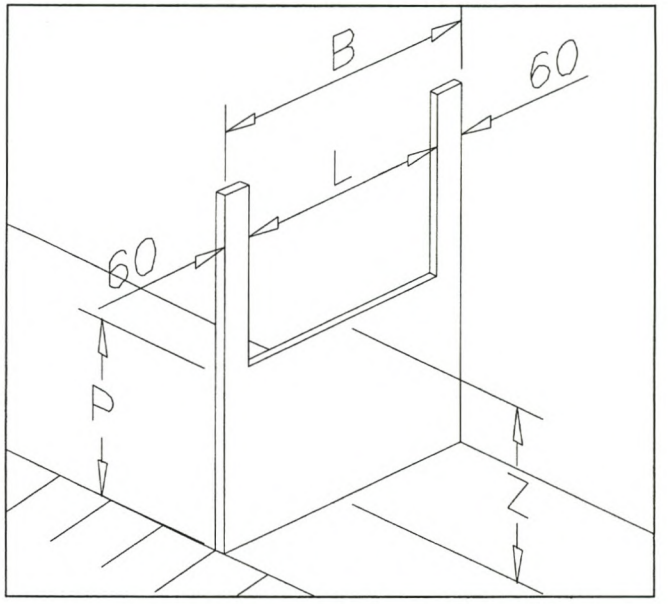

Water levels (mm):		Regime**:
h_v	t	
101.5	5.5	a
102.5	22.5	a
106.0	39.5	b
110.0	54.5	b
119.0	80.0	b
137.0	114.0	b
154.0	138.0	b
190.0	181.5	b

** a = Plunging Nappe; b = Surface Nappe

Test No: B5

Configuration:	
B =	0.6 m
L =	0.478 m
P =	0.292 m
Z =	0.292 m

† Kindsvater & Carter equation

Flow - Weir:	
h_o =	0.0665 m
Q_o† =	0.0149 m^3/s
Flow - Manometer:	
d_1 =	0.300 m
d_2 =	0.213 m
C_d =	0.628
h_W =	0.017 m
Q_m =	0.0150 m^3/s

† IMFT (adapted as described in Chapter 4)

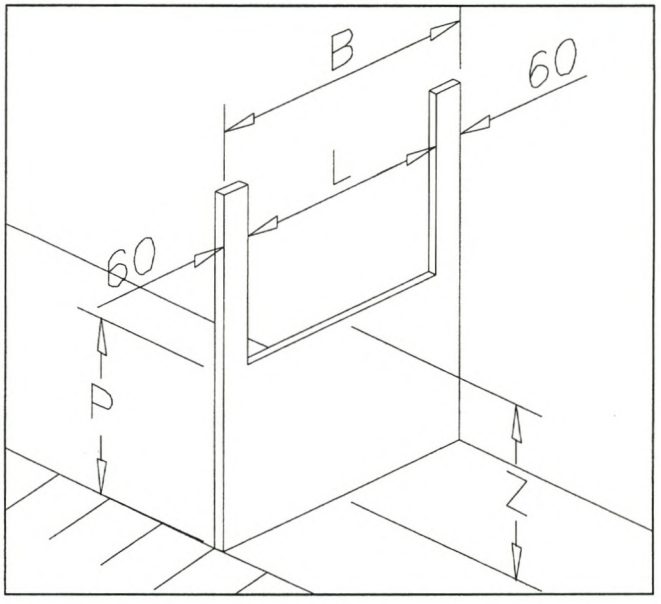

Water levels (mm):		Regime**:
h_v	t	
66.5	7.0	a
69.5	23.0	b
75.0	42.0	b
80.0	55.0	b
86.0	66.5	b
95.0	80.5	b
121.0	114.0	b

** a = Plunging Nappe; b = Surface Nappe

Test No: B6

Configuration:	
B =	0.6 m
L =	0.478 m
P =	0.292 m
Z =	0.292 m

Flow - Weir:	
h_o =	0.2065 m
Q_o† =	0.0808 m^3/s

Flow - Manometer:	
d_1 =	0.300 m
d_2 =	0.213 m
C_d =	0.628
h_W =	0.551 m
Q_m =	0.0852 m^3/s

† IMFT (adapted as described in Chapter 4)

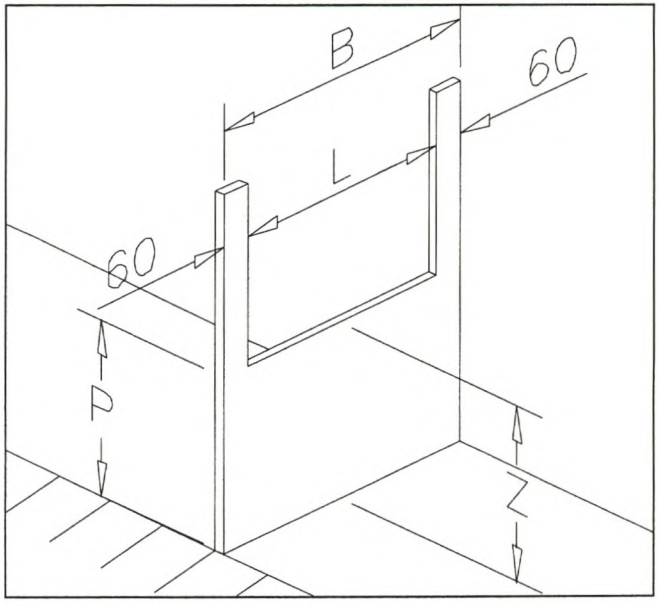

Water levels (mm):		Regime**:
h_v	t	
206.5	10.5	a
206.5	25.5	a
206.5	42.0	a
208.0	56.5	a
209.5	67.5	a
212.0	81.5	a
214.5	96.0	a
218.5	111.5	a
222.0	124.0	a
230.0	151.0	b
240.5	176.0	b
261.0	215.0	b
290.5	259.5	b
329.5	309.0	b

** a = Plunging Nappe; b = Surface Nappe

Test No: B7

Configuration:	
B =	0.6 m
L =	0.478 m
P =	0.292 m
Z =	0.292 m

Flow - Weir:	
h_o =	0.0495 m
Q_o † =	0.0096 m^3/s

Flow - Manometer:	
d_1 =	0.300 m
d_2 =	0.213 m
C_d =	0.628
h_W =	0.007 m
Q_m =	0.0096 m^3/s

† IMFT (adapted as described in Chapter 4)

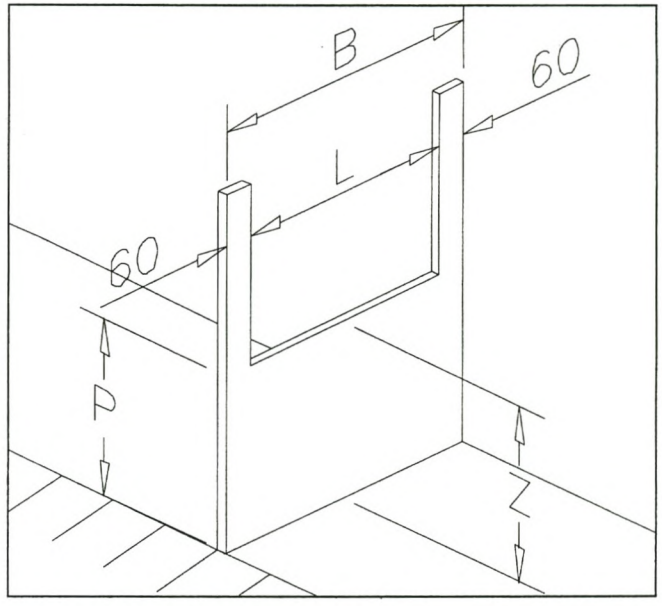

Water levels (mm): h_v	t	Regime**:
49.5	2.5	a
53.5	22.5	b
55.0	26.5	b
59.5	39.5	b
66.0	52.0	b
77.0	68.0	b
91.0	85.0	b

** a = Plunging Nappe; b = Surface Nappe

Test No: C1

Configuration:	
B =	1.0 m
L =	0.799 m
P =	0.504 m
Z =	0.504 m

Flow - Weir:	
h_o =	0.1990 m
Q_o† =	0.1278 m^3/s

Flow - Magflow‡:	
V_{min} =	0.000 V (0 l/s)
V_{max} =	4.970 V (300 l/s)
V =	2.02 V
Q_m =	0.1219 m^3/s

† IMFT (adapted as described in Chapter 4)

‡ Device was not reliable!

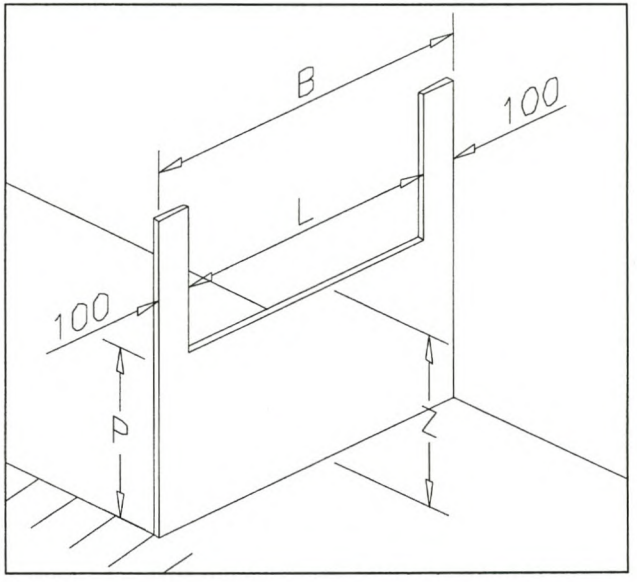

Water levels (mm):		Regime**:
h_v	t	
199.0	2.0	a
199.0	15.5	a
199.5	27.5	a
200.5	41.0	a
203.0	54.5	a
205.5	67.0	a
209.0	83.0	a
212.0	96.0	a
216.0	110.5	a-b
222.0	130.5	a-b
228.0	148.0	b
237.5	169.5	b
249.0	193.5	b
260.5	213.0	b
276.5	237.5	b
299.0	269.0	b

** a = Plunging Nappe; b = Surface Nappe

Test No: C2

Configuration:	
B =	1.0 m
L =	0.799 m
P =	0.504 m
Z =	0.504 m

Flow - Weir:	
h_o =	0.0680 m
Q_o† =	0.0259 m^3/s

Flow - Magflow‡:	
V_{min} =	0.000 V (0 l/s)
V_{max} =	4.970 V (300 l/s)
V =	0.387 V
Q_m =	0.0234 m^3/s

† IMFT (adapted as described in Chapter 4)

‡ Device was not reliable!

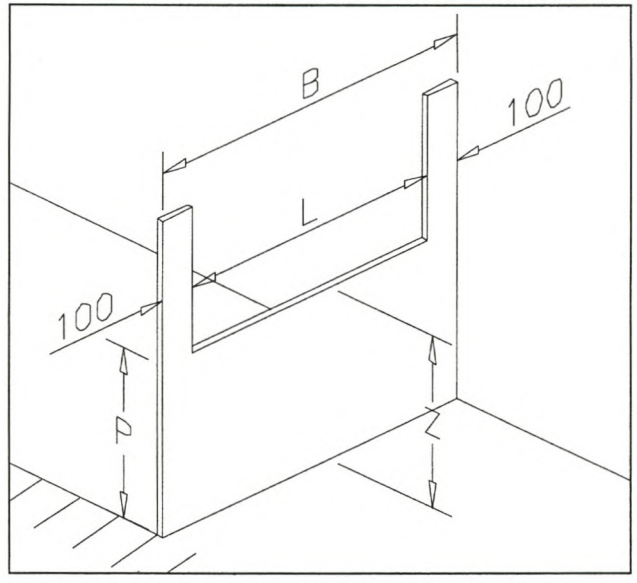

Water levels (mm):		Regime**:
h_v	t	
68.0	3.5	a
69.0	8.5	a
69.2	11.0	a
69.5	13.5	b
70.5	18.5	b
71.5	22.5	b
73.0	28.0	b
74.5	33.0	b
76.5	38.5	b
78.0	44.2	b
83.1	56.5	b
87.0	64.5	b
91.5	72.0	b
95.0	77.5	b
100.0	85.5	b
107.0	95.0	b

** a = Plunging Nappe; b = Surface Nappe

Test No: C3

Configuration:	
B =	1.0 m
L =	0.799 m
P =	0.504 m
Z =	0.504 m

Flow - Weir:	
h_o =	0.2645 m
Q_o† =	0.1943 m^3/s

Flow - Magflow‡:	
V_{min} =	0.000 V (0 l/s)
V_{max} =	4.970 V (300 l/s)
V =	3.100 V
Q_m =	0.1871 m^3/s

† IMFT (adapted as described in Chapter 4)

‡ Device was not reliable!

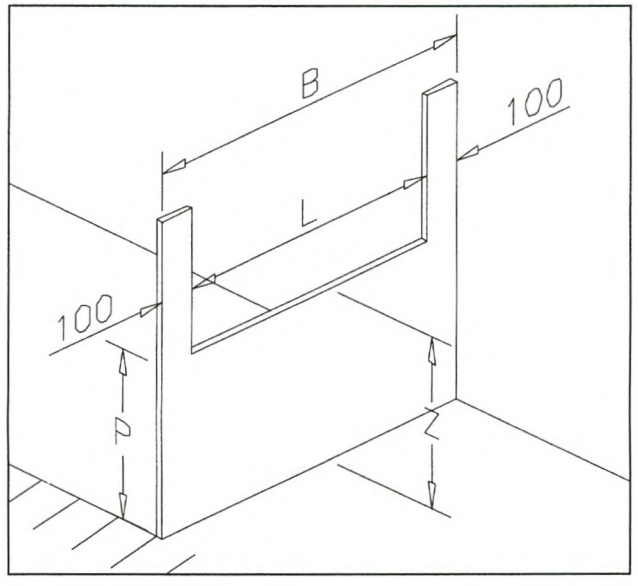

Water levels (mm):		Regime**:
h_v	t	
264.5	9.0	a
264.5	16.0	a
264.0	23.0	a
264.0	34.0	a
264.5	48.5	a
266.0	61.0	a
269.0	80.5	a
273.0	101.5	a
279.5	127.5	a
287.5	160.0	a
297.0	191.0	b
305.0	210.5	b
314.0	230.0	b
326.0	254.0	b
340.5	280.0	b
355.5	304.5	b
386.5	348.5	b

** a = Plunging Nappe; b = Surface Nappe

Test No: C4

Configuration:	
B =	1.0 m
L =	0.799 m
P =	0.504 m
Z =	0.504 m

Flow - Weir:	
h_o =	0.1285 m
Q_o† =	0.0669 m^3/s

Flow - Magflow‡:	
V_{min} =	0.000 V (0 l/s)
V_{max} =	4.970 V (300 l/s)
V =	1.030 V
Q_m =	0.0622 m^3/s

† IMFT (adapted as described in Chapter 4)

‡ Device was not reliable!

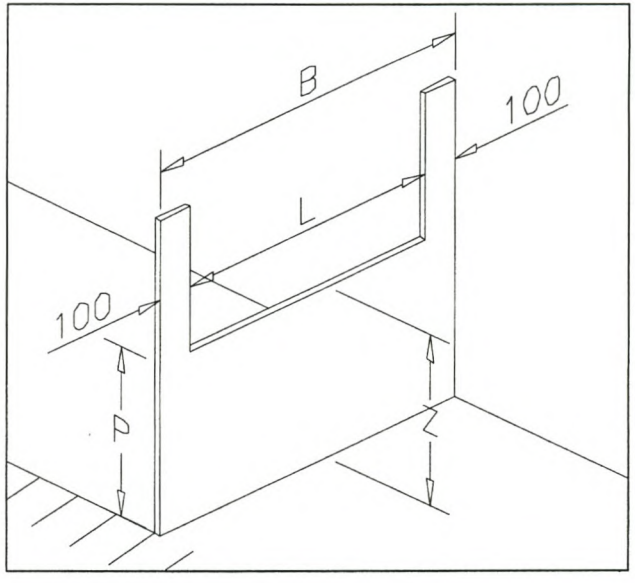

Water levels (mm):		Regime**:
h_v	t	
128.5	11.0	a
130.0	25.5	a
131.5	34.0	b
133.0	42.0	b
135.0	50.0	b
137.0	57.5	b
139.0	65.0	b
143.0	77.5	b
146.0	86.5	b
152.5	102.0	b
157.0	112.5	b
162.5	123.0	b
169.5	136.0	b
179.0	150.5	b
192.0	169.0	b
204.5	186.0	b

** a = Plunging Nappe; b = Surface Nappe

Test No: C5

Configuration:	
B =	1.0 m
L =	0.799 m
P =	0.504 m
Z =	0.504 m

Flow - Weir:	
h_o =	0.3155 m
Q_o† =	0.2539 m^3/s

Flow - Magflow‡:	
V_{min} =	0.000 V (0 l/s)
V_{max} =	4.970 V (300 l/s)
V =	4.110 V
Q_m =	0.2481 m^3/s

† IMFT (adapted as described in Chapter 4)

‡ Device was not reliable!

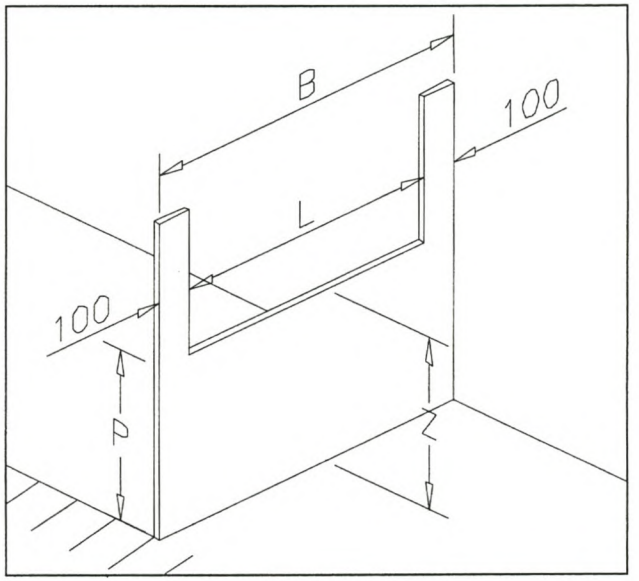

Water levels (mm):		Regime**:
h_v	t	
315.5	16.5	a
315.5	35.0	a
315.0	54.0	a
318.0	82.0	a
321.5	106.5	a
325.0	127.5	a
330.5	152.0	a
335.0	172.0	a
340.5	188.5	a
346.0	211.0	a
351.5	231.0	b
362.0	252.5	b
375.5	281.0	b
397.0	320.0	b
416.5	353.0	b
439.0	387.0	b
464.5	422.0	b

** a = Plunging Nappe; b = Surface Nappe

APPENDIX III
EXAMPLE CALCULATIONS
1. MODULAR FLOW CONDITIONS – COMPOUND WEIRS

The data of Test No. A8-F3 is taken for this example:

DATA:

$L_1 = 0.401$m $\quad L_{2a} = 0.500$m $\quad L_{2b} = 0.699$m
$P_1 = 0.102$m $\quad T_1 = 0.071$m $\quad h_o = 0.1415$m
$B = 2.000$m $\quad Q_m = 0.0815\text{m}^3/\text{s}$ (manometer)

SOLUTION:

Set $H_o = h_o = 0.1415$m

Step 1: Discharge over Notch 1

$$H_o / L_1 = \frac{0.1415}{0.401} = 0.3529 > 0.35 \quad \therefore n = 0.174\left(\frac{0.401}{0.1415}\right)^{0.517} - 0.1 = 0.198$$

$$L_{e1} = 0.401 - 0.198 \times 0.1415 = 0.373m$$

$$\frac{H_o}{P_1} = \frac{0.1415}{0.102} = 1.387 < 1.867 \qquad \therefore C_{d1} = 0.627 + 0.018 \times \frac{0.1415}{0.102} = 0.6520$$

$$Q_{o1} = 0.6520 \times \frac{2}{3} \times \sqrt{2g} \times 0.373 \times 0.1415^{3/2} = 0.038 m^3/s$$

Step 2: Discharge over Notch 2a

$$\frac{H_o - T_1}{L_{2a}} = \frac{0.1415 - 0.071}{0.500} = 0.141 < 0.35 \quad \therefore n = 0.2$$

$$L_{e2a} = 0.500 - \frac{1}{2} \times 0.2 \times (0.1415 - 0.071) = 0.493m \quad \text{(Note: only one side is contracted)}$$

$$\frac{H_o - T_1}{P_{2a}} = \frac{0.1415 - 0.071}{0.102 + 0.071} = 0.4075 < 1.867 \qquad \therefore C_{d2a} = 0.627 + 0.018 \times \frac{0.1415 - 0.071}{0.102 + 0.071} = 0.6343$$

$$Q_{o2a} = 0.6343 \times \frac{2}{3} \times \sqrt{2g} \times 0.493 \times (0.1415 - 0.071)^{3/2} = 0.0173 m^3/s$$

Step 3: Discharge over Notch 2b

$$\frac{H_o - T_1}{L_{2b}} = \frac{0.1415 - 0.071}{0.699} = 0.101 < 0.35 \quad \therefore n = 0.2$$

$$L_{e2b} = 0.699 - \frac{1}{2} \times 0.2 \times (0.1415 - 0.071) = 0.692m \quad \text{(Note: only one side is contracted)}$$

$$\frac{H_o - T_1}{P_{2b}} = \frac{0.1415 - 0.071}{0.102 + 0.071} = 0.4075 < 1.867 \qquad \therefore C_{d2b} = 0.627 + 0.018 \times \frac{0.1415 - 0.071}{0.102 + 0.071} = 0.6343$$

$$Q_{o2b} = 0.6343 \times \frac{2}{3} \times \sqrt{2g} \times 0.692 \times (0.1415 - 0.071)^{3/2} = 0.0243 m^3/s$$

Step 4: Total Discharge & Updated Energy Level

$$Q_o = Q_{o1} + Q_{o2a} + Q_{o2b} = 0.038 + 0.0173 + 0.0243 = 0.0796 m^3/s$$

Approach velocity:

$$v = \frac{Q_o}{A} = \frac{Q_o}{B(P_1 + h_o)} = \frac{0.0796}{2 \times (0.102 + 0.1415)} = 0.163 m/s$$

Update total energy head:

$$H_o = h_o + \frac{v^2}{2g} = 0.1415 + \frac{0.163^2}{2g} = 0.1429m$$

Use this value and go back to step 1. Iterate until H_o is constant.

Final answer: $H_o = 0.1429m$
$Q_o = 0.0821 m^3/s$

Error:

$$\frac{Q_o - Q_m}{Q_m} \times 100 = \frac{0.0821 - 0.0815}{0.0815} \times 100 = 0.74\%$$

2. NON-MODULAR FLOW CONDITIONS – VILLEMONTE'S METHOD (SINGLE NOTCH WEIR)

The data of Test No. A1 (full-width weir) is taken for this example:

DATA:

$L = 2.000\text{m}$ $\quad h_o = 0.1061\text{m}$
$P = 0.173\text{m}$ $\quad h_v = 0.1273\text{m}$
$Z = 0.383\text{m}$ $\quad t = 0.0876\text{m}$
$B = 2.000\text{m}$ $\quad Q_o = 0.1359\text{m}^3/\text{s}$ (free-flow discharge at weir)

SOLUTION:

Set $H_v = h_v = 0.1273\text{m}$

Step 1: Estimate Discharge over Weir

$$\frac{H_v}{P} = \frac{0.1273}{0.173} = 0.736 < 1.867 \qquad \therefore C_d = 0.627 + 0.018 \times \frac{0.1273}{0.173} = 0.6402$$

$$Q_f = 0.6402 \times \frac{2}{3} \times \sqrt{2g} \times 2.000 \times 0.1273^{3/2} = 0.1717 m^3/s$$

$$Q_s = Q_f \left[1 - \left(\frac{t}{h_v}\right)^{1.5}\right]^{0.385} = 0.1717 \times \left[1 - \left(\frac{0.0876}{0.1273}\right)^{1.5}\right]^{0.385} = 01240 m^3/s$$

Step 2: Updated Energy Level

Approach velocity:

$$v = \frac{Q_s}{A} = \frac{Q_s}{B(P + h_v)} = \frac{0.1240}{2 \times (0.173 + 0.1273)} = 0.206 m/s$$

Update total energy head:

$$H_v = h_v + \frac{v^2}{2g} = 0.1273 + \frac{0.206^2}{2g} = 0.1295 m$$

Use this value and go back to step 1. Iterate until H_v is constant.

Final answer: $H_v = 0.1295 m$
$Q_s = 0.1274 m^3/s$

Error:

$$\frac{Q_s - Q_o}{Q_o} \times 100 = \frac{0.1274 - 0.1359}{0.1359} \times 100 = -6.3\%$$

3. NON-MODULAR FLOW CONDITIONS – WESSELS' METHOD (SINGLE NOTCH WEIR)

The data of Test No. A1 (full-width weir) is taken for this example:

DATA:

$L = 2.000\text{m}$ $\quad h_o = 0.1061\text{m}$
$P = 0.173\text{m}$ $\quad h_v = 0.1273\text{m}$
$Z = 0.383\text{m}$ $\quad t = 0.0876\text{m}$
$B = 2.000\text{m}$ $\quad Q_o = 0.1359\text{m}^3/\text{s}$ (free-flow discharge at weir)

SOLUTION:

Step1: Estimate h_o with Wessels' Method:

$$b = -0.34074 - 0.30623\frac{t}{h_v} = -0.34074 - 0.30623\frac{0.0876}{0.1273} = -0.5515$$

$$c = 0.62879\left(\frac{t}{h_v}\right)^2 + 0.10159\frac{t}{h_v} - 0.6096 = -0.2419$$

$$\alpha = \frac{-b + \sqrt{b^2 - 4c}}{2} = \frac{-(-0.5515) + \sqrt{0.5515^2 - 4\times(-0.2419)}}{2} = 0.8396$$

$$h_o = h_v\frac{\sqrt{1-(t/h_v)^2}}{\alpha} = 0.1273\frac{\sqrt{1-(0.0876/0.1273)^2}}{0.8396} = 0.1100m$$

Step 2: Estimate Discharge over Weir

Set $\quad H_o = h_o = 0.1100\text{m}$

$$\frac{H_o}{P} = \frac{0.1100}{0.173} = 0.636 < 1.867 \qquad \therefore C_d = 0.627 + 0.018\times\frac{0.1100}{0.173} = 0.638$$

$$Q_s = 0.638\times\frac{2}{3}\times\sqrt{2g}\times 2.000\times 0.1100^{3/2} = 0.137m^3/s$$

Step 3: Updated Energy Level

Approach velocity:

$$v = \frac{Q_s}{A} = \frac{Q_s}{B(P+h_o)} = \frac{0.137}{2\times(0.173+0.1100)} = 0.242m/s$$

Update total energy head:

$$H_o = h_o + \frac{v^2}{2g} = 0.1100 + \frac{0.242^2}{2g} = 0.1130m$$

Use this value and go back to step 2. Iterate until H_o is constant.

Final answer: $H_o = 0.1133m$

$Q_s = 0.1439m^3/s$

Error:

$$\frac{Q_s - Q_o}{Q_o} \times 100 = \frac{0.1439 - 0.1359}{0.1359} \times 100 = 5.9\%$$

4. NON-MODULAR FLOW CONDITIONS – COMPOUND SHARP-CRESTED WEIR

The data of Test No. A8 is taken for this example:

DATA:

$L_1 = 0.401$m $\quad L_{2a} = 0.500$m $\quad L_{2b} = 0.699$m
$P_1 = 0.102$m $\quad T_1 = 0.071$m $\quad h_o = 0.1754$m
$B = 2.000$m $\quad Z = 0.313$m $\quad Q_o = 0.1331\text{m}^3/\text{s}$ (free-flow)
$h_v = 0.1972$m $\quad t = 0.1435$m

CALCULATION OF SUBMERGENCE RATIO:

$$A_v = L_1 \times h_v + (L_{2,a} + L_{2,b}) \times (h_v - T_1) = 0.401 \times 0.1972 + (0.500 + 0.699) \times (0.1972 - 0.071) = 0.230 m^2$$

$$A_t = L_1 \times t + (L_{2,a} + L_{2,b}) \times (t - T_1) = 0.401 \times 0.1435 + (0.500 + 0.699) \times (0.1435 - 0.071) = 0.144 m^2$$

$$S' = \frac{A_t}{A_v} = \frac{0.144}{0.230} = 0.63$$

SOLUTION:

Set $H_v = h_v = 0.1972$m

Step 1: Discharge over Notch 1

$$H_v / L_1 = \frac{0.1972}{0.401} = 0.492 > 0.35 \quad \therefore n = 0.174\left(\frac{0.401}{0.1972}\right)^{0.517} - 0.1 = 0.151$$

$$L_{e1} = 0.401 - 0.151 \times 0.1972 = 0.371 m$$

$$\frac{H_v}{P_1} = \frac{0.1972}{0.102} = 1.933 > 1.867 \qquad \therefore C_{d1} = 0.689\left(\frac{0.102}{0.102 + 0.1972}\right)^{0.04} = 0.660$$

$$Q_{f1} = 0.660 \times \frac{2}{3} \times \sqrt{2g} \times 0.371 \times 0.1972^{3/2} = 0.063 m^3/s$$

$$Q_{s1} = Q_{f1}\left[1 - \left(\frac{t}{h_v}\right)^{1.5}\right]^{0.385} = 0.063 \times \left[1 - \left(\frac{0.1435}{0.1972}\right)^{1.5}\right]^{0.385} = 0.043 m^3/s$$

Step 2: Discharge over Notch 2a

$$\frac{H_v - T_1}{L_{2a}} = \frac{0.1972 - 0.071}{0.500} = 0.252 < 0.35 \quad \therefore n = 0.2$$

$$L_{e2a} = 0.500 - \frac{1}{2} \times 0.2 \times (0.1972 - 0.071) = 0.487m \quad \text{(Note: only one side is contracted)}$$

$$\frac{H_v - T_1}{P_{2a}} = \frac{0.1972 - 0.071}{0.102 + 0.071} = 0.729 < 1.867 \qquad \therefore C_{d2a} = 0.627 + 0.018 \times \frac{0.1972 - 0.071}{0.102 + 0.071} = 0.640$$

$$Q_{f2a} = 0.640 \times \frac{2}{3} \times \sqrt{2g} \times 0.487 \times (0.1972 - 0.071)^{3/2} = 0.041 m^3/s$$

$$Q_{s2a} = Q_{f2a}\left[1 - \left(\frac{t - T_1}{h_v - T_1}\right)^{1.5}\right]^{0.385} = 0.041 \times \left[1 - \left(\frac{0.1435 - 0.071}{0.1972 - 0.071}\right)^{1.5}\right]^{0.385} = 0.033 m^3/s$$

Step 3: Discharge over Notch 2b

$$\frac{H_v - T_1}{L_{2b}} = \frac{0.1972 - 0.071}{0.699} = 0.181 < 0.35 \quad \therefore n = 0.2$$

$$L_{e2b} = 0.699 - \frac{1}{2} \times 0.2 \times (0.1972 - 0.071) = 0.686m \quad \text{(Note: only one side is contracted)}$$

$$\frac{H_v - T_1}{P_{2b}} = \frac{0.1972 - 0.071}{0.102 + 0.071} = 0.729 < 1.867 \qquad \therefore C_{d2b} = 0.627 + 0.018 \times \frac{0.1972 - 0.071}{0.102 + 0.071} = 0.640$$

$$Q_{f2b} = 0.640 \times \frac{2}{3} \times \sqrt{2g} \times 0.686 \times (0.1972 - 0.071)^{3/2} = 0.058 m^3/s$$

$$Q_{s2b} = Q_{f2b}\left[1 - \left(\frac{t - T_1}{h_v - T_1}\right)^{1.5}\right]^{0.385} = 0.058 \times \left[1 - \left(\frac{0.1435 - 0.071}{0.1972 - 0.071}\right)^{1.5}\right]^{0.385} = 0.047 m^3/s$$

Step 4: Total Discharge & Updated Energy Level

$$Q_s = Q_{s1} + Q_{s2a} + Q_{s2b} = 0.043 + 0.033 + 0.047 = 0.123 m^3/s$$

Approach velocity:

$$v = \frac{Q_s}{A} = \frac{Q_s}{B(P_1 + h_v)} = \frac{0.123}{2 \times (0.102 + 0.1972)} = 0.206 m/s$$

Update total energy head:

$$H_v = h_v + \frac{v^2}{2g} = 0.1972 + \frac{0.206^2}{2g} = 0.1994m$$

Use this value and go back to step 1. Iterate until H_v is constant.

Final answer: $H_v = 0.1995m$
$Q_s = 0.127m^3/s$

Step 5: Determine if Villemonte Formula was Valid:

Obtain an estimate of the free-flow water head (h_o) for the above Q_s. A rough estimate will suffice, therefore:

$$Q_s = 0.127 = C_d \frac{2}{3}\sqrt{2g}\sum\left(L_i \times h_i^{1.5}\right) \qquad \text{take } C_d = 0.60$$

$$\therefore h_o = 0.1770$$

Calculate area of vena contracta:

$$A_o = L_1 \times h_o + (L_{2,a} + L_{2,b}) \times (h_o - T_1) = 0.401 \times 0.177 + (0.500 + 0.699) \times (0.177 - 0.071) = 0.198m^2$$

$$A_{co} = 0.6 \times \frac{1}{2} A_o = 0.6 \times \frac{1}{2} \times 0.198 = 0.059m^2$$

$$\therefore \frac{A_{co}}{A_{t=0}} = \frac{0.059}{B \times Z} = \frac{0.059}{2 \times 0.313} = 0.094 < 0.130$$

Villemonte is therefore valid and the calculation is finished.

Error:

$$\frac{Q_s - Q_o}{Q_o} \times 100 = \frac{0.127 - 0.1331}{0.1331} \times 100 = -4.6\%$$

APPENDIX IV
GRAPH DEVELOPED BY WESSELS FOR SUBMERGED WEIRS